Westinghouse Non-Proprietary Class 3

WCAP-8859-A

TRANFLO Steam Generator Code Description

Westinghouse Electric Company LLC

WCAP-8859-A

TRANFLØ Steam Generator

Code Description

R. E. Land

Reactor Protection Analysis I

September 1976

Approved Version
June 2001

Edited by:
J. C. Reck

APPROVED: _____
C. Eicheldinger, Manager
Nuclear Safety Department

Westinghouse Electric Company LLC
Nuclear Services Division
P.O. Box 355
Pittsburgh, PA 15230-0355

WCAP-8859-A

TABLE OF CONTENTS

SECTION B

NRC Safety Evaluation Report

SECTION A

NRC Acceptance Letter for Referencing of Licensing Topical Report WCAP-8821 (P)/8859 (NP), "TRANFLO Steam Generator Code Description," and WCAP-8822 (P)/8860 (NP), "Mass and Energy Release Following a Steam Line Rupture"

UNITED STATES
NUCLEAR REGULATORY COMMISSION
WASHINGTON, D. C. 20555

Mr. E. P. Rahe, Jr., Manager
Nuclear Safety Department
Westinghouse Electric Corporation
Box 355
Pittsburgh, Pennsylvania 15230

Dear Mr. Rahe:

Subject: Acceptance for Referencing of Licensing Topical Report WCAP-8821 (P)/8859 (NP), "TRANFLO Steam Generator Code Description", and WCAP-8822 (P)/8860 (NP), "Mass and Energy Release Following a Steam Line Rupture"

We have completed our review of the subject topical reports submitted September 29, 1976 by Westinghouse Electric Corporation letters NS-CE-1219 and NS-CE-1220, respectively. We find these reports are acceptable for referencing in license applications to the extent specified and under the limitations delineated in the reports and the associated NRC evaluation which is enclosed. The evaluation defines the basis for acceptance of the reports.

We do not intend to repeat our review of the matters described in the reports and found acceptable when the reports appear as references in license applications except to assure that the material presented is applicable to the specific plant involved. Our acceptance applies only to the matters described in the reports.

In accordance with procedures established in NUREG-0390, it is requested that Westinghouse publish accepted versions of these reports, proprietary and non-proprietary, within three months of receipt of this letter. The accepted versions should incorporate this letter and the enclosed evaluation between the title page and the abstract. The accepted versions shall include an -A (designating accepted) following the report identification symbol.

Should our criteria or regulations change such that our conclusions as to the acceptability of the reports are invalidated, Westinghouse and/or the applicants referencing the topical reports will be expected to revise and resubmit their respective documentation, or submit justification for the continued effective applicability of the topical reports without revision of their respective documentation.

Sincerely,

Cecil O. Thomas

Cecil O. Thomas, Chief
Standardization & Special
Projects Branch
Division of Licensing

Enclosure: As stated

Report Nos. and Titles: WCAP-8821 (Proprietary) and WCAP-8859 (Non Proprietary), TRANFLO Steam Generator Code Description

WCAP-8822 (Proprietary) and WCAP-8860 (Non-Proprietary) Mass and Energy Releases Following A Steam Line Rupture

Report Date: September, 1976
Originating Organization: Westinghouse
Reviewed By: Containment Systems Branch, Office of Nuclear Reactor Regulation

Summary of Topical Report

The above topical reports describe: (1) a method utilizing the MARVEL code for the calculation of mass and energy releases to the containment following a postulated break in a main steam line, and (2) the TRANFLO code which predicts the breakflow quality assumed in the MARVEL calculation. The reports are issued in Proprietary (P) and Non-Proprietary (non-P) versions. The application of the MARVEL code is discussed in WCAP-8822 (P) and WCAP-8860 (non-P). The resulting mass and energy release data calculated using MARVEL are included in Appendix A of the above topical reports as part of Westinghouse Standard 12.2 Rev. 1.

The Westinghouse standard presents data for a spectrum of break sizes as a function of power level. The standard also provides a prescription for modifying the data tables to account for the specific plant conditions of any 3 or 4-loop Westinghouse plant, with Model D or Model 51 steam generators. The MARVEL code that is used to generate the mass and energy release data for steam line breaks is also used for various

types of accident and control studies, including startup of an inactive loop, loss of reactor coolant flow, reactivity insertion incidents, steam line break accident, and steam generator tube rupture accident. A description of the MARVEL code is given in WCAP-8843 which is under a separate review by the NRC.

The MARVEL code provides a multiloop description of the primary system including the core, pressurizer, coolant loops, and steam generator. The code describes the core power excursion during a steam line break and the resulting heat flow to the primary sytsem which can then be transferred to the steam generator and into the containment.

A specific input to MARVEL for the calculation of mass and energy releases is the quality of the flow emanating from the postualted steam line break as a function of time. This input is calculated by the TRANFLO code, which is described in WCAP-8821 (P) and WCAP-8859 (non-P). Quality is a measure of dryness of the flow, ranging from 1.0 (dry steam) to 0 (saturated liquid). An increment of 0.1 is conservatively added to the qualities predicted by TRANFLO before they are input to MARVEL. TRANFLO is a multinode blowdown code similar to SATAN-VI and RELAP-4. The code provides a detailed description of a single steam generator which includes the U-tube region, downcomer region, steam dome and steam separation equipment. The integral feedwater preheater of the Westinghouse Model D steam generator is modeled as is the downcomer injection of the MODEL 51 steam generator. The primary system is not modeled in TRANFLO except in the steam generator. The primary system temperature is input as a table of hot leg temperature versus time, which is calculated using the MARVEL code. The primary loop flow rate is input and assumed to be constant.

Since both MARVEL and TRANFLO require input from each other, iterations may be required between the two codes to obtain a convergent solution.

Summary of Regulatory Evaluation

The staff has reviewed the above cited topical reports and prepared a detailed evaluation. Since portions of the staff's evaluation were considered to be proprietary by Westinghouse, a complete version of the evaluation is presented only in the proprietary version of this report.

The staff has concluded that the TRANFLO and MARVEL codes as described in WCAP-8821 (P)/WCAP-8859 (non-P) and WCAP-8822 (P)/WCAP-8860 (non-P), are acceptable for calculating mass and energy release data following a MSLB. The following model modifications were proposed by Westinghouse, and have been reviewed and found acceptable by the staff:

(1) the steam generator water level calculation was modified to include a pressure depedency, and

(2) heat transfer to steam during tube bundle uncovery has been accounted for.

The mass and energy release data in Appendix A to WCAP-8822 (p)/WCAP-8860 (non-P) should be revised to reflect these changes. The impact of these modifications on earlier plants that used the TRANFLO-MARVEL method has been evaluated. Based on the sensitivity study performed by Westinghouse, we conclude that the second modification could result in higher temperatures in the lower compartment of an ice condenser plant. Consequently, additional analysis may be required to justify the adequacy of equipment qualification in ice condenser containments.

The MARVEL code as described in WCAP-8843, used in performing transient analyses, is currently under a separate review by the NRC. Following the completion of that review, we may require additional analysis to be performed by Westinghouse.

With the exception of the above considerations, we have concluded that the TRANFLO-MARVEL method described in WCAP-8821 (P)/WCAP-8859 (non-P) and WCAP-8822 (P)/WCAP-8860 (non-P), provides a conservative method for calculating mass and energy release to the containment following a main steamline break.

Our review of the TRANFLO code has been confined to the acceptability of the model to provide input for long term containment analysis and did not include considerations for use of the code for other purposes.

In the calculation of mass and energy release data in Appendix A to WCAP-8822 (P) and WCAP-8860 (non-P), Westinghouse has listed the assumptions made for initial steam generator inventory and feedwater system operation during the accident, and has provided a prescription for calculation of steam system operation. We require that applicants using these mass and energy release data provide justification by comparing the in-plant design with the assumptions made by Westinghouse, and provide and justify any modifications made to the tables to account for the specific design of their systems.

SECTION C

WCAP-8859-A Text

TABLE OF CONTENTS

TABLE OF CONTENTS (Cont'd)

TABLE OF CONTENTS (Cont'd)

LIST OF ILLUSTRATIONS

LIST OF ILLUSTRATIONS (Continued)

LIST OF ILLUSTRATIONS (Continued)

LIST OF ILLUSTRATIONS (Continued)

LIST OF ILLUSTRATIONS (Continued)

LIST OF TABLES

ABSTRACT

A comprehensive model of a steam generator capable of treating all types of high energy breaks is presented. Fluid condition may be saturated, subcooled, or superheated. Geometry and flow conditions for two different steam generator models are presented, but the geometrical model is sufficiently flexible to simulate a wide variety of non-standard systems.

Comparisons of model predictions with available experimental data and other computer models show satisfactory agreement. Sensitivity of computer results to special equipment in the steam generators is also illustrated.

1.0 INTRODUCTION

The impact of a "secondary system high energy line break" occurring inside containment on the integrity of in-containment safety systems as well as the containment integrity itself has long been an important part of reactor plant safety evaluations. The ability to accurately predict the events following a high energy secondary system rupture is a basic requirement for adequately performing these evaluations.

The factors which affect the nature of line rupture events can be segregated into three basic groups: (1) energy input from the primary plant; (2) effects of the steam generator design and geometry; and (3) the thermo-hydraulic conditions inside the steam generator. Any simulation which attempts to define the nature of a high energy line break event must be able to treat all of these elements as well as the interaction and feedback among them.

A computer code formulation, called TRANFLØ, has been developed which addresses each of the above items. The code uses an elemental volume approach in which the spatial solution is achieved by dividing the system into a finite number of regions of uniform conditions. The temporal solution is then governed by the integral forms of the conservation equations in each particular region.

This approach to solving complicated thermo-hydraulic problems has been used as a design tool in many other areas for several years. Particular examples of computer formulation using similar techniques are the SATAN[1] and WFLASH[2] codes currently used in loss-of-coolant analyses.

The following material describes the mathematical details, solution techniques, code description and input requirements of the TRANFLØ code as well as providing verification and documentation of results achieved with the code.

2.0 CODE DESCRIPTION

An elemental control volume approach is used in the TRANFLØ code to calculate the thermodynamic and hydraulic behavior of steam/water systems undergoing rapid changes. Fluid conditions may be subcooled, two-phase, or superheated. Fluid flows are assumed to be one-dimensional.

Geometrical modeling is accomplished by using multiple independent fluid control volumes, inter-connected by appropriate flow paths to allow mass and energy exchange. Each nodal volume is represented by a mass and energy which are assumed to exist homogeneously throughout the volume. Flows and pressure drops associated with each flow path are applied one-dimensionally between center points of connected control volumes. Mass may be introduced or removed from the system model by predefined flow leaks into or out of any control volume. Energy may also be added to the system from a specified heat source represented by a continuous pass tube bundle with hot compressed water as a working fluid.

TRANFLØ computationally solves for system conditions by satisfying the mass and energy conservation equations for all control volumes, and by balancing the system pressure differences between control volumes via the momentum equation. An implicit backward differencing technique[3] which numerically integrates the conservation equations is used to continually adjust control volume energies and masses with time. All remaining thermodynamic properties are determined from the mass and energy of the fluid by assuming equilibrium throughout each volume. These conditions are then used for successive calculations. The time steps are determined by an input specification which limits the maximum allowable fractional change of mass or energy in any node over one time step.

The effects of two phase flow on pressure losses and steam/water separation are modeled. The influence of gravity on phase separation in low velocity regions is also modeled.

Heat transfer from the tube bundle heat source is determined from the specified conditions of the working fluid at the tube entrance, the thermodynamic conditions in the control volumes, and the tube wall characteristics. Appropriate time dependent heat transfer coefficients are determined from among a variety of correlations spanning all regimes from forced convection to subcooled liquid through nucleate and transition boiling, to stable film boiling and forced convection to steam. Selection of the appropriate heat transfer coefficients is made independently for each control volume containing a section of the heat source. Cooling of the working fluid as it supplies energy to the system is included in the solution.

Special logic is included in the coding formulation to allow modeling of steam/water separation equipment in any flow path. This modeling includes total phase separation, directionally dependent phase separation, or may be specified by the user in separate subroutines. The capability to calculate subcooled, saturated, and superheated critical flows out of leak paths is also available.

3.0 CODE MODELING

3.1 FUNDAMENTAL EQUATIONS

The governing equations for determining the dependent state variables of pressure, temperature, enthalpy, mass and mass flow rate are developed from the mass, energy, and momentum conservation equations. The equations for an upstream node "i" connected to a downstream node "j" by connector "k" are used in the following form:

$$\frac{dM_i}{dt} = \sum W_{in} - \sum W_{out} - \sum W_{\ell} \tag{1}$$

$$\frac{dU_i}{dt} = \sum h_{in} W_{in} - \sum h_{out} W_{out} - \sum h_{\ell} W_{\ell} + \sum Q_{\text{heat source}} \tag{2}$$

$$\frac{dW_k}{dt} = \frac{1}{L_k} (DP_k + DPX_k + DPF_k + DPE_k + E_k) \tag{3}$$

where

$$DP_k = P_i - P_j \tag{4}$$

$$DPX_k = -0.316 \left(\frac{AF * VIS}{DE|W|}\right)^{0.25} \frac{\nu_{eff} * X}{2g_c * 144 * DE * AF^2} * W * |W| \tag{5}$$

$$DPF_k = - \frac{FD * \nu_{eff}}{2g_c * 144 * AF^2} * W * |W| \tag{6}$$

$$DPE_k = - \left(\frac{1}{AN_i} + \frac{1}{AN_j}\right)\left(\frac{VM_j}{AN_j} - \frac{VM_i}{AN_i}\right)\frac{1}{2g_c * 144} * W^2 \tag{7}$$

$$E_k = \left(\frac{1}{\nu_i} + \frac{1}{\nu_j}\right)\frac{Z_i - Z_i}{288} \tag{8}$$

Definitions of the nomenclature used above are given in Appendix C.

The constituant state equations relating the above equations come from the steam tables which provide the functional relationship between mass, energy, and pressure of a node, i.e.,

$$P_i = P_i\ (U_i,\ M_i) \tag{9}$$

Leak flows out of a node are functions of the pressure and enthalpy and therefore are, in turn, functions of mass and energy such that

$$WL_\ell = WL_\ell\ (P_i,\ h_i) = WL_\ell\ (U_i,\ M_i) \tag{10}$$

Combining equations 1, 2, 3, 9, and 10 for a system of "n" nodes and "m" connectors gives 2n + m differential equations which can be solved for the mass, energy and flowrates for each node. The mathematical solution of these equations is described in Appendix B.

3.2 GEOMETRY

In general the user may describe any steam/water system he chooses with the TRANFLØ code. There are no specific limitations on the number of control volumes or interconnecting flow paths that may be used other than those set by the computer capability. All that need be specified is the volume, elevation, and nodal area for each node and the length, flow area, hydraulic diameter, pressure loss coefficients, and upstream and downstream nodes for each flow path.

Nodes should be selected as much as possible to coincide with obvious physical volumes, and flow paths should reflect all possible paths for mass transfer between these volumes. Since the code uses homogeneous values to represent the thermodynamic conditions throughout a node, regions where this is known to be an inappropriate approximation should be divided into several nodes.

As much as possible, flow connectors should be kept simple. For example, paths which have sharp area changes should not be combined with those which have no area change. Two separate connectors should be used. This is done to avoid the problem of defining a single pressure drop coefficient which is appropriate for a path having many subchannels with very different loss characteristics. However, channels expected to have similar loss characteristics and for which a single coefficient is easily defined should be combined.

Special attention must be given to defining the loss coefficients discussed above in order that the appropriate information is provided to the code. To ensure this the following discussions give a brief description of the loss coefficients used by TRANFLØ.

Form Loss

Form loss for a connector is calculated using equation (6),

$$\Delta P_{\substack{\text{Form}\\ \text{loss}}} = FD*(\text{Flowrate})^2 * \upsilon_{eff}/2g_c*144*(\text{Flow Area})^2$$

Commonly this form loss is defined in terms of either a minimum area and a resistance coefficient, k, or a flow coefficient, C, as follows:

$$\Delta P = k*(\text{Flow rate})^2 * \upsilon_{eff}/2g_c*144*(A_{min})^2$$

$$\Delta P = (\text{Flow rate})^2 * \upsilon_{eff}/2g_c*144*C^2*(A_{min})^2$$

Thus

$$FD = k\ (\text{Flow area}/A_{min})^2 = (\text{Flow area}/C*A_{min})^2$$

Inertial Length

TRANFLØ uses an "inertial length" in the momentum equation, equation (3), to model the inertial or length/area characteristics of the flow path. The inertial length is defined as

$$\text{Inertial length} = \int_i^j \frac{dx}{A(x)}$$

where A(x) is the flow area along the connector length. For connectors joining two nodes of different area this reduces to

$$\text{Inertial length} = \frac{X_i}{A_i} + \frac{X_j}{A_j}$$

where A_i is the flow area of node i and X_i is the length of the connector in node i, and X_j and A_j are similar numbers for node j.

Hydraulic Diameter

The standard definition of hydraulic diameter of a flow path is used in TRANFLØ,

$$D_H = 4* \text{ Flow Area/Wetted Perimeter}$$

For connectors between nodes of different areas, the effective hydraulic diameter is determined as follows:

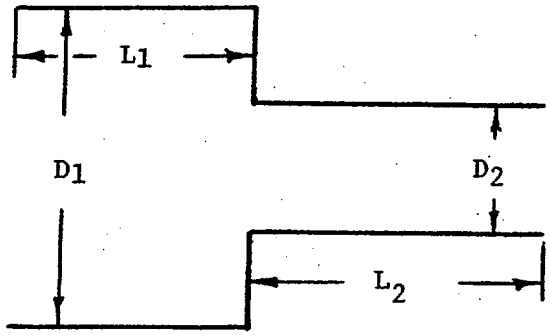

The pressure drop from (1) to (2) is proportional to

$$\frac{f_1 L_1}{D_1} + \frac{f_2 L_2}{D_2} = \left(\frac{fL}{D}\right)_{\text{effective.}}$$

Since the flow is constant throughout the connector the friction factors are assumed equal. Thus

$$\frac{L_{eff}}{D_{eff}} = \frac{L_1 + L_2}{D_{eff}} = \frac{L_1}{D_1} + \frac{L_2}{D_2}$$

or

$$D_{eff} = \frac{L_1 + L_2}{\frac{L_1}{D_1} + \frac{L_2}{D_2}}$$

The details of geometrical input data are given in Appendix A.

3.3 SPECIAL CONNECTORS

Often in steam/water systems some flow paths may have special properties, either by design or as a result of their geometry, which result in higher pressure losses or which may cause phase separation of the steam and water. The TRANFLØ code includes the capability to model some of these effects as standard options. For a flow path any of the following flow characteristics may be specified:

- All steam flow
- All water flow
- Steam flow in positive direction, water flow in negative direction
- Water flow in positive direction, steam flow in negative direction
- Steam flow in positive direction, two-phase flow in negative direction
- Water flow in positive direction, two-phase flow in negative direction
- Cross-flow through a regularly spaced tube bundle.

Because many other variations of characteristics can be postulated, the user also has the option to program any desired connector modeling for

individual flow path in a modular subroutine. Examples of this approach can be found in section 4.3.

3.4 HEAT TRANSFER

The option is available in TRANFLØ for simulating energy addition to any control volume. This is done by using an internal model of a single pass tube bundle having hot pressurized water flowing through it. A segment, or segments, of the tube pass may be specified to transfer heat to any selected volume. Heat flux between the tubes and the control volume is determined independently for each tube segment and is dependent upon the conditions in the control volume. Cooling of consecutive segments of the tube pass is calculated using an energy balance which matches the integrated heat flux over the time step with the energy loss of the working fluid. The heat transfer calculation uses the average of tube segment inlet and outlet temperatures.

Values of heat flux are determined from the following correlations:

1. Dittus-Boelter correlation for forced convection to subcooled water

$$H^{w}_{fc} = \frac{0.023}{D_H} P_r^{0.4} R_e^{0.8} k_w \qquad [16]$$

2. Heineman correlation for forced convection to super-heated steam

$$H^{s}_{fc} = \frac{0.0133}{D_H} P_r^{0.333} R_e^{0.84} k_s \qquad [22]$$

3. Thom correlation for local boiling in subcooled water

$$q^{w}_{lb} = 193\, e^{P/630} (T_{wall} - T_{sat})^2 \qquad [17]$$

4. Schrock and Grossman correlation for forced convection vaporization (used when void fraction > 0.9)

$$H_{fv} = 2.5\, H_{fc}^{w} \Big/ \left[\left(\frac{\mu_w^{0.1}}{\mu_s^{0.1}}\right)\left(\frac{\upsilon_w^{0.5}}{\upsilon_s^{0.5}}\right)\left(\frac{1}{\chi} - 1\right)^{0.9}\right]^{0.75} \qquad [21]$$

5. Conditions for departure from nucleate boiling are determined using the MacBeth correlation for both subcooled and saturated conditions.

$$q_{crit} = 1.7583\, h_{fg} \left(\frac{G}{10^6}\right)^{0.51} (1-\chi)/D_H^{0.1} \qquad [19]$$

6. Transition boiling is calculated using the Westinghouse transition boiling correlation [4].

7. Dougall and Rohsenow correlation for stable film boiling to two-phase mixtures

$$H_{fb} = \frac{0.023 k_s}{D_H}\left[\frac{D_H G[(1-\chi)\upsilon_w + X\upsilon_s]}{\upsilon_s \mu_s}\right]^{0.8} P_r^{0.4} \qquad [20]$$

8. Sandberg et. al. correlation for stable film boiling in subcooled liquid

$$H_{fb} = 0.0193\, R_e^{0.8}\, P_r^{1.23} \left(\frac{\upsilon_w}{\upsilon_s}\frac{\upsilon_{sc}}{\upsilon_{sat}}\right)^{0.068} \frac{k_s}{D_H} \qquad [18]$$

3.5 PHASE SLIP AND WATER ENTRAINMENT IN VERTICAL FLOW

The effects of velocity differences between the steam and water phases in flow paths is included in the problem solution by using an experimental phase slip correlation. The homogeneous void fraction in the

node feeding any given connector is used in the following equation to define flowing quality in that connector:

$$\chi_f = -2.5 + 3\,\chi_a\left(1 - \frac{\nu_w}{\nu_s}\right) + \left\{\left[2.5 - 3\,\chi_a\left(1 - \frac{\nu_w}{\nu_s}\right)\right]^2 + 6\,\chi_a\left(\frac{\nu_w}{\nu_s}\right)\right\}^{1/2}$$

The equation comes from the A. A. Armand two-phase flow correlation [5]. Additionally, the effective specific volume used in the form and frictional pressure loss equation (see Section 3.1) are found using the Armand correlation and the following equations.

1. $\nu_{eff} = \nu_w$ for $\chi_a < 0.01$

2. $\nu_{eff} = \nu_s$ for $\chi_a > 0.99$

3. $\nu_{eff} = \gamma\,\nu_w$ for $0.01 \leq \chi_a \leq 0.99$

   where

   $\gamma = (1-\chi_f)^{1.75}/(1-\chi_a)^{1.42}$ for $0.01 \leq \chi_a \leq 0.61$

   $\gamma = 0.48\,(1-\chi_f)^{1.75}/(1-\chi_a)^{2.2}$ for $0.61 \leq \chi_a \leq 0.90$

   $\gamma = 1.73\,(1-\chi_f)^{1.75}/(1-\chi_a)^{1.64}$ for $0.90 \leq \chi_a \leq 0.95$

   $\gamma = \left[\chi_f + 1.26(1-\chi_f)\left(\frac{\nu_w}{\nu_s}\right)^{1/2}\right]^2\left(\frac{\nu_s}{\nu_w}\right)$ for $0.95 \leq \chi_a \leq 0.99$ (Reference 6)

The effects of gravity separation on entrained water in vertical flows is also included in the code. When the superficial steam velocity for a flow path is less than that for which droplet entrainment is predicted by Davis [7], the flowing quality for the vertical path is set equal to 1.0. For superficial steam velocities slightly higher than the Davis correlation, a transition region is assumed in which that quality varies from all steam to that given by Armand. Specifically, if the steam velocity determined by

$$V_s = (\text{Flowrate})(\nu_s)/\text{Flow area}$$

is between 100% and 180% of the critical velocity given by Davis, a linear fit of flow quality between pure steam and $\chi_{f\ \text{Armand}}$ is used. For values greater than 180% of the critical velocity Armand is used directly. The value of 180% was determined by fitting predicted results to experimental test data for which this natural separation phenomenon should be dominant (see Section 5.1.3).

3.6 CRITICAL FLOW

The mass flowrates from leaks which simulate critical flow situations are determined using either the Moody correlation (saturated mixtures) [8] or the Zaloudek correlation (subcooled fluid)[9].

4.0 APPLICATION TO STEAM GENERATORS

The TRANFLØ code was created specifically for modeling U-tube, recirculating steam generators of the type built by Westinghouse, although it is not limited to this use. There currently are two basic steam generator designs which are either in use at operating power plants or scheduled to go into use in future plants. Computer models of both have been developed and used for analyzing a variety of different accidental transients. A detailed description of both models follows.

4.1 NON-PREHEAT (MODEL 51) STEAM GENERATOR

The steam generators most commonly found in older Westinghouse plants are units designated as Model 51 steam generators. Typical characteristics of these units are shown in Table 4.1-1. They are a non-preheat design having a circular feedwater sparger entering the re-circulation path in the region of the upper downcomer at a level several feet above the tubes. Steam/water separation is accomplished by three (3) swirl vane type centrifugal separators and two (2) parallel banks of Peerless chevron separators. Total unit inventory is approximately 100,000 - 120,000 lbm across the power operating range. A schematic cross-sectional view of a typical unit is shown in Figure 4.1-1.

The TRANFLØ computer model for Model 51 steam generators is shown in Figure 4.1-2 and consists of sixteen (16) elemental control volumes and eighteen (18) flow connectors. The physical locations of the nodes are also indicated on Figure 4.1-1. Descriptions of each node and connector and the input data (as described in Appendix A) are provided in Tables 4.1-2 and 4.1-3. As noted in Table 4.1-3, certain flow paths have special characteristics pertaining to pressure losses, heat transfer, and steam/water separation. Details of these special characteristics are given in Section 4.3.

TABLE 4.1-1

MODEL 51 STEAM GENERATOR TYPICAL DESIGN PARAMETERS

Power	838 Mwt
Primary Flow	9310 lbm/sec
Coolant Inlet Temperature	608.3 °F
Coolant Outlet Temperature	544.2 °F
Coolant Average Temperature	576.3 °F
Primary Operating Pressure	2250 psia
Feedwater Temperature	429 °F
Steam Flow Rate	1000 lbm/sec
Steam Pressure	796 psia
Steam Temperature	518 °F
Primary Pressure Drop	30 psi
Circulation Ratio	3.25
Heat Transfer Area	51,500 ft^2
Number of Tubes	3388
Secondary Mass at Full Power	105,000 lbm

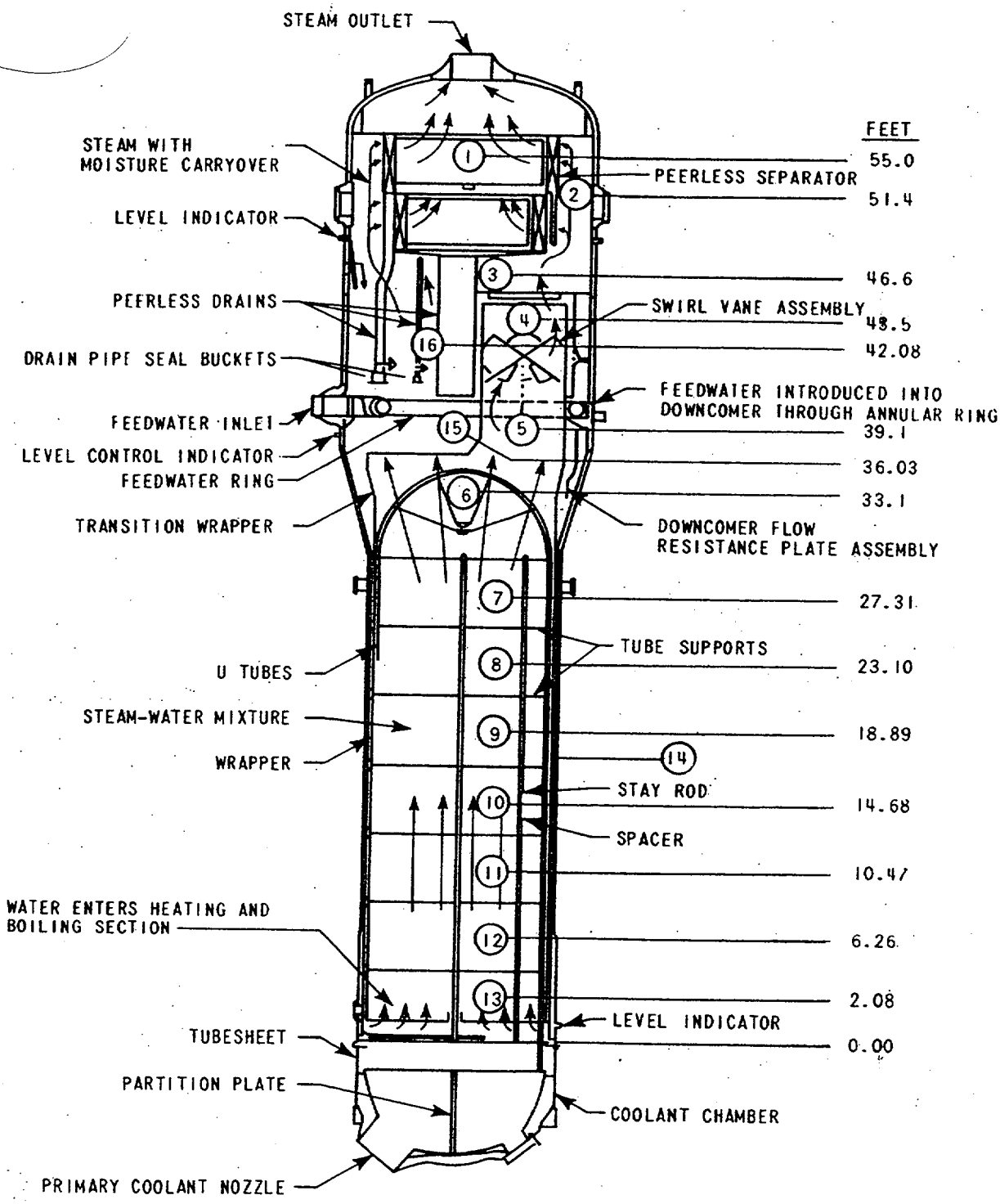

Figure 4.1-1 51 Series Steam Generator Schematic

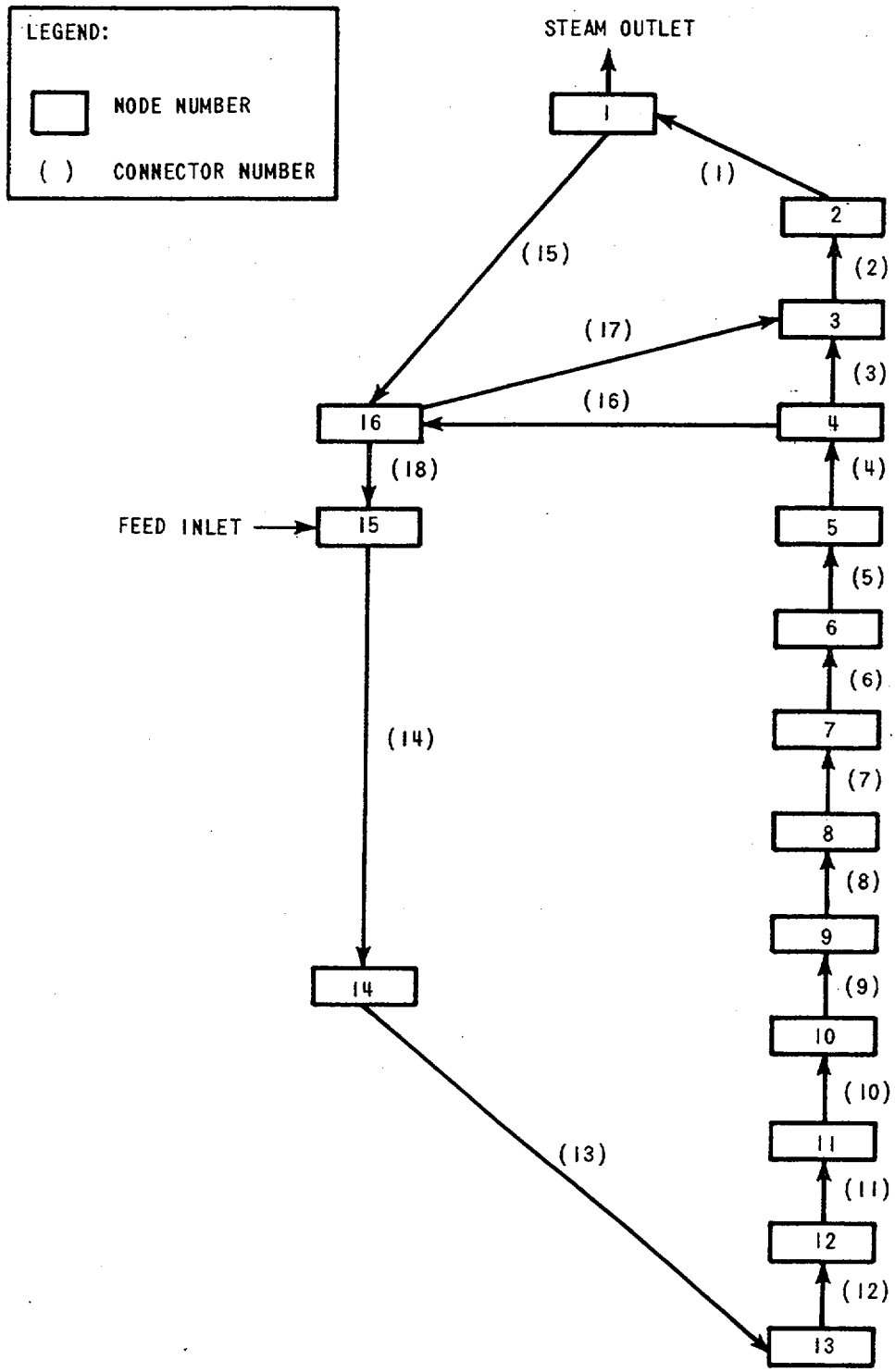

Figure 4.1-2a 51 Series Steam Generator Computer Model

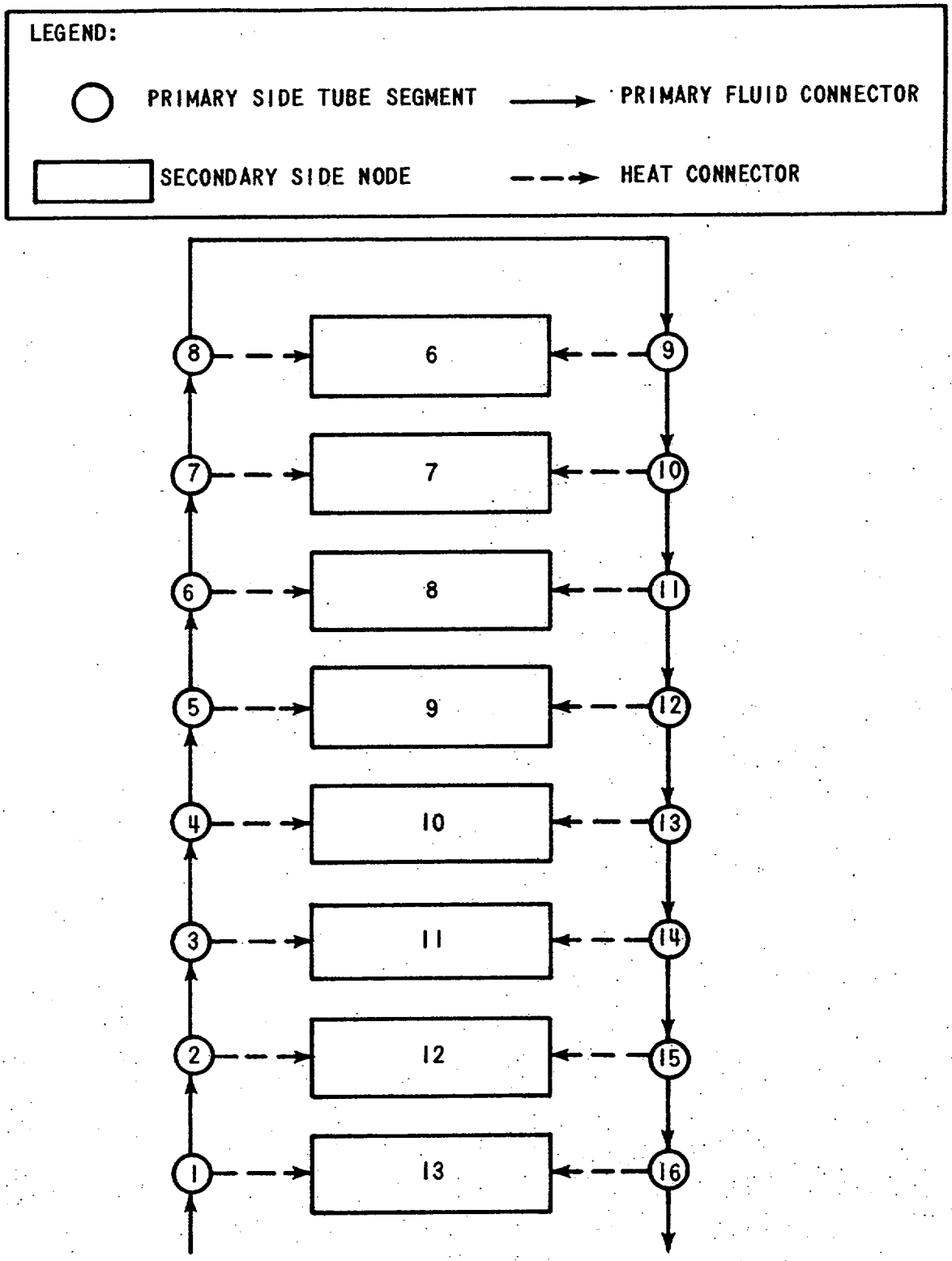

Figure 4.1-2b 51 Series Steam Generator Computer Model—Heat Connectors and Primary Coolant Segments

TABLE 4.1-2

MODEL 51 STEAM GENERATOR COMPUTER MODEL - NODE DESCRIPTIONS

Node	Description
1	Region in upper head of the steam generator including the secondary separators and drains
2	Region between the secondary separators and the steam generator shell
3	Region between the upper steam generator deck plate and the bottom of the secondary separators
4	Region in the swirl vane cylinders above the center of the swirl vanes
5	Region in the swirl vane cylinders below the center of the swirl vanes
6	Region below the swirl vane cylinders and above the top tube support plate
7 - 12	Regions between each adjacent set of tube support plates
13	Region between the lower tube support plate and the tube sheet

TABLE 4.1-2 (Continued)

MODEL 51 STEAM GENERATOR COMPUTER MODEL - NODE DESCRIPTIONS

Node	Description
14	Region in the downcomer between the tube sheet and the downcomer orifice plate
15	Region between the downcomer orifice plate and the feed ring
16	Region between the feed ring and the upper steam generator deck plate

Input Data

Node	Area (ft^2)	Volume (ft^3)		Elevation (ft)
1	[		(a)	55.0
2				51.3
3				46.6
4				43.5
5				39.1
6				33.1
7				27.3
8				23.1
9				18.9
10				14.7
11				10.5
12				6.3
13				2.1
14				16.7
15				36.0
16	]	]		42.1

TABLE 4.1-3

MODEL 51 STEAM GENERATOR COMPUTER MODEL - CONNECTOR DESCRIPTIONS

Connector	Hydraulic Diameter (ft)	Area (ft^2)	Length (ft)	Nodes Connected
1	[		]	(a) 2-1
2				3-2
3				4-3
4				5-4
5				6-5
6				7-6
7				8-7
8				9-8
9				10-9
10				11-10
11				12-11
12				13-12
13				14-13
14				15-14
15				1-16
16				4-16
17				16-3
18	]		[	16-15

Special Connectors

3 Water separation due to swirl vanes is included in this flow path.

15 Secondary separator drains; positive flow is assumed to be saturated water. Elevation head is corrected for height of water in the drain pipes.

MODEL 51 STEAM GENERATOR COMPUTER MODEL - CONNECTOR DESCRIPTIONS

Special Connectors (Cont'd)

16	Swirl vane drains; positive flow is assumed to be saturated water. Elevation head is corrected to include centrifugal force inparted by the swirl vanes.

4.2 INTEGRAL PREHEATER (MODEL D) STEAM GENERATOR

Typical operating characteristics of the newer Westinghouse integral preheater type steam generators, commonly called Model D units, are shown in Table 4.2-1. Feedwater enters the recirculation loop of model D units through a baffled preheater located on the cold leg side of the u-tubes just above the tube sheet. Steam/water separation is accomplished via twelve (12) centrifugal type swirl vane separators and two (2) parallel banks of Peerless chevron separators. The total steam generator inventory typically varies between 100,000 and 160,000 lb_m between full and zero load conditions. A schematic view is shown in Figure 4.2-1.

Model D steam generators are simulated in the TRANFLØ code using twenty-five (25) nodes and thirty-six (36) flow paths as shown in Figure 4.2-2. As before, the locations of the nodes are indicated on Figure 4.2-1. Node and connector information are provided by Tables 4.2-2 and 4.2-3 and special connector effects are discussed in Section 4.3.

4.3 SPECIAL STEAM GENERATOR CONNECTOR LOGIC

Certain flow paths in the steam generator code models represent the flow passage through equipment specifically designed to separate the water and steam phases of the flow. The separative capability of these devices cannot adequately be modeled using any of the special connectors described in Section 3.3. Therefore, some additional connector logic is required when representing these devices in a system.

4.3.1 SWIRL VANES

One flow path having special properties is that which represents the flow through the centrifugal swirl vane separators. These devices

TABLE 4.2-1

MODEL D STEAM GENERATOR TYPICAL DESIGN PARAMETERS

Power	856 Mwt
Primary Flow	9860 lbm/sec
Coolant Inlet Temperature	616.9 °F
Coolant Outlet Temperature	557.0 °F
Coolant Average Temperature	587.0 °F
Primary Operating Pressure	2250 psia
Feedwater Temperature	440 °F
Steam Flow Rate	1050 lbm/sec
Steam Pressure	1000 psia
Steam Temperature	545 °F
Primary Pressure Drop	33 psi
Circulation Ratio	2.4
Heat Transfer Area	48,300 ft^2
Number of Tubes	4578
Secondary Mass at Full Power	104,000 lbm

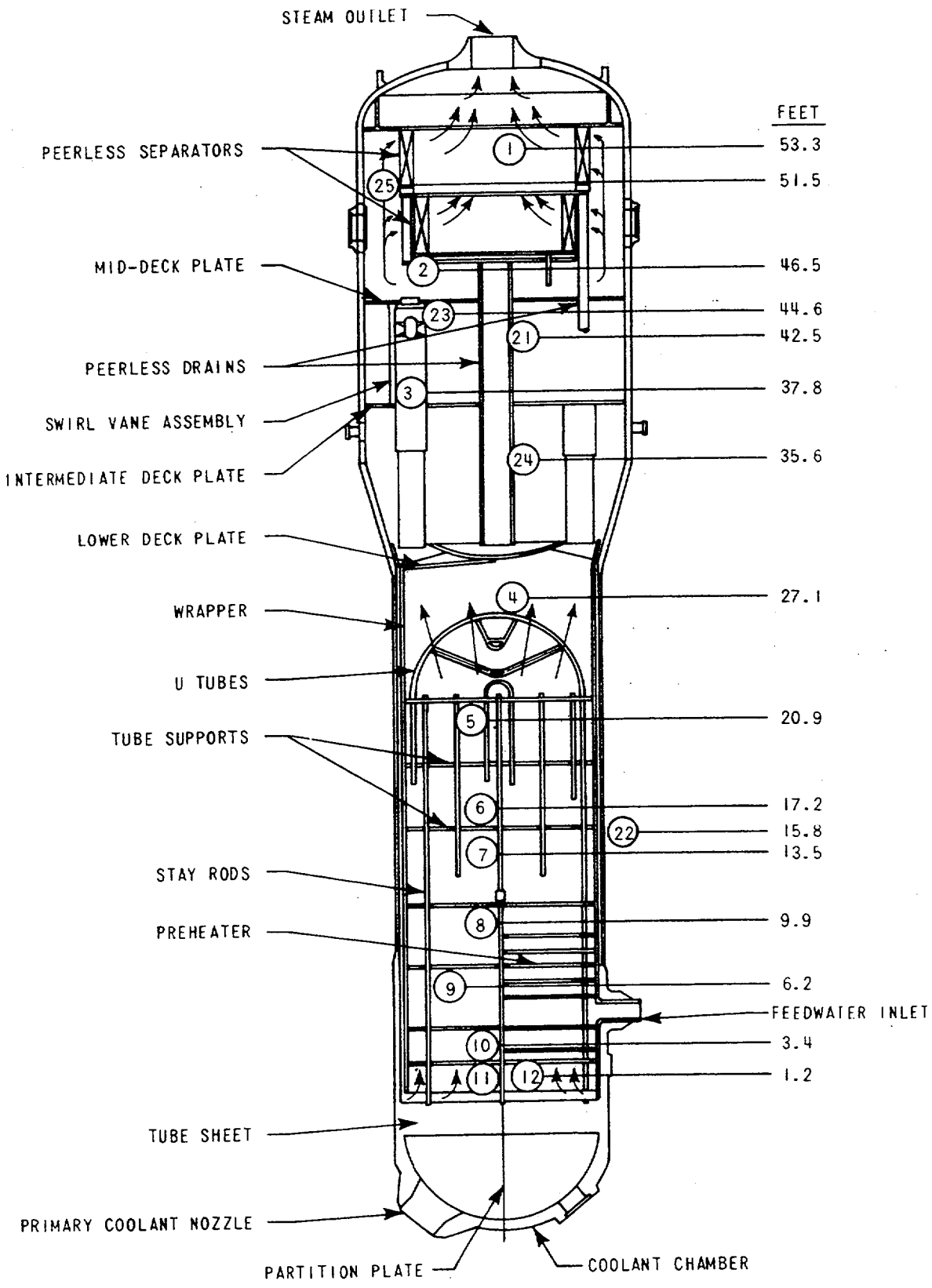

Figure 4.2-1 Model D Steam Generator Schematic

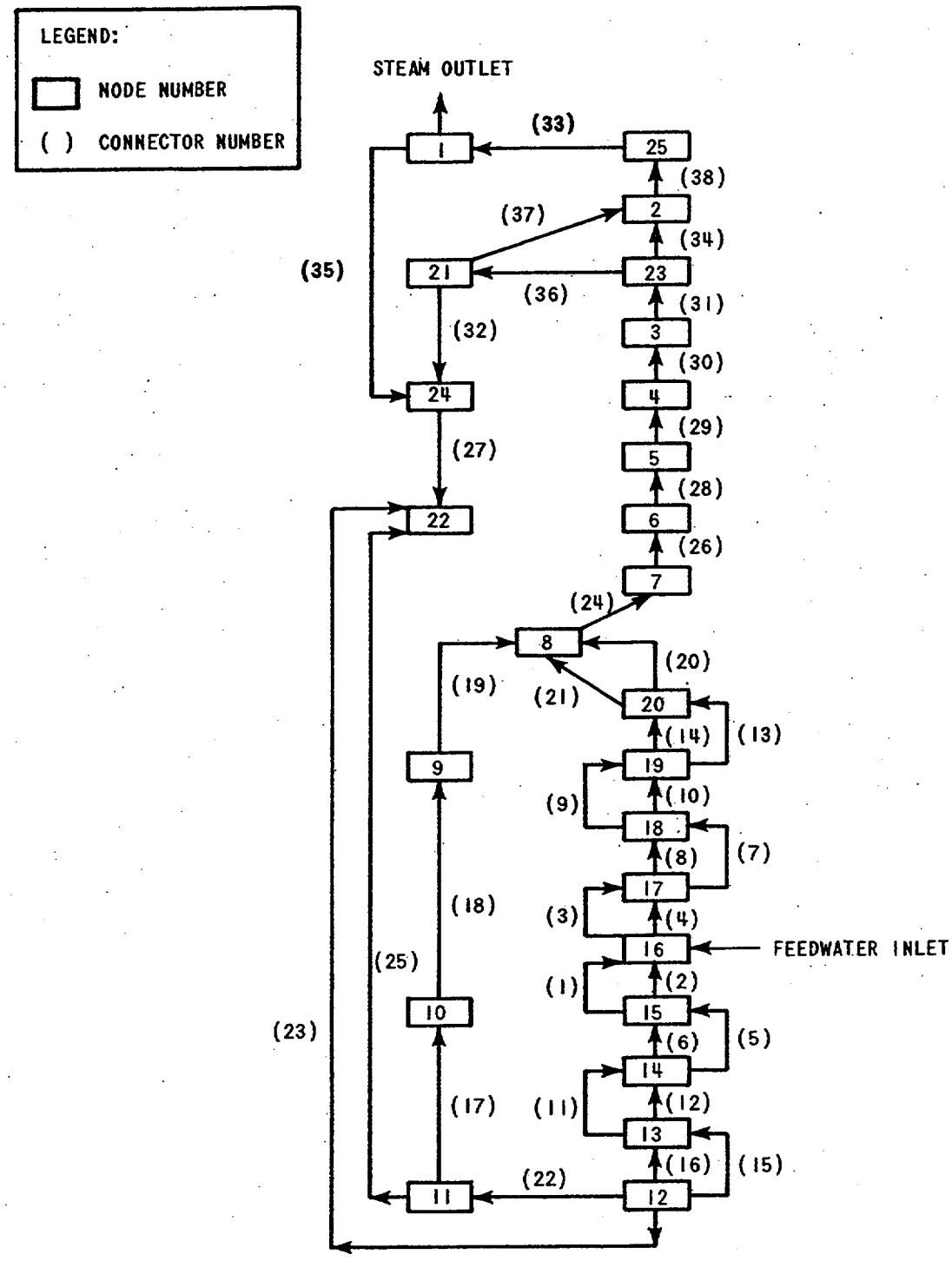

Figure 4.2-2a Model D Steam Generator Computer Model

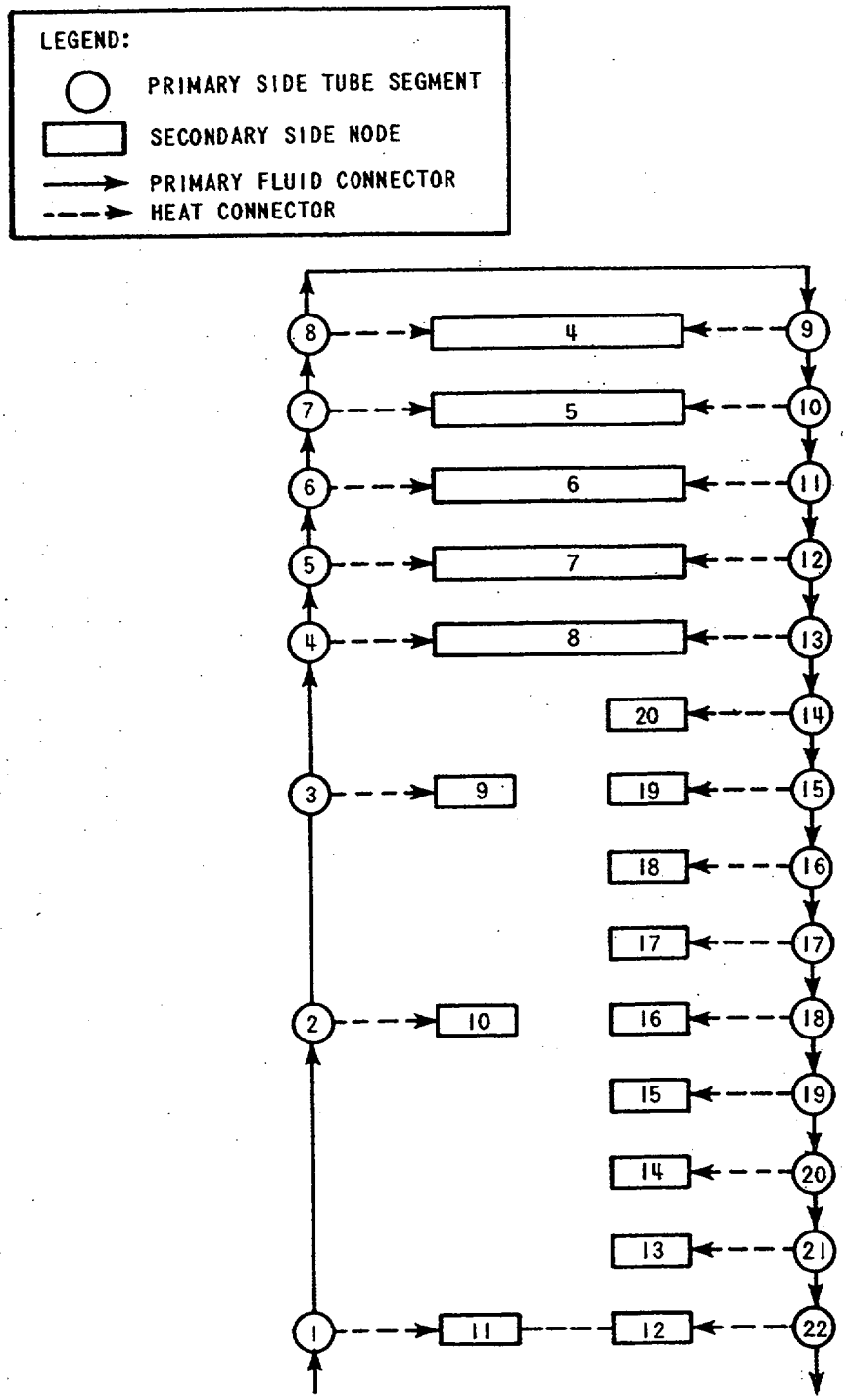

Figure 4.2-2b Model D Steam Generator Computer Model Heat Connectors and Primary Coolant Segments

TABLE 4.2-2

MODEL D STEAM GENERATOR COMPUTER MODEL - NODE DESCRIPTIONS

Node	Description
1	Region in upper head of the steam generator including the secondary separators and drains
2	Region between the mid-deck plate (immediately above the swirl vanes) and the bottom of the secondary separators
3	Region in the swirl vane cylinders below the center of the swirl vanes
4	Region below the swirl vane cylinders and above the top tube support plate
5-7	Regions between each adjacent set of tube support plates above the top of the pre-heater box
8	Region between the fourth tube support plate, the top of the preheater baffle, and the fifth tube support plate
9-10	Regions between adjacent sets of tube support plates on the hot leg side of the tube bundle below the top of the preheater box
11	Region between the tube sheet and the lower tube support plate on the hot leg side of the tube bundle

TABLE 4.2-2 (Continued)

MODEL D STEAM GENERATOR COMPUTER MODEL - NODE DESCRIPTIONS

Node	Description
12	Region between the tubesheet and the lower tube support plate on the cold leg side of the tube bundle
13-20	Regions between adjacent baffle plates in the preheater
21	Region between the intermediate and mid-deck plates outside of the swirl vanes and secondary separator drains
22	Region in the downcomer annulus between the tubesheet and lower deck plate
23	Region in the swirl vane cylinders above the center of the swirl vanes
24	Region between the lower and intermediate deck plates outside of the swirl vanes and secondary separator drains
25	Region between the secondary separators and the steam generator shell

TABLE 4.2-2 (Continued)

MODEL D STEAM GENERATOR COMPUTER MODEL - NODE DESCRIPTIONS

Input Data

Node	Area (ft^2)	Volume (ft^3)		Elevation (ft)
1	[	]	(a)	53.3
2				46.5
3				37.8
4				27.1
5				20.9
6				17.2
7				13.5
8				9.9
9				6.2
10				3.4
11				1.2
12				1.2
13				2.7
14				3.4
15				4.0
16				5.3
17				6.7
18				7.6
19				8.5
20				9.4
21				42.5
22				15.8
23				44.6
24				35.6
25				51.5

TABLE 4.2-3

MODEL D STEAM GENERATOR COMPUTER MODEL - CONNECTOR DESCRIPTIONS

Connector	Hydraulic Diameter (ft)	Area (ft^2)	Length (ft)	Nodes Connected
1				(a) 15-16
2				15-16
3				16-17
4				16-17
5				14-15
6				14-15
7				17-18
8				17-18
9				18-19
10				18-19
11				13-14
12				13-14
13				19-20
14				19-20
15				12-13
16				12-13
17				11-10
18				10-9
19				9-8
20				20-8
21				20-8
22				12-11
23				12-22
24				8-7
25				11-22
26				7-6
27				24-22

TABLE 4.2-3 (Continued)

MODEL D STEAM GENERATOR COMPUTER MODEL - CONNECTOR DESCRIPTIONS

Connector	Hydraulic Diameter (ft)	Area (ft^2)	Length (ft)	Nodes Connected
28	[			(a) 6-5]
29				5-4
30				4-3
31				3-23
32				21-24
33				25-1
34				23-2
35				1-24
36				23-21
37				21-2
38				2-25

Special Connectors

1,3,5,7,9 11,13,15, 21,22,29	Represent flow paths across the u-tubes.
33	Secondary separator drains; positive flow is assumed to be saturated water. Elevation head is corrected for height of water in the drain pipes.
34	Water separation due to swirl vanes is included in this flow path.
36	Swirl vane drains; positive flow is assumed to be saturated water. Elevation head is corrected to include centrifugal force imparted by the swirl vanes.

operate by imparting a radial force component to the water phase of the flow as it passes through the vanes forcing it to the outside of the swirl vane cylinder as shown in Figure 4.3.1-1. As the water reaches the top of the cylinder, it is trapped by the annular scrubber and returned to the downcomer. The steam phase is allowed to continue flowing upward out of the swirl vane through the center opening in the scrubber.

The effects of the swirl vanes are modeled in TRANFLØ by correcting the void fraction of the flow through the device using the following formula:

[ ] (a)

where η_{sv} is the efficiency of the swirl vanes as specified by the user. A graphical representation of the effects of this relationship on swirl vane quality is shown in Figure 4.3.1-2 using a value of 0.7 for η_{sv}.

[ ] (a)

Investigations of the sensitivity of transient results to the swirl vane modeling, and particularly to the value of η_{sv} are discussed in Section 5.3.2. The adequacy and conservatism of this model are also evaluated.

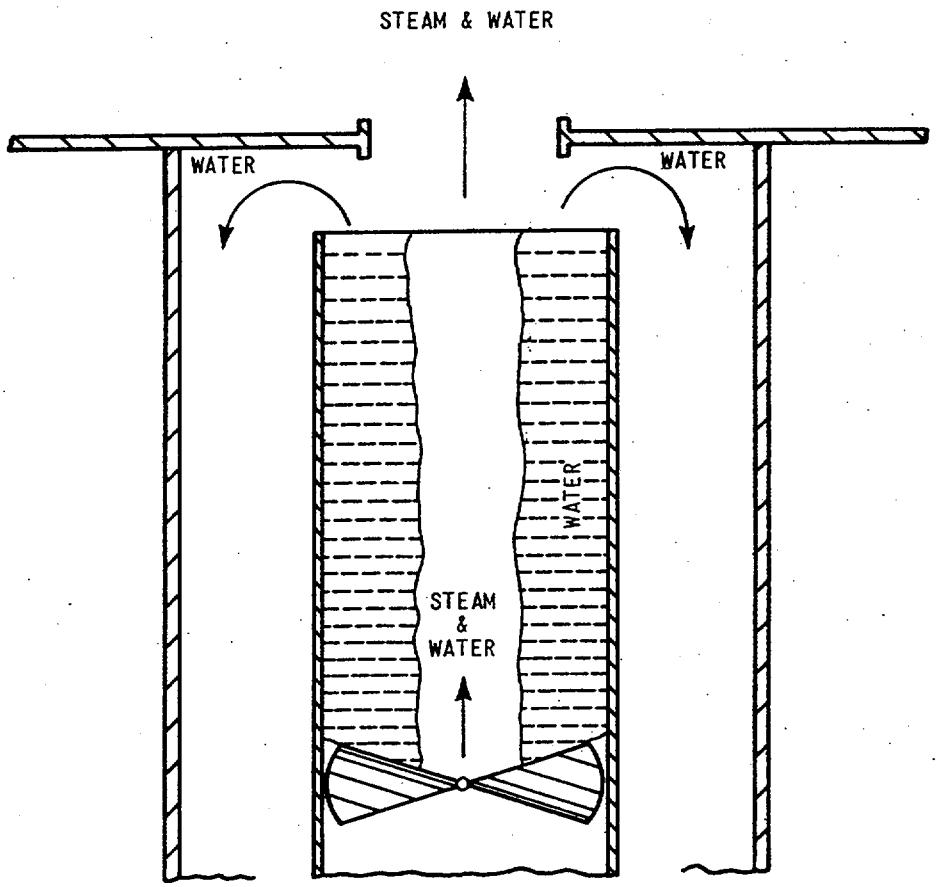

Figure 4.3.1-1 Swirl Vane Schematic Model

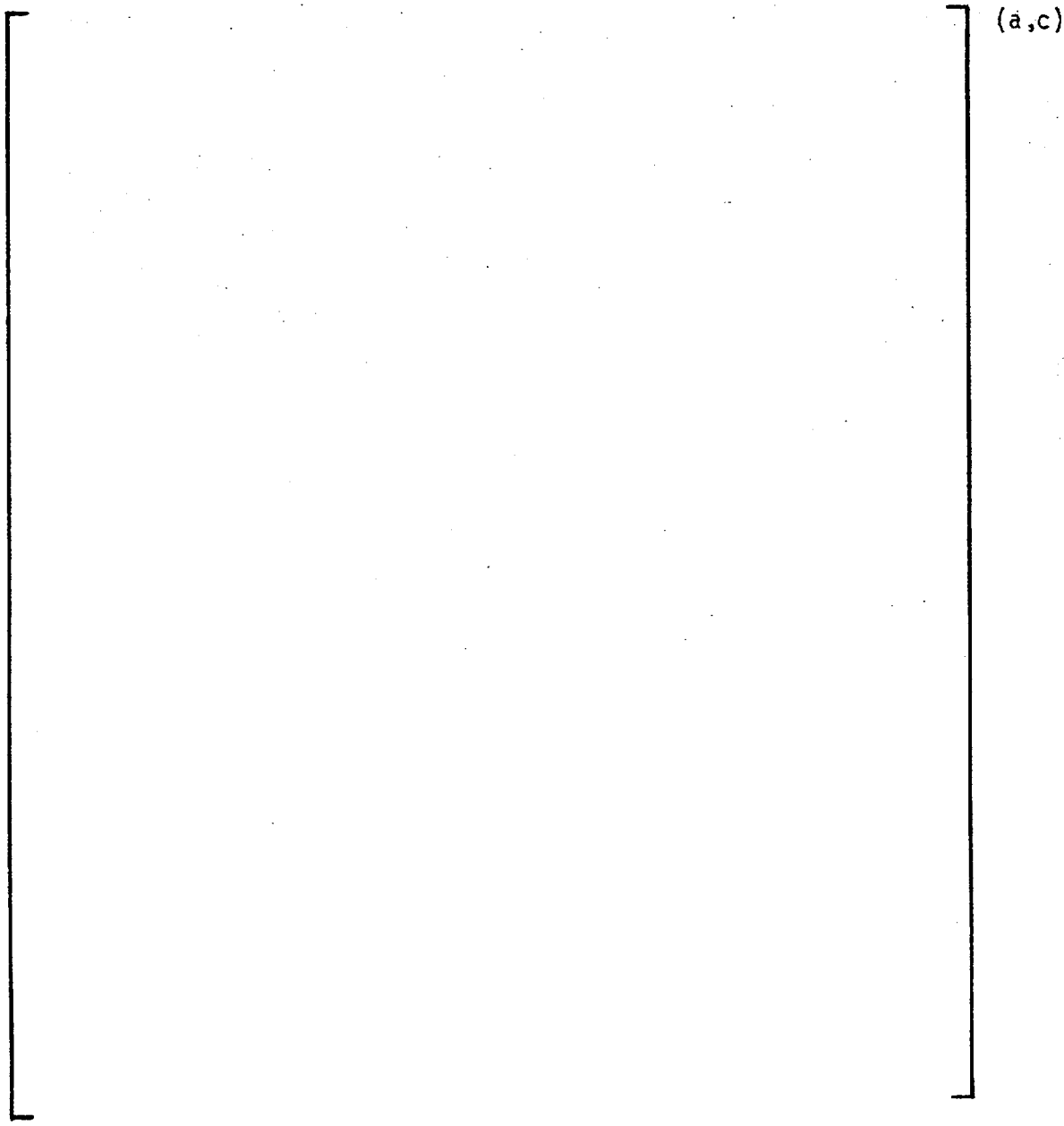

Figure 4.3.1-2a TRANFLO Swirl Vane Separation Model - Void Correction

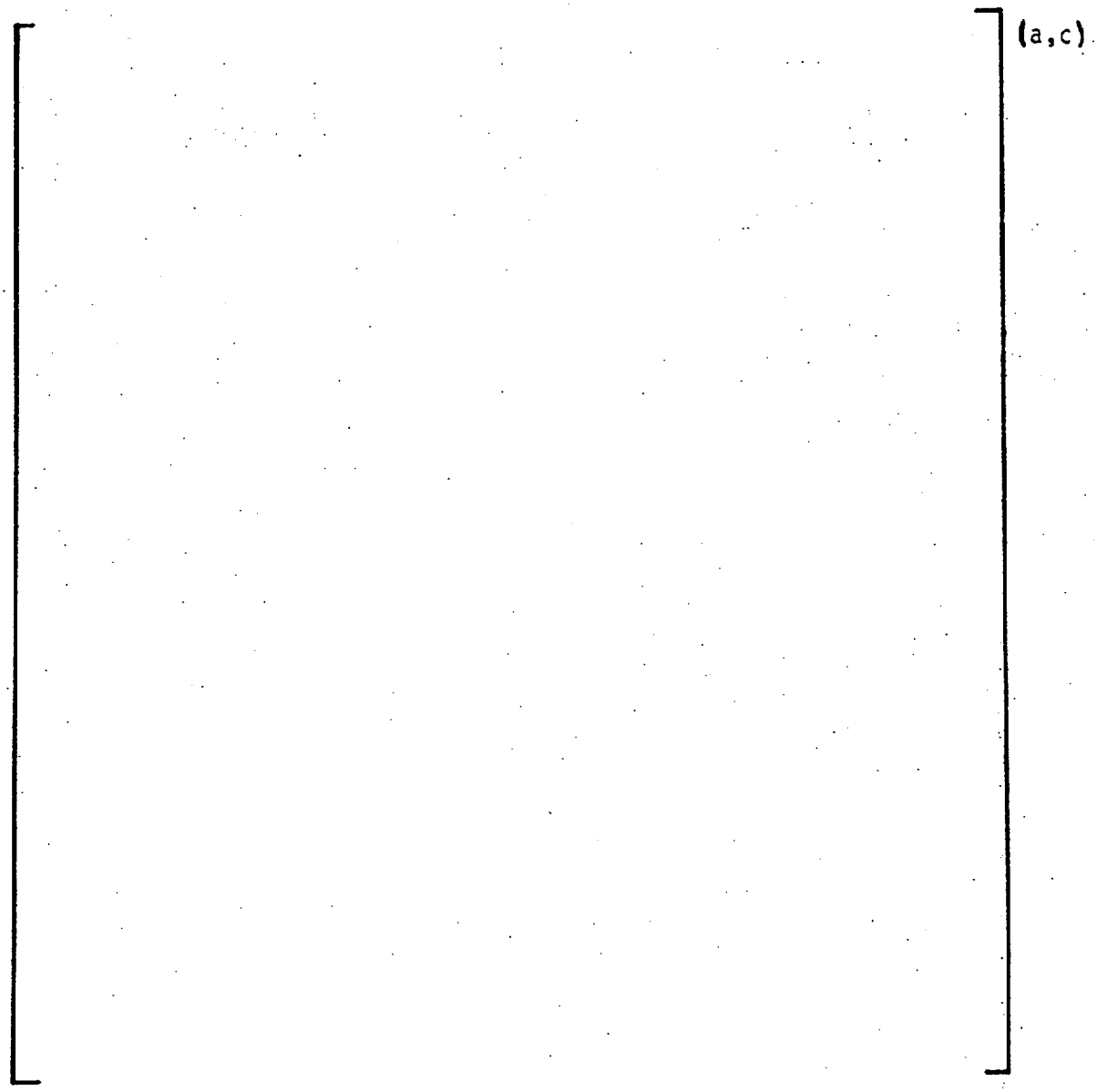

Figure 4.3.1-2b TRANFLO Swirl Vane Separation Model - Quality Correction

4.3.2 PEERLESS CHEVRON SEPARATORS

The chevron separators are also designed specially to extract water from the flow passing through them. Their operation depends again upon the higher momentum of the water phase forcing water droplets to the outer edge of a flow path when a change in flow direction occurs. The separation mechanism is shown schematically in Figure 4.3.2-1. Water which is trapped by the hooked vanes as shown in Figure 4.3.2-1 drains back into the downcomer through a series of drain pipes. The drain flow rate is controlled by the elevation head and the pressure drop between the chevrons and the exit of the drain lines.

The model of the secondary separators in TRANFLØ was chosen such that conservative, high quality releases for a steam line break are always calculated. [ ](a) Sensitivity of results to this model is also evaluated in Section 5.3.2.

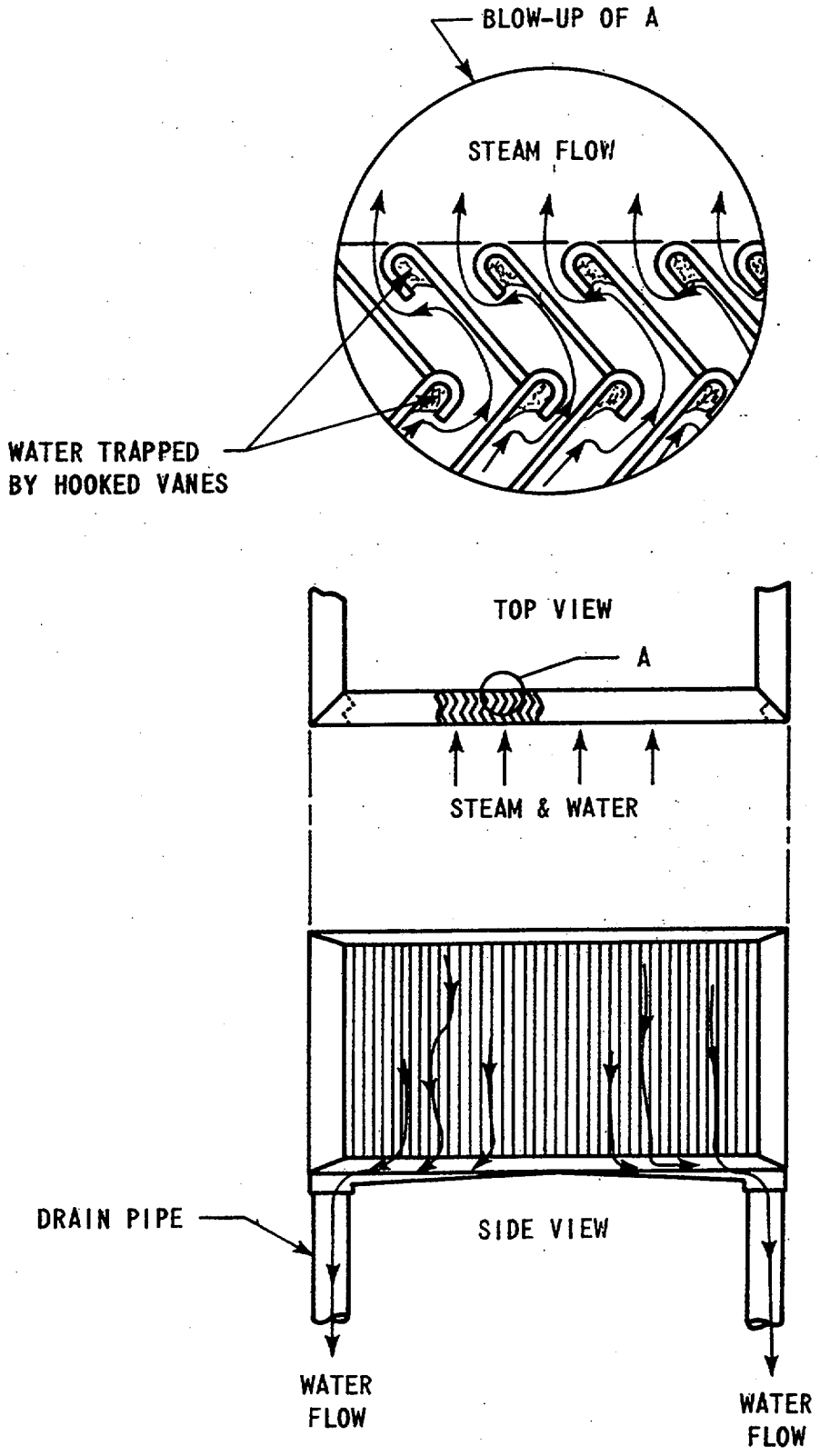

Figure 4.3.2-1 Chevron Separator Schematic Model

5.0 CODE VERIFICATION

5.1 SMALL VESSEL BLOWDOWNS

For the purpose of verifying the adequacy of TRANFLØ for calculating blowdown results, the code has been used to predict the pressure and mass flow time transients for a number of experimental small vessel blowdowns. Included are experiment B53B done at Battelle Northwest [10], experiments 7, 12, and 14 done at Frankfurt/Main [11], and several blowdowns from the series conducted by CISE as part of the CIRENE-3 program [10][11]. A discussion of these comparisons follows.

5.1.1 FRANKFURT/MAIN TEST 7

The test vessel and the computer model used are shown in Figures 5.1.1-1 and 5.1.1-2.

At the beginning of test number 7, the vessel is approximately half full of water. The break location is at approximately 23.75 feet elevation and thus is initially located in the steam space. The diameter of the break is 5.71 inches.

Comparisons between measured and predicted results using a Moody discharge coefficient (C_D) of 0.60 are shown in Figures 5.1.1-3 through 5.1.1-6. The comparisons show good agreement until the pressure is low enough for the subcooled water at the bottom of the vessel to start flashing. It is believed at this time that the heater bundle and supports act as inherent separators keeping the steam quality high at the break location and therefore the critical flow rate low. The support structure is not defined in the published literature and therefore any separation which may occur could not be included in the computer model. The resultant lower quality calculated at the break location would produce the higher mass flow rate seen in Figure 5.1.1-3. Figure 5.1.1-4

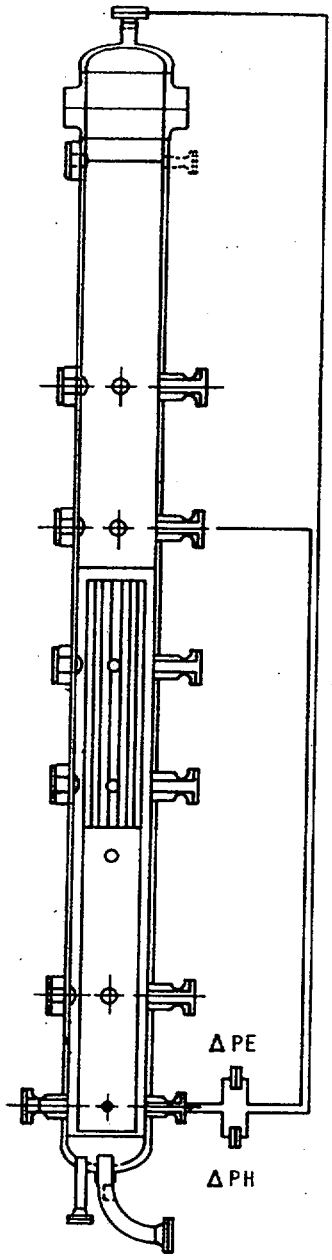

Figure 5.1.1-1 Frankfurt/Main Test Vessel Schematic

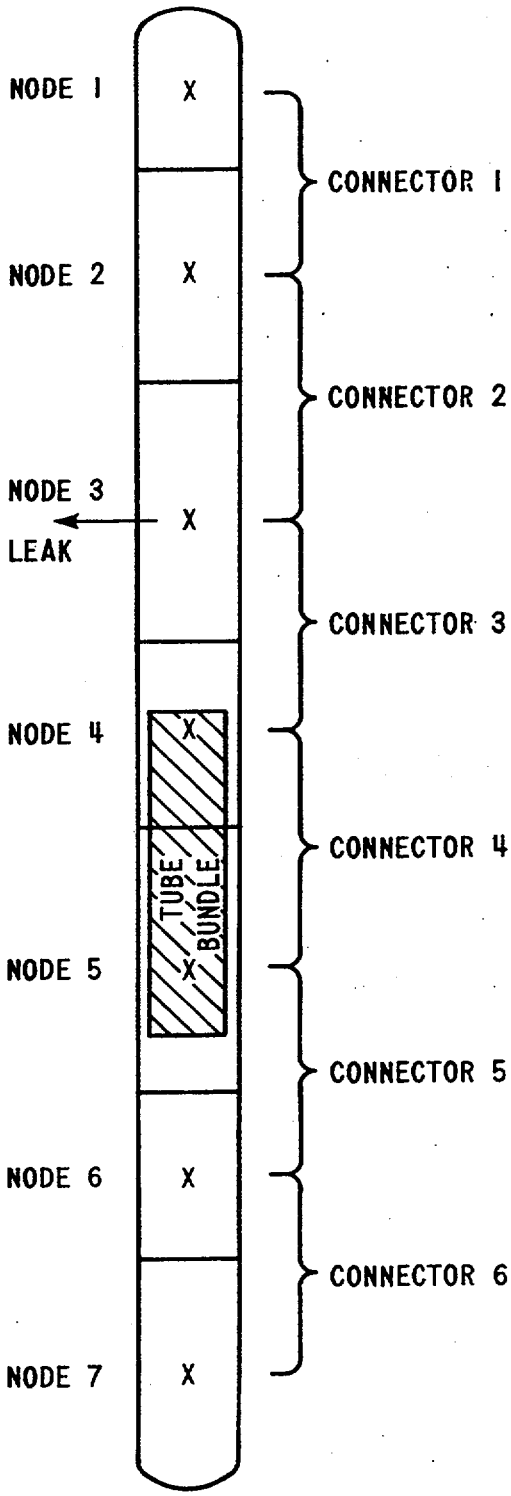

Figure 5.1.1-2 Computer Model Used for Frankfurt/Main Test Calculation

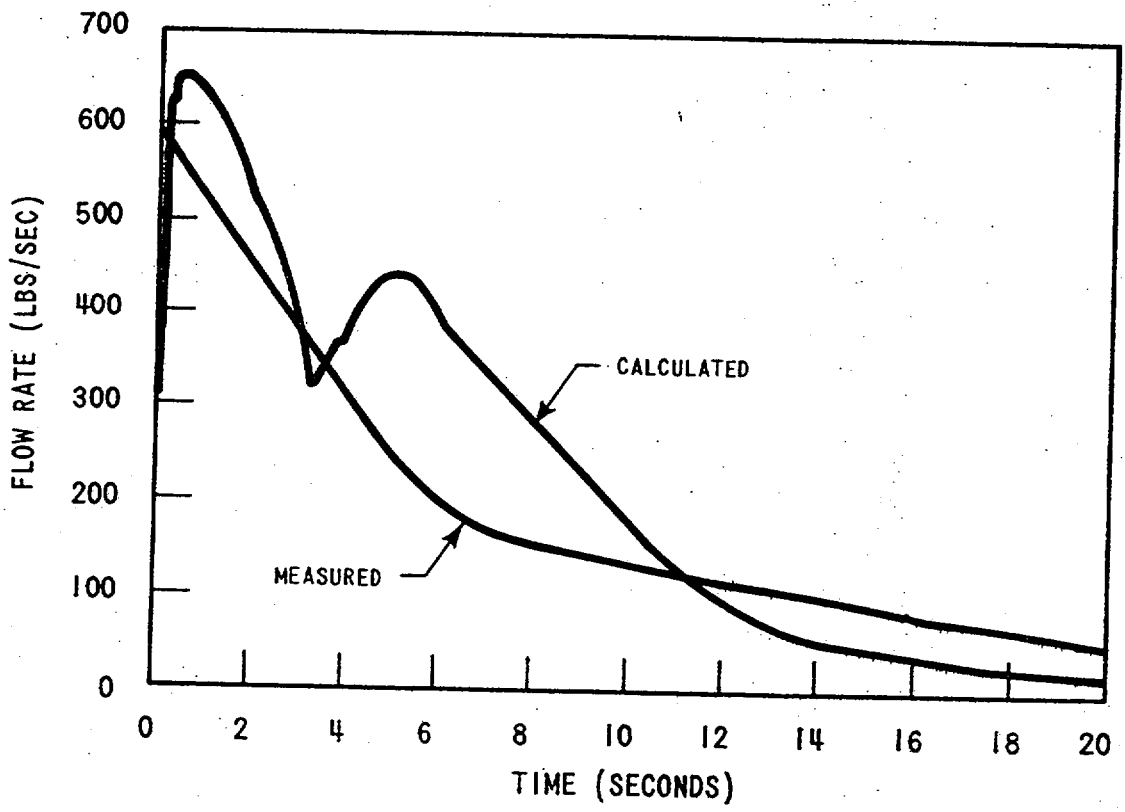

Figure 5.1.1-3 Comparison of Calculated and Measured Flow Rate for Frankfurt Test 7

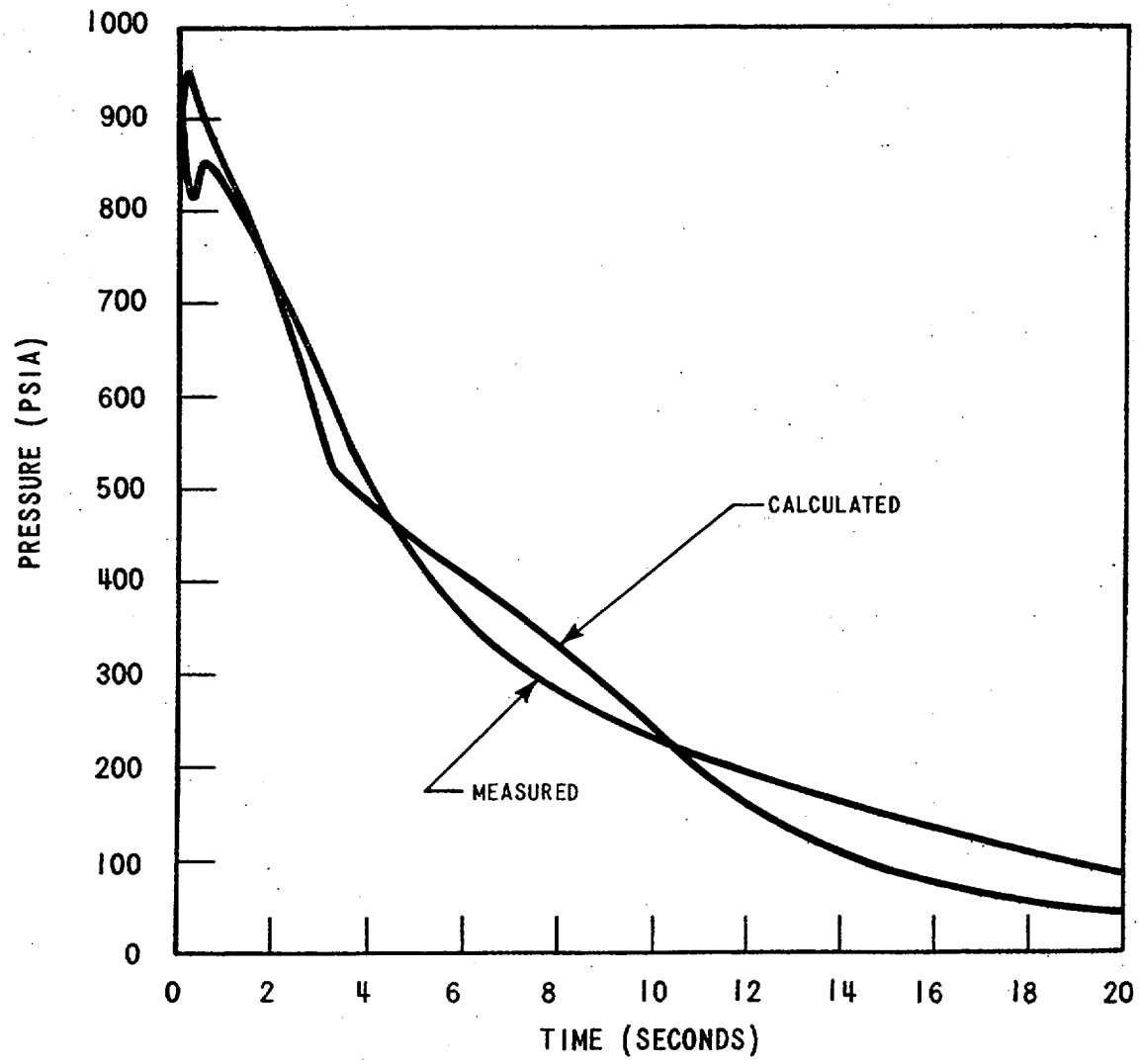

Figure 5.1.1-4 Comparison of Calculated and Measured Pressure for Frankfurt Test 7

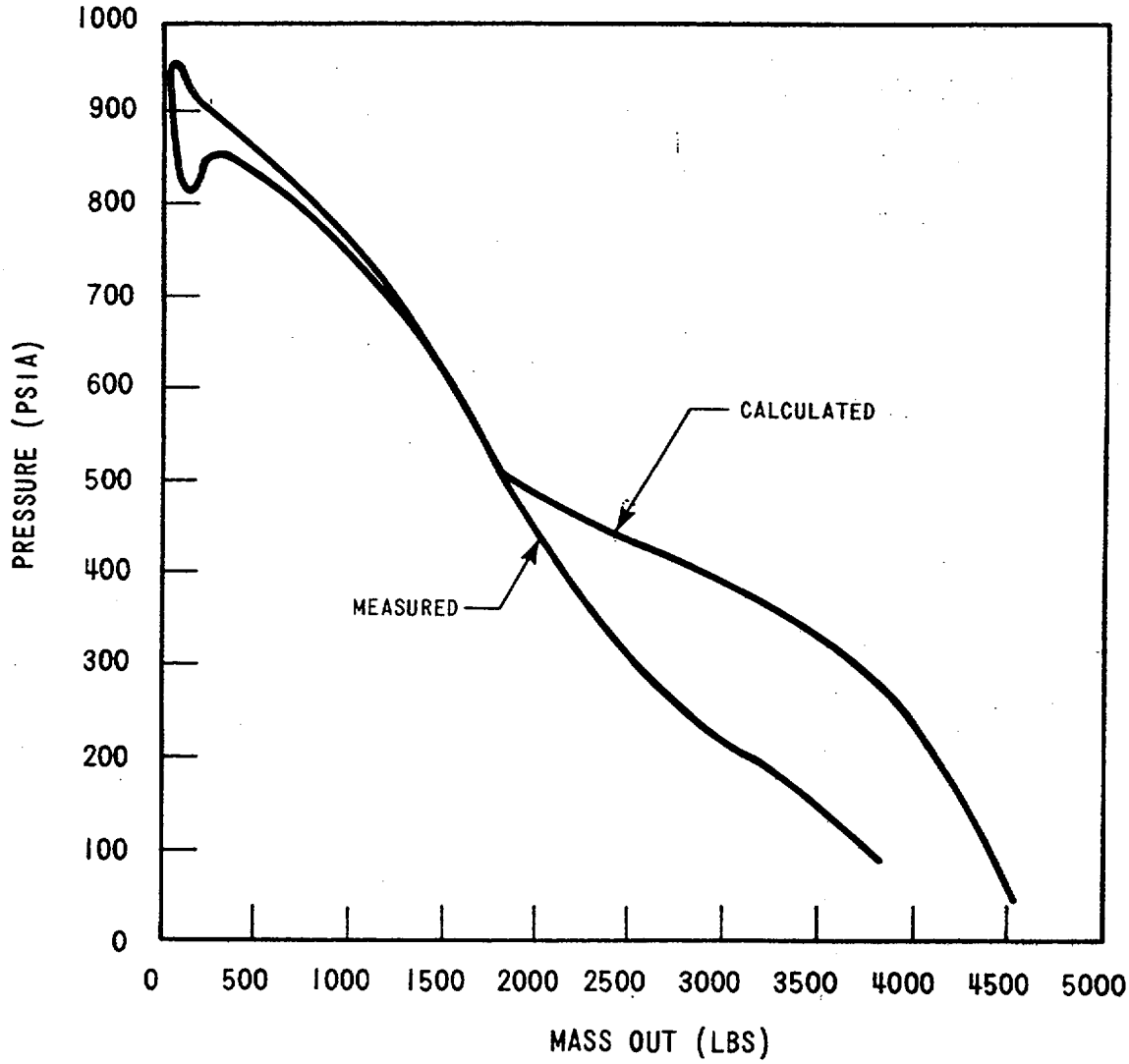

Figure 5.1.1-5 Comparison of Calculated and Measured Pressure Vs. Mass for Frankfurt Test 7

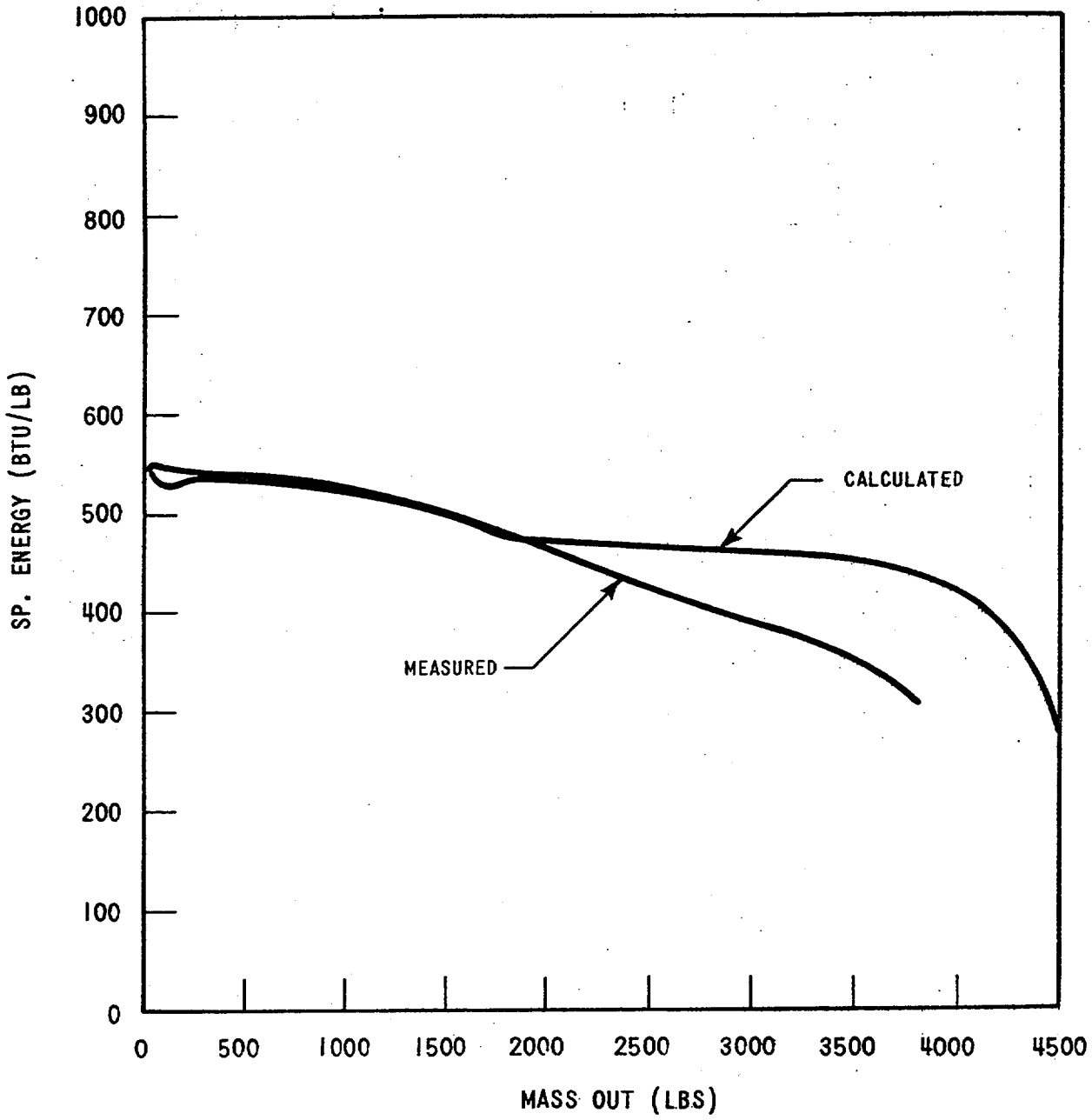

Figure 5.1.1-6 Comparison of Calculated and Measured Energy Vs Mass for for Frankfurt Test 7

shows the comparison between measured and calculated pressure as a function of time, and Figures 5.1.1-5 and 5.1.1-6 show the quantitative comparisons of pressure and specific energy of the fluid remaining in the tank as a function of the mass having left the vessel. The last two figures provide an indication of how well the code predicts the energy removal by the blowdown. Again the variances between measured and calculated results, beginning at a mass of about 1700 lb_m on Figure 5.1.1-6, indicates some separation occurs in the heater bundle which is not accounted for by the computer model. This can be verified by comparing Figures 5.1.1-3 and 5.1.1-6 and noting that the point of variation of the mass flow rates corresponds to the point at which the specific energy results begin to deviate from each other.

5.1.2 FRANKFURT/MAIN TEST 12

The computer model used for test 12 is the same as used in test 7. However the initial water level in this test is above the break location such that the quality of the break flow is very low during the initial portion of the transient. The break diameter, at 5.5 inches, is slightly smaller than test 7. Calculated and measured results are compared in Figures 5.1.2-1 through 5.1.2-4 which show very good agreement throughout the transient. The discharge coefficient is 0.60.

5.1.3 FRANKFURT/MAIN TEST 14

Again the same computer model is used but a much smaller break diameter (1.97 inches) is simulated. The test vessel in this case is almost completely filled with water. Comparison of results (C_D=0.65) are given by Figures 5.1.3-1 through 5.1.3-4.

Throughout almost this entire transient TRANFLØ predicts the occurrence of natural separation in the vertical flows. Also, it was found that the pressure versus the mass remaining in the vessel was sensitive to

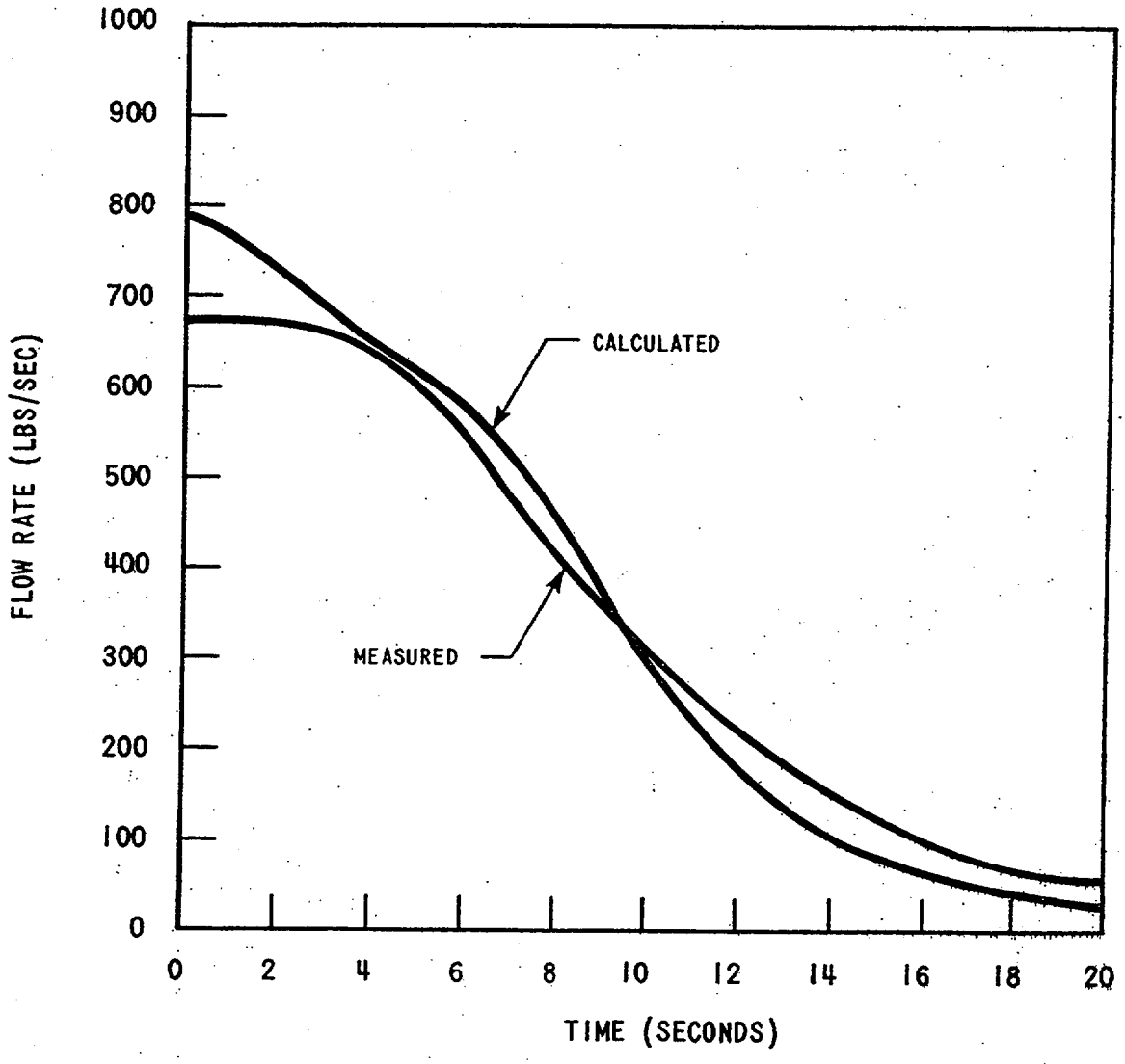

Figure 5.1.2-1 Comparison of Calculated and Measured Flow Rate for Frankfurt Test 12

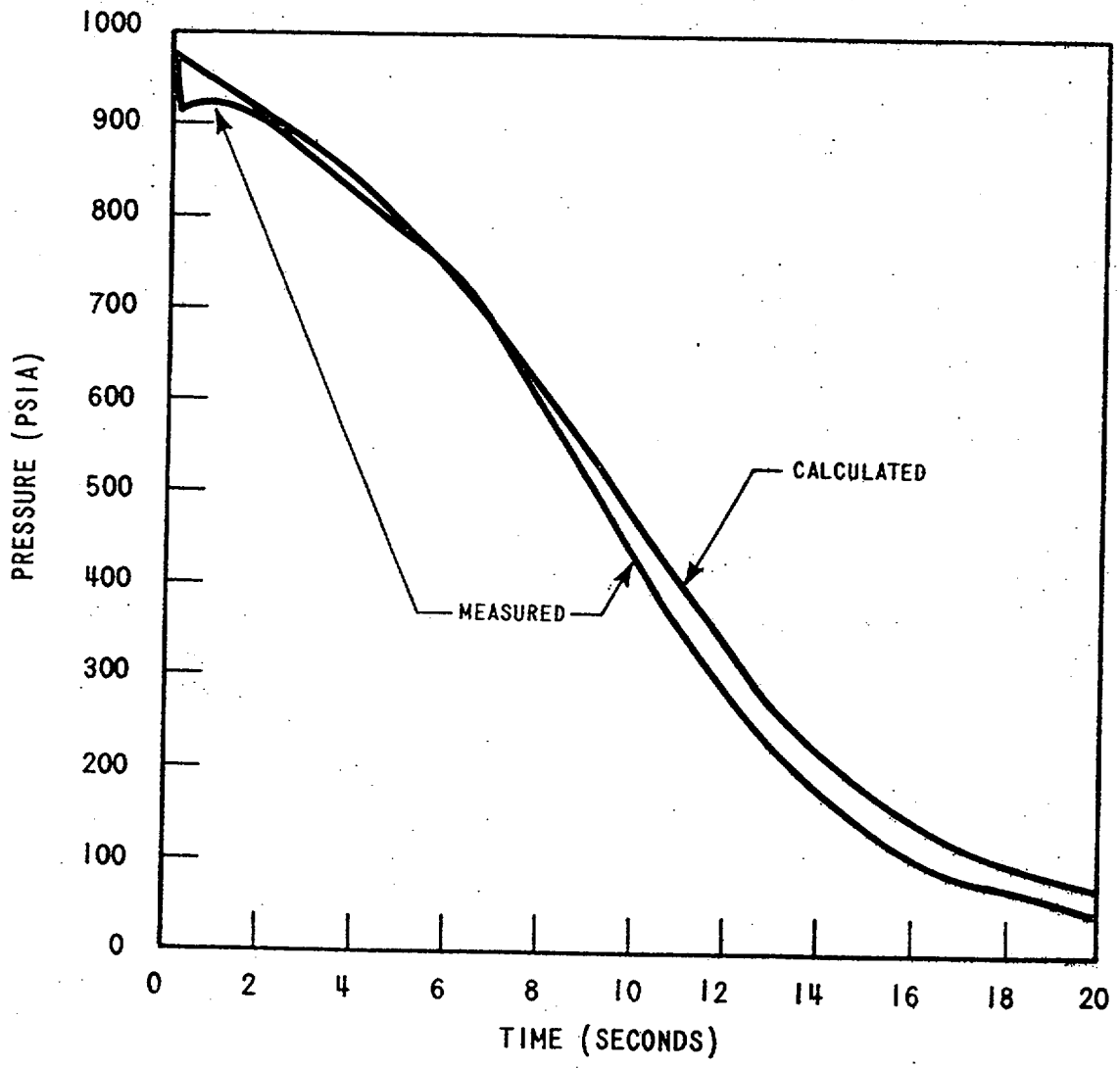

Figure 5.1.2-2 Comparison of Calculated and Measured Pressure for Frankfurt Test 12

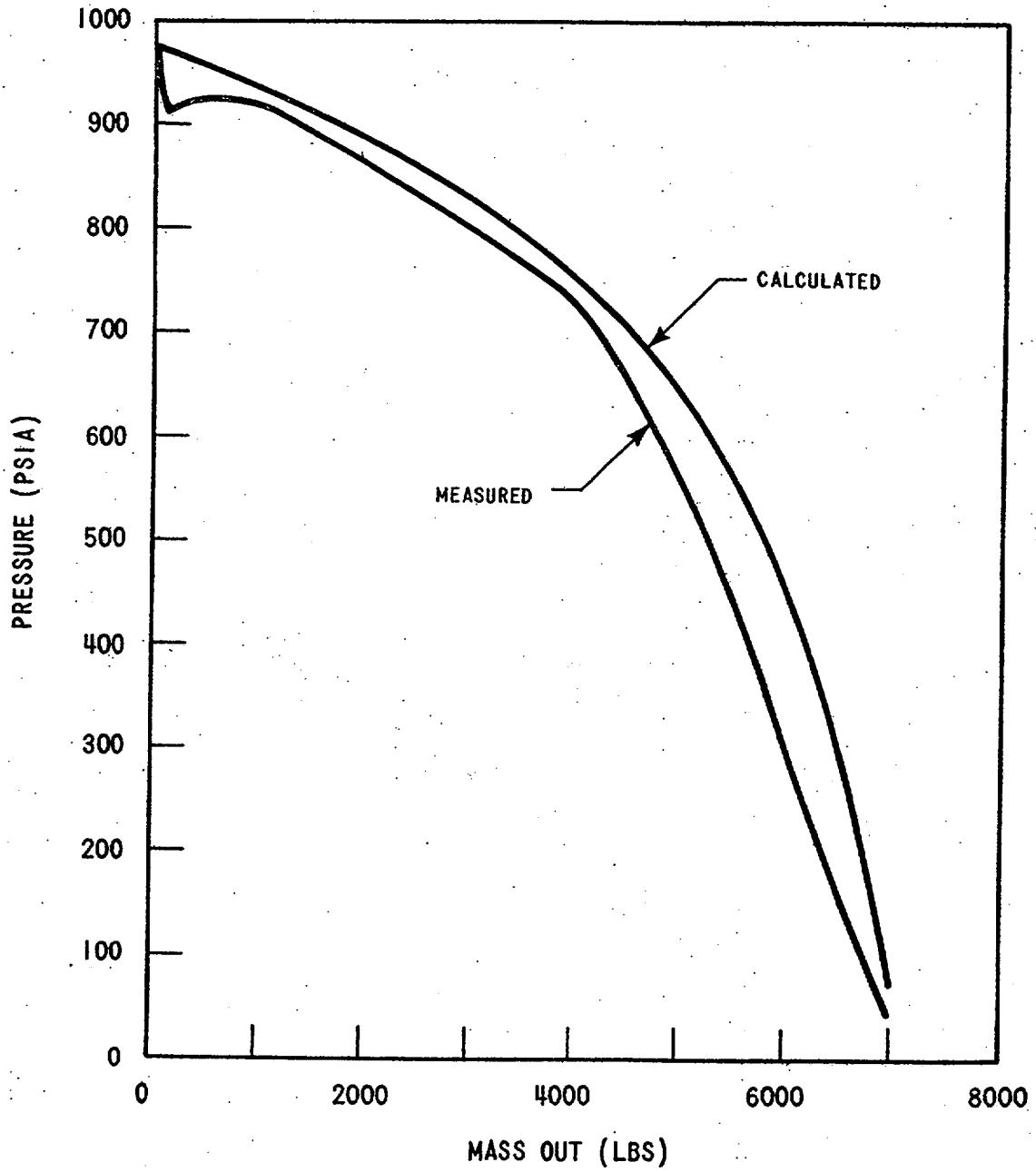

Figure 5.1.2-3 Comparison of Calculated and Measured Pressure Vs. Mass for Frankfurt Test 12

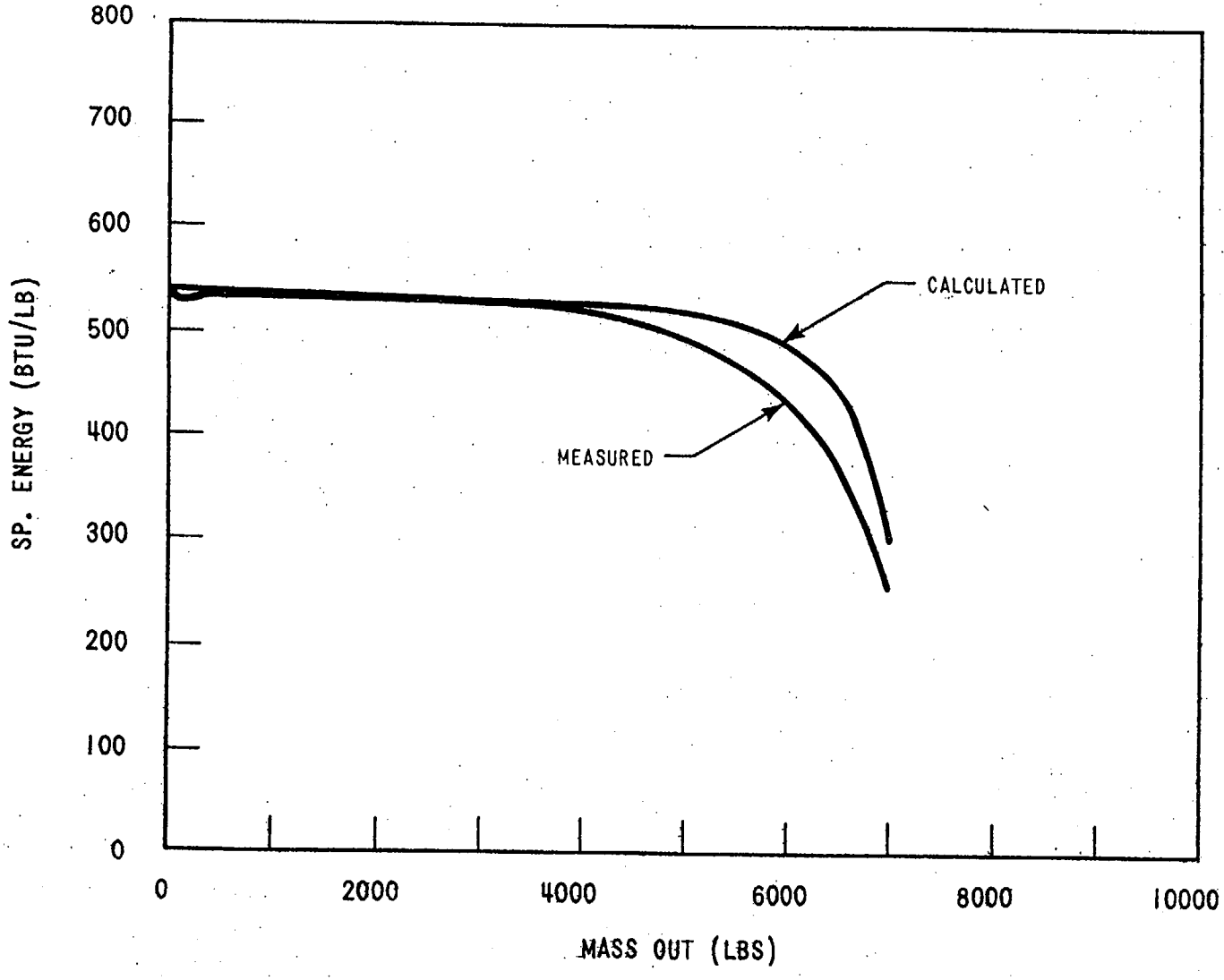

Figure 5.1.2-4 Comparison of Calculated and Measured Energy Vs. Mass for Frankfurt Test 12

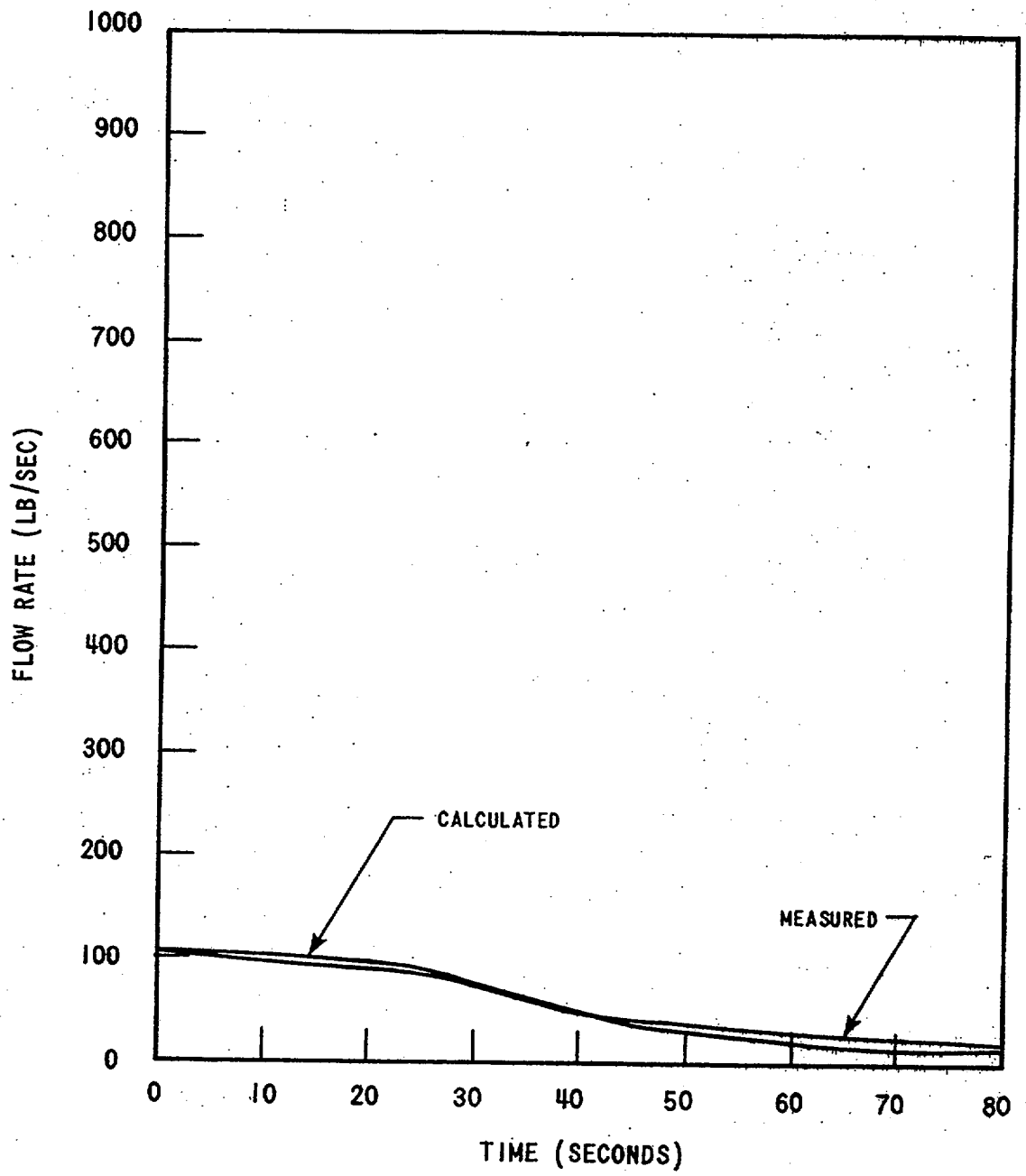

Figure 5.1.3-1 Comparison of Calculated and Measured Flow Rate for Frankfurt Test 14

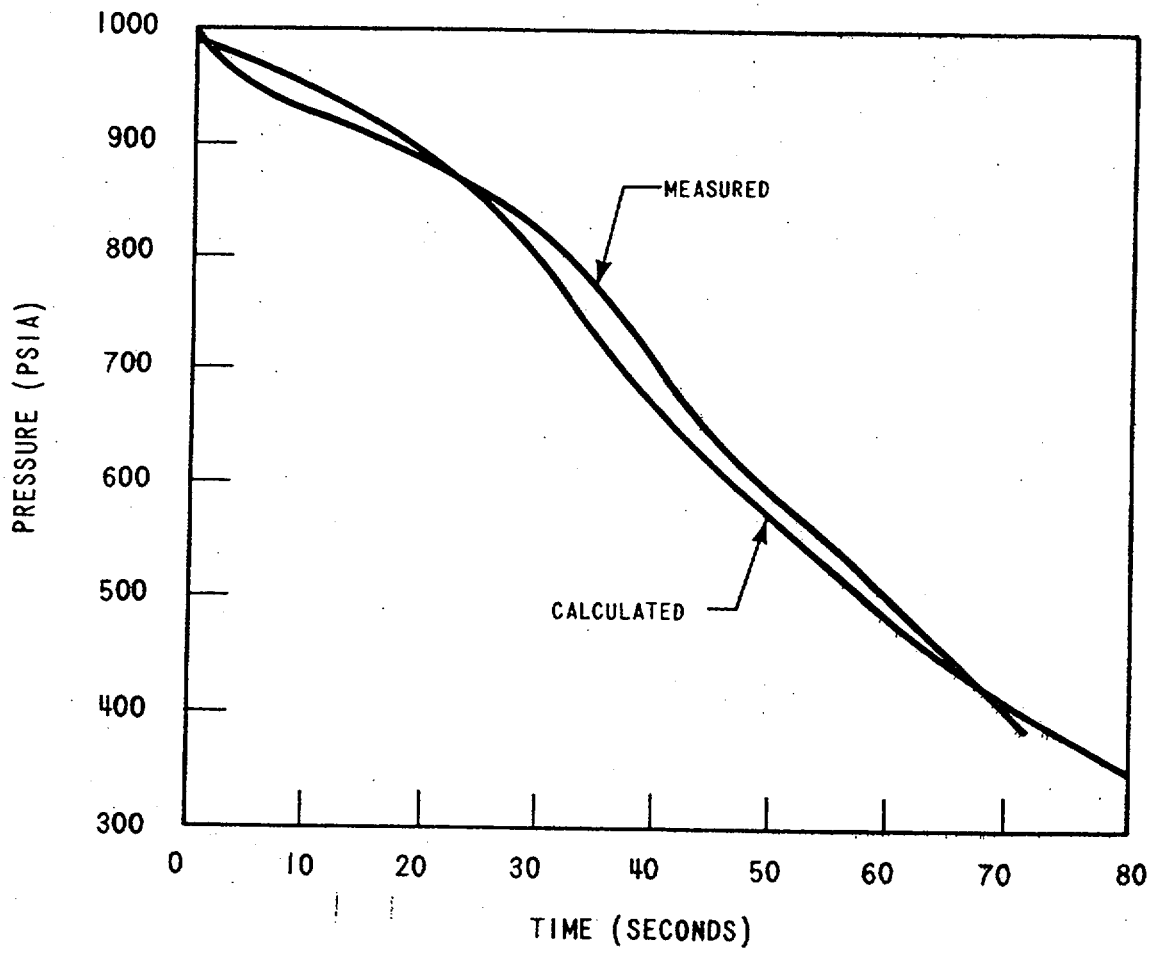

Figure 5.1.3-2 Comparison of Calculated and Measured Pressure for Frankfurt Test 14

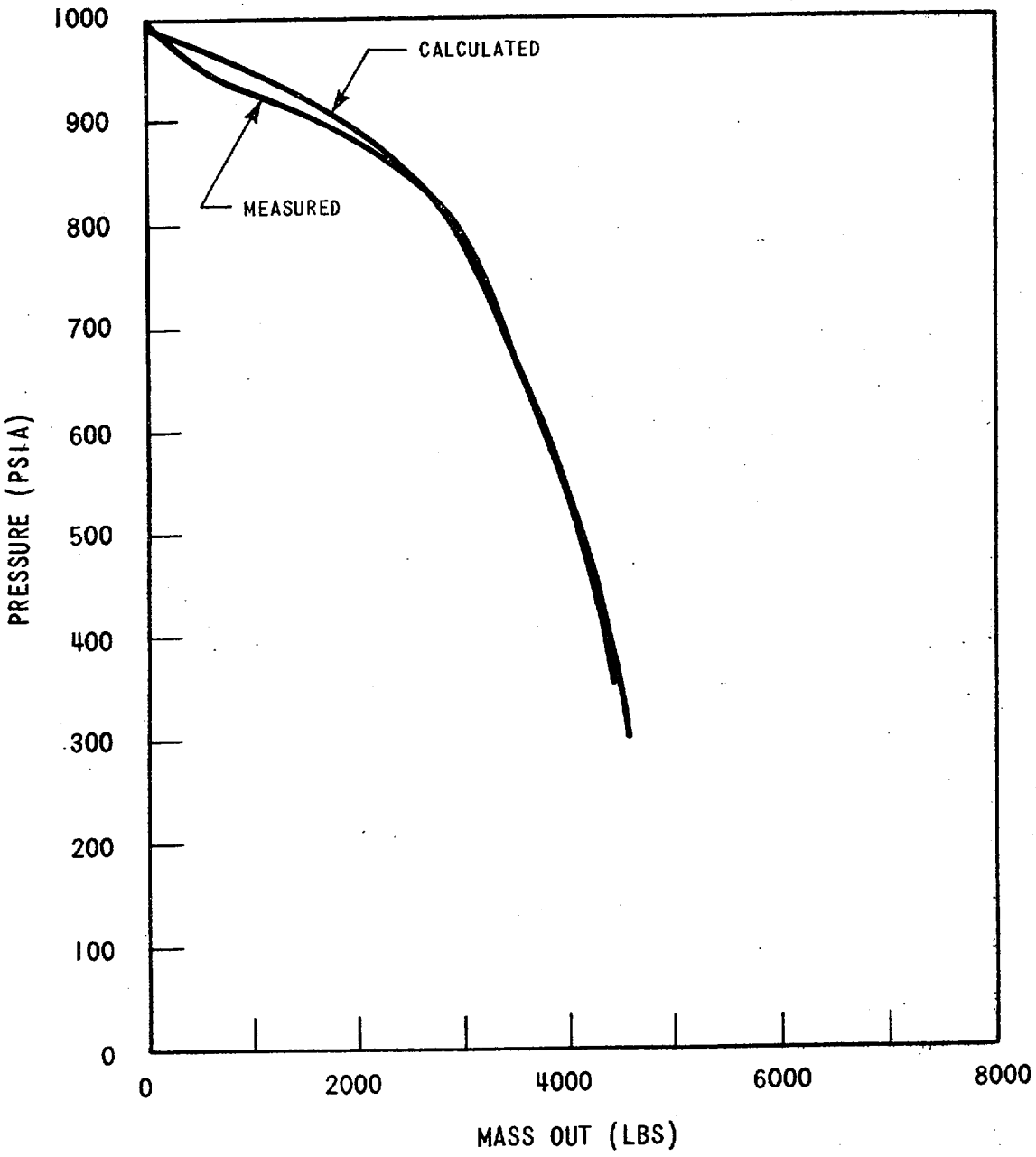

Figure 5.1.3-3 Comparison of Calculated and Measured Pressure Vs. Mass for Frankfurt Test 14

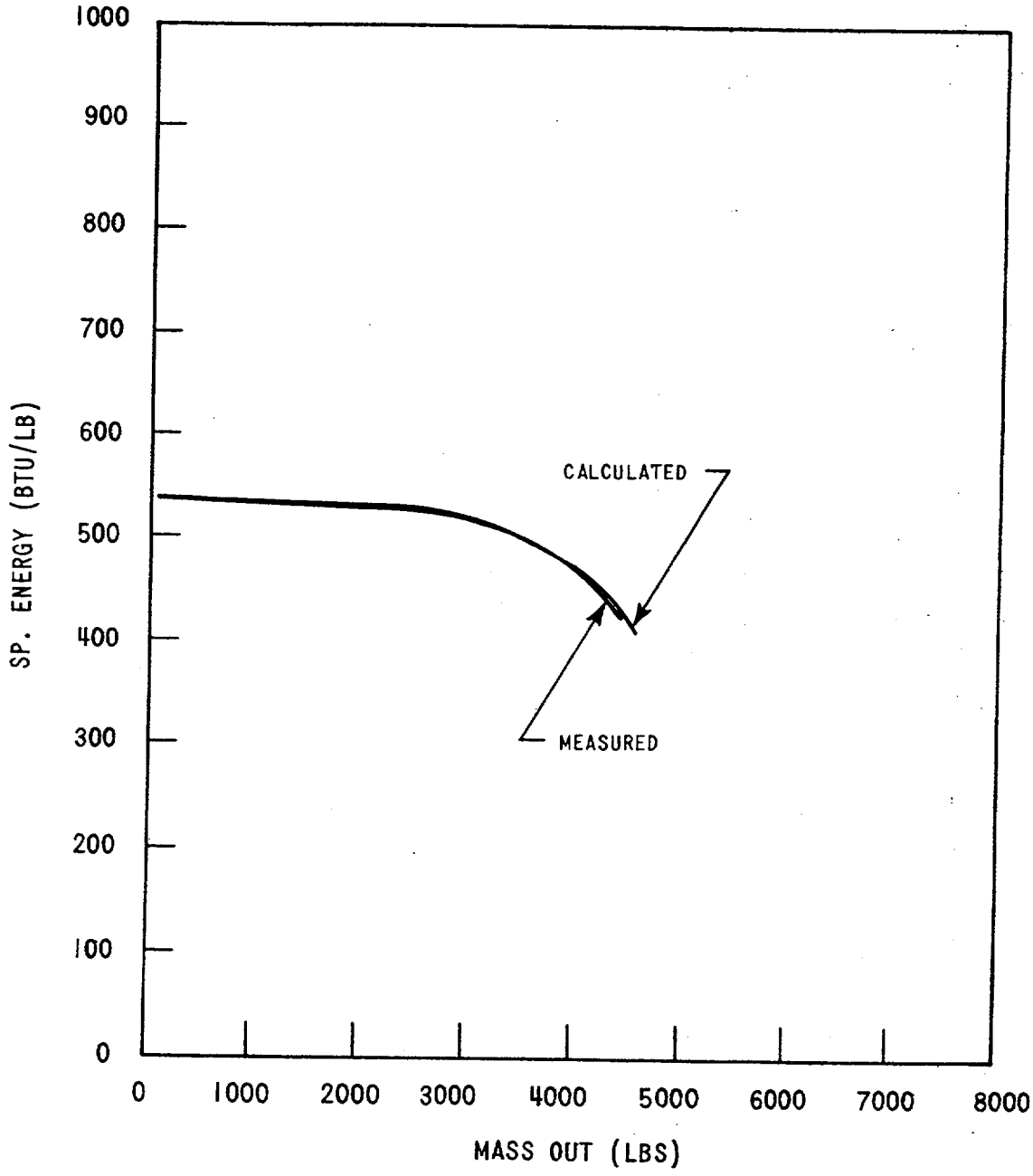

Figure 5.1.3-4 Comparison of Calculated and Measured Energy Vs. Mass for Frankfurt Test 14

any changes in the natural separation model. In this particular test the steam superficial velocities in the lower region of the hot vessel were found to be of the magnitude of the Davis critical velocity from approximately 2 seconds into the transient until the transient was terminated at 100 seconds. The value of superficial steam velocity at which the transition from using flowing quality predicted by Armand to a corrected value of quality accounting for some partial fall back due to gravity was found to have significant impact on the comparisons shown in Figures 5.1.3-3 and 5.1.3-4. Thus several cases were run in which the point of transition was changed. A value of 180% for the multiplier on the Davis critical velocity, as described in Section 3.5, was chosen because it resulted in good agreement to the test data. All other blowdown predictions were made using this same separation model.

5.1.4 BATTELLE NORTHWEST TEST B53B

The test vessel and computer model used for prediction of the Battelle tests are shown in Figure 5.1.4-1. Experimental results for this test did not include the mass flow rate but did indicate the water level in the vessel during the blowdown. The TRANFLØ code does not directly predict a level but a calculated water level was determined by collapsing all the water in that nodal volume where the transition from water to steam occurs. The comparison of this level with the test results are shown in Figure 5.1.4-2. Because of the longer entrance length to the nozzle, a C_D=0.80 is used. Initially the predicted level is too low due to the assumption that all liquid is at the bottom of the node. Later, as the transient situation stabilizes, the level prediction shows good agreement with the measured result. It is possible that the initial difference in level is an indication of frothing occurring at the steam/water interface which the code does not predict. Favorable comparisons between the mass and pressure transients were obtained as shown

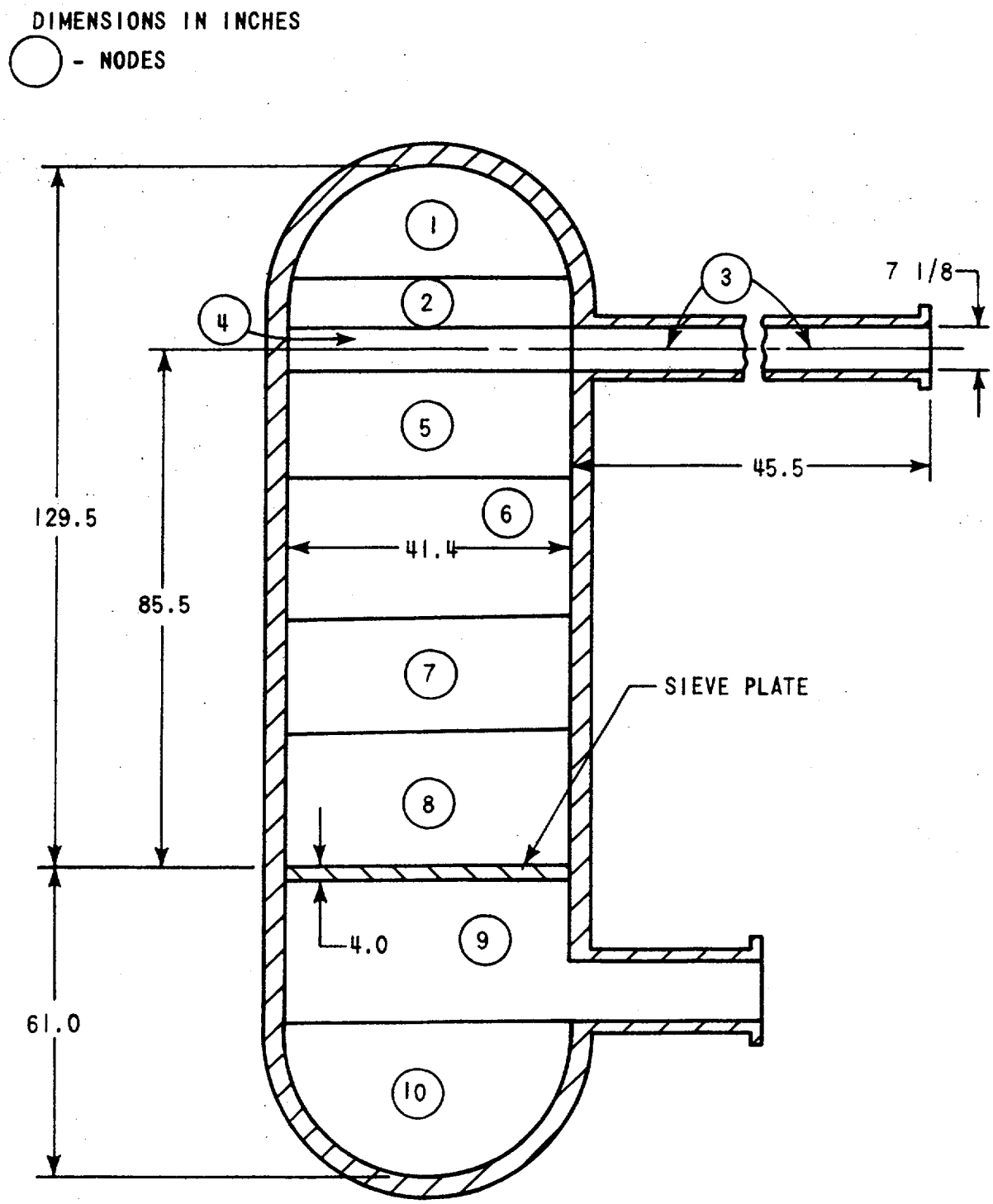

Figure 5.1.4-1 Battelle B53B Test Vessel Schematic

in Figures 5.1.4-3 and 5.1.4-4. It is important to note that natural separation also has significant impact on this transient as in the Frankfurt/Main Test 12. It is felt that the close predictions of pressure and remaining mass are further justification for the separation model described in Section 3.6.

5.1.5 CISE TESTS

The CISE experimental test work was carried out using a 3 m^3 test vessel at the Betulla plant of C.C.R. Euratom at Ispra. A total of sixteen different blowdown tests were conducted using three different break locations, two initial conditions, and five different break diameters. A tabulation of the tests and the test procedures are provided in Reference 12. A selection of several of these tests have been modeled using TRANFLØ. The actual test vessel and the code model are shown in Figures 5.1.5-1 and 5.1.5-2.

5.1.5.1 CISE Test 1

Test Case 1 is a blowdown from the upper nozzle shown in Figure 5.1.5-1. The initial pressure is 51 kg/cm^2 (725 psia) and the initial water level is approximately 248 cm (8.14 ft) below the nozzle. The blowdown orifice is 5 inches in diameter.

Figures 5.1.5.1-1 and 5.1.5.1-2 show comparisons between predicted and experimental results for vessel pressure and mass remaining in the test vessel using a C_D=0.55. The excellent agreement between the two again indicates the adequacy of the gravity separation model for upward vertical flows.

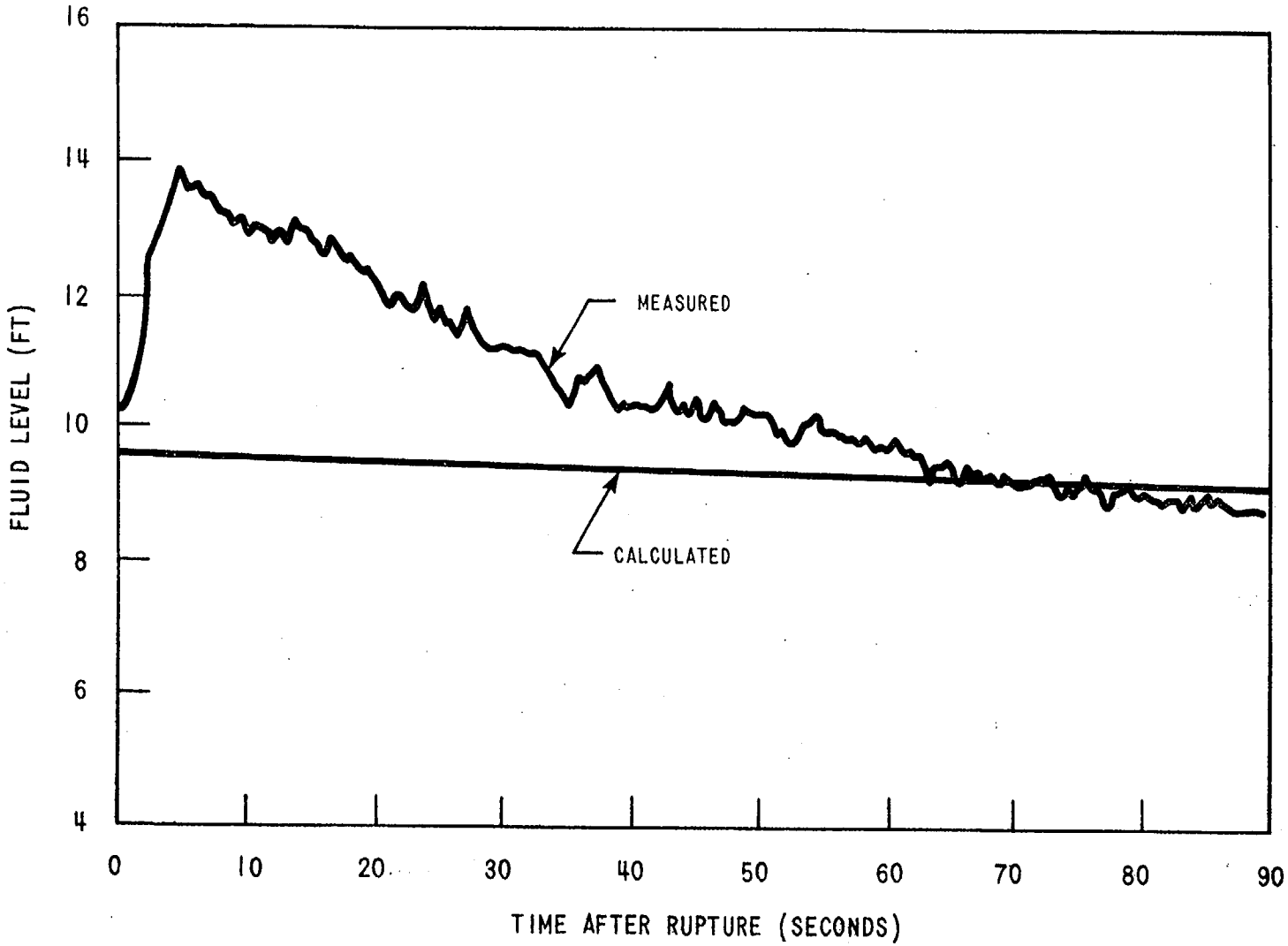

Figure 5.1.4-2 Liquid Level of Fluid Remaining in Vessel, Battelle Test B53B

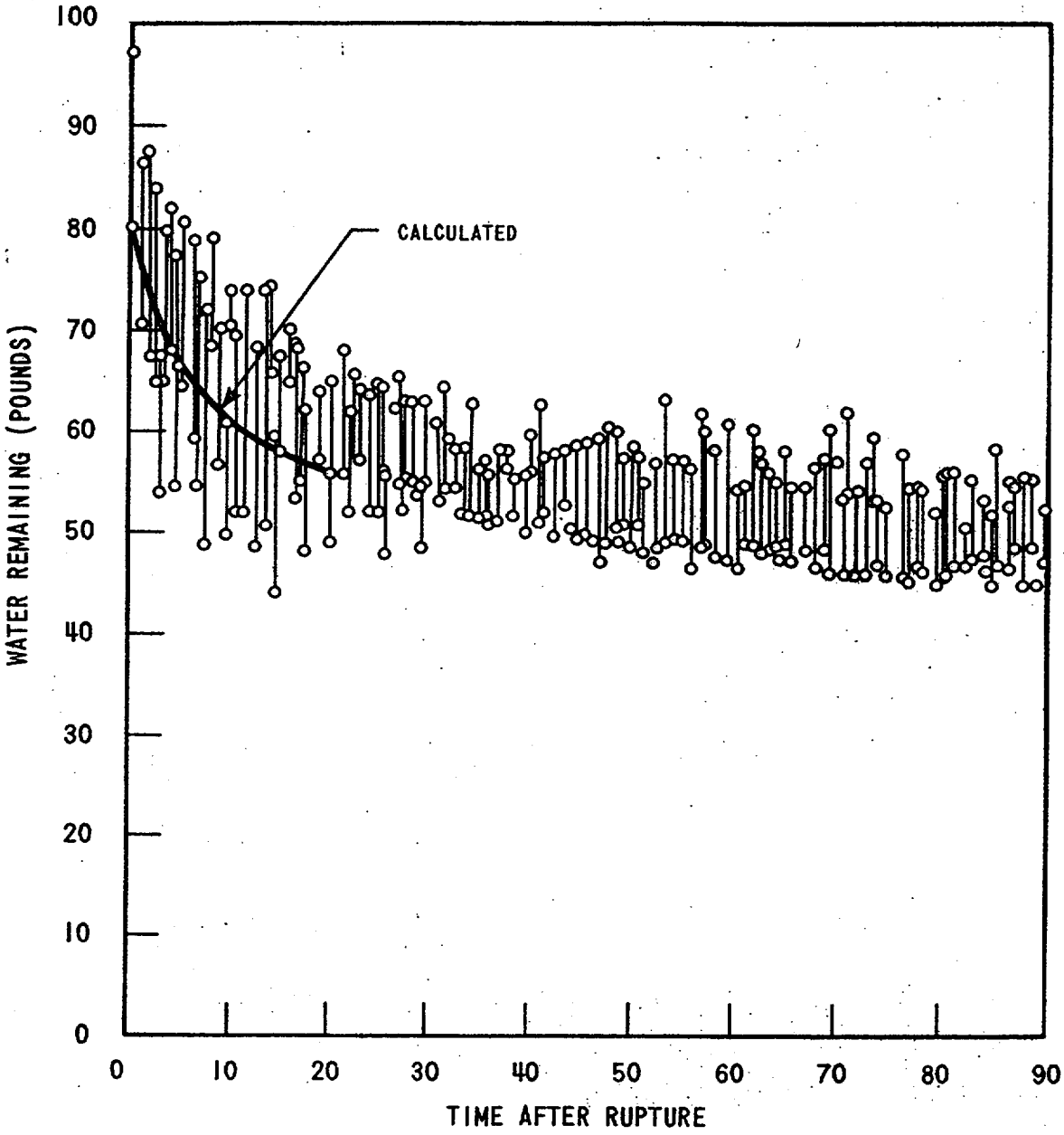

Figure 5.1.4-3 Weight of Water in Vessel as Function of Time for Battelle Test B53B

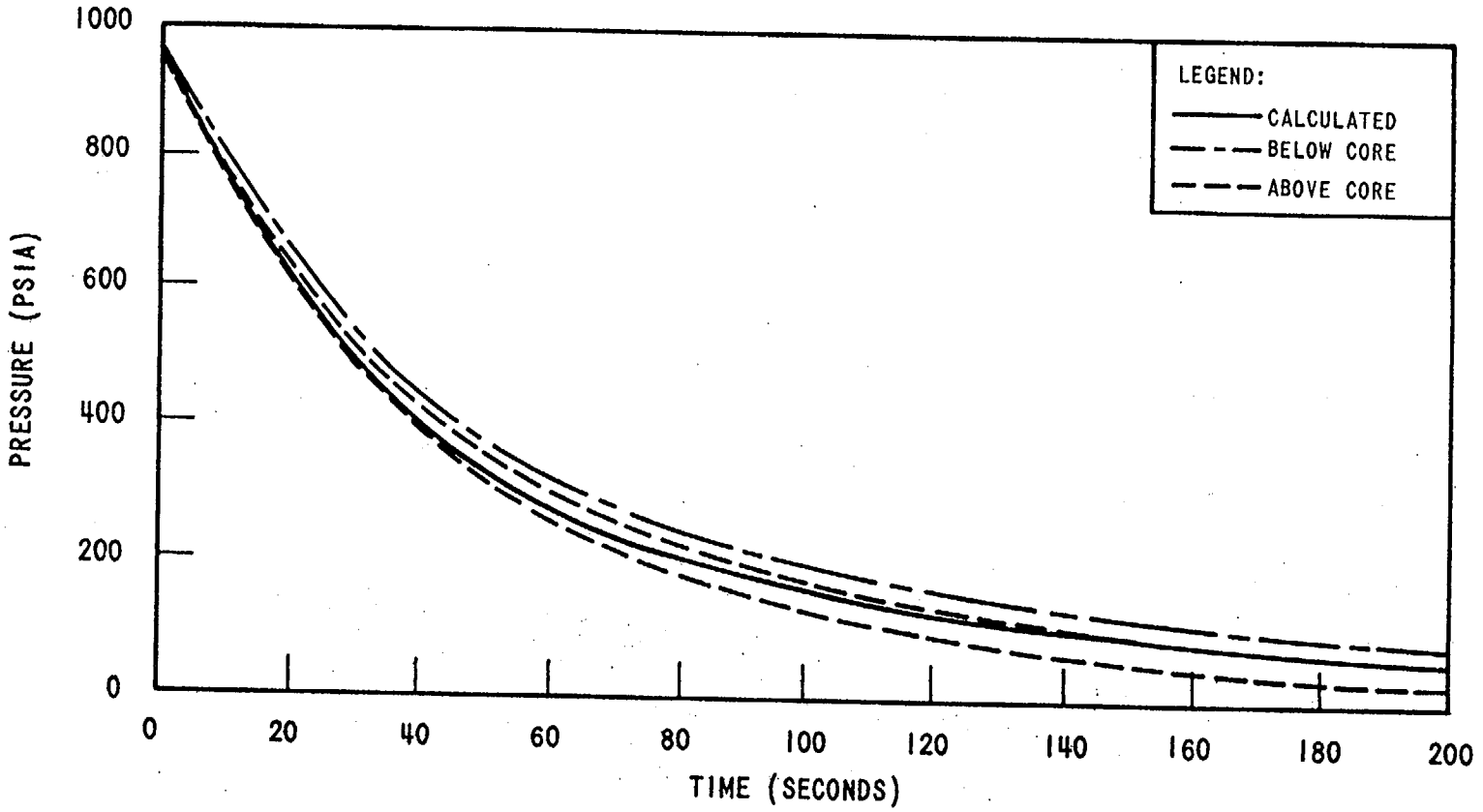

Figure 5.1.4-4 Comparison of Calculated and Measured Pressure for Battelle Test B53B

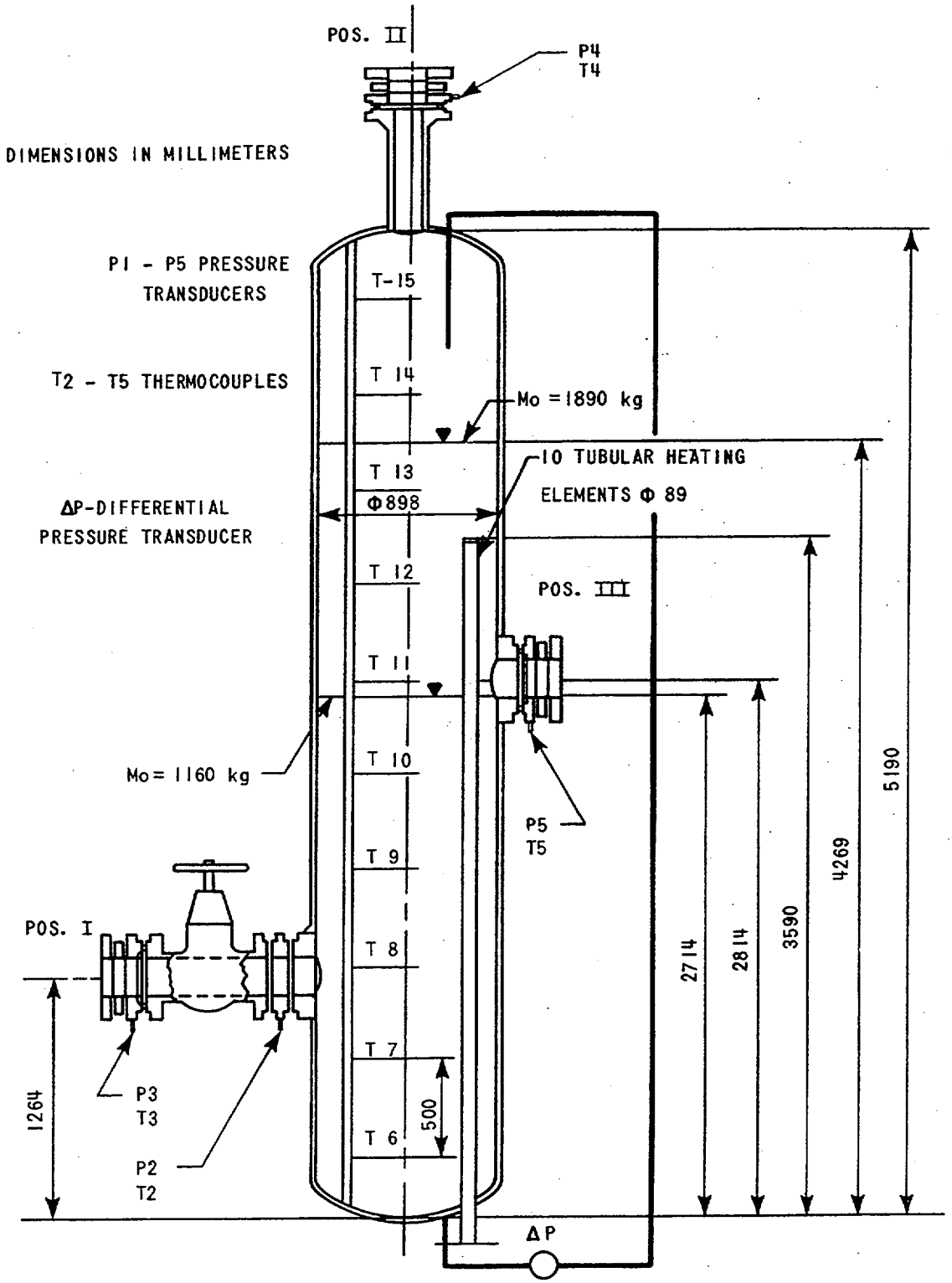

Figure 5.1.5-1 CISE Test Vessel Schematic

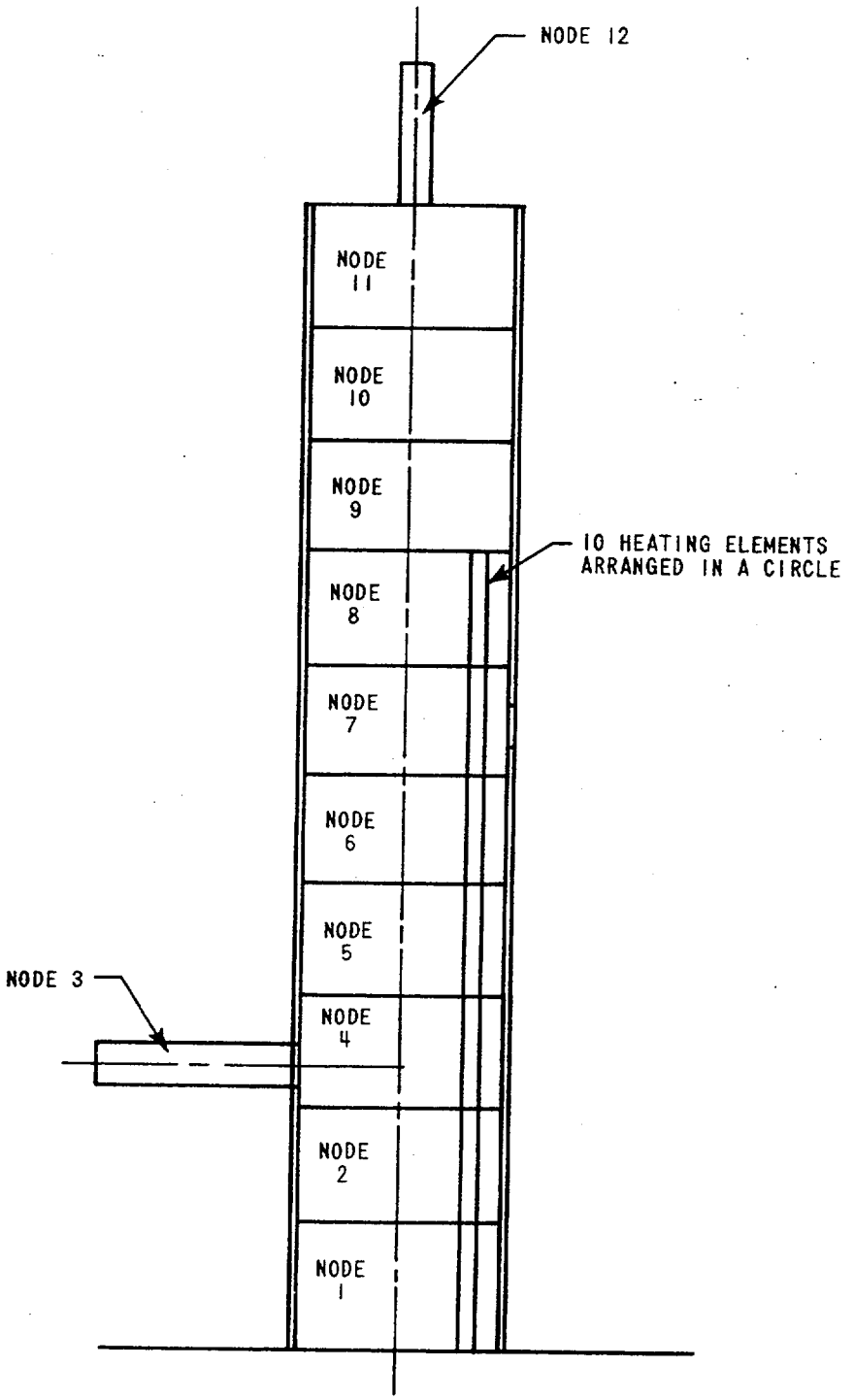

Figure 5.1.5-2a Computer Model Used for CISE Test Calculations

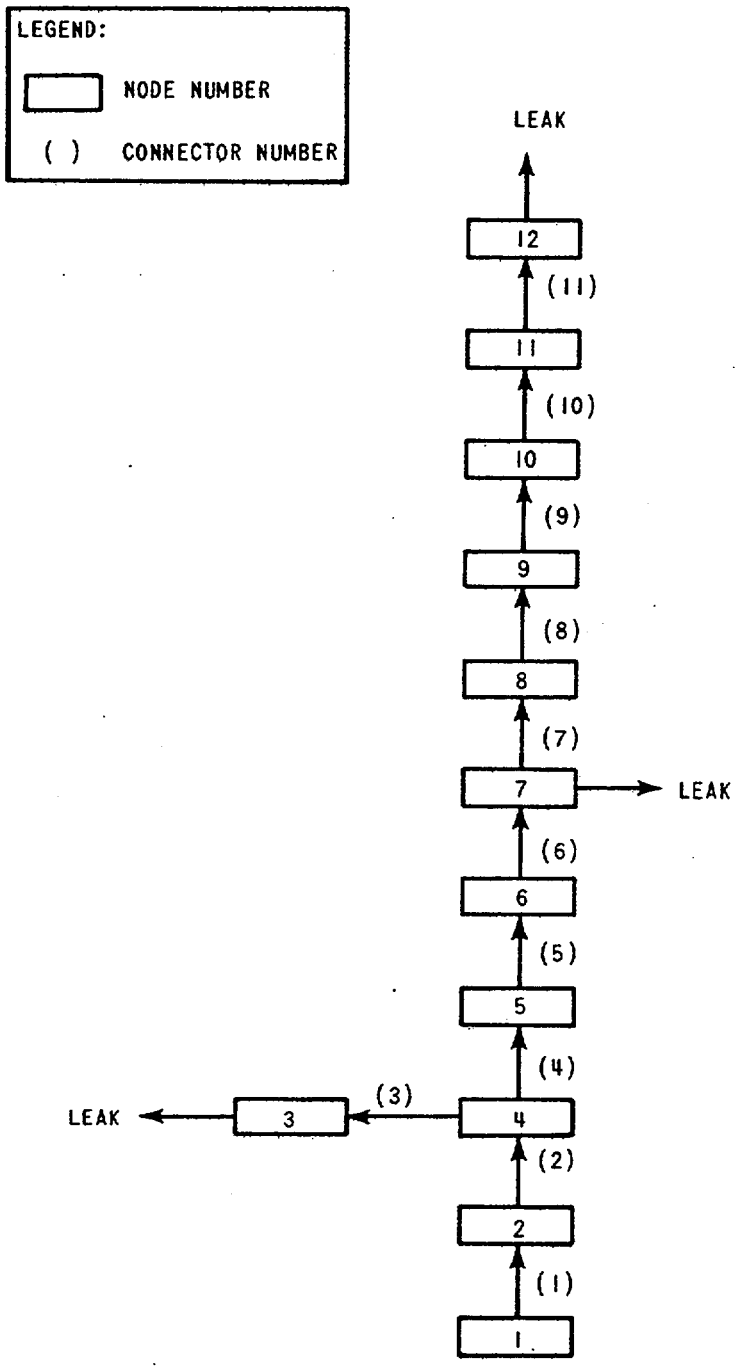

Figure 5.1.5-2b Computer Model Used for CISE Test Calculations

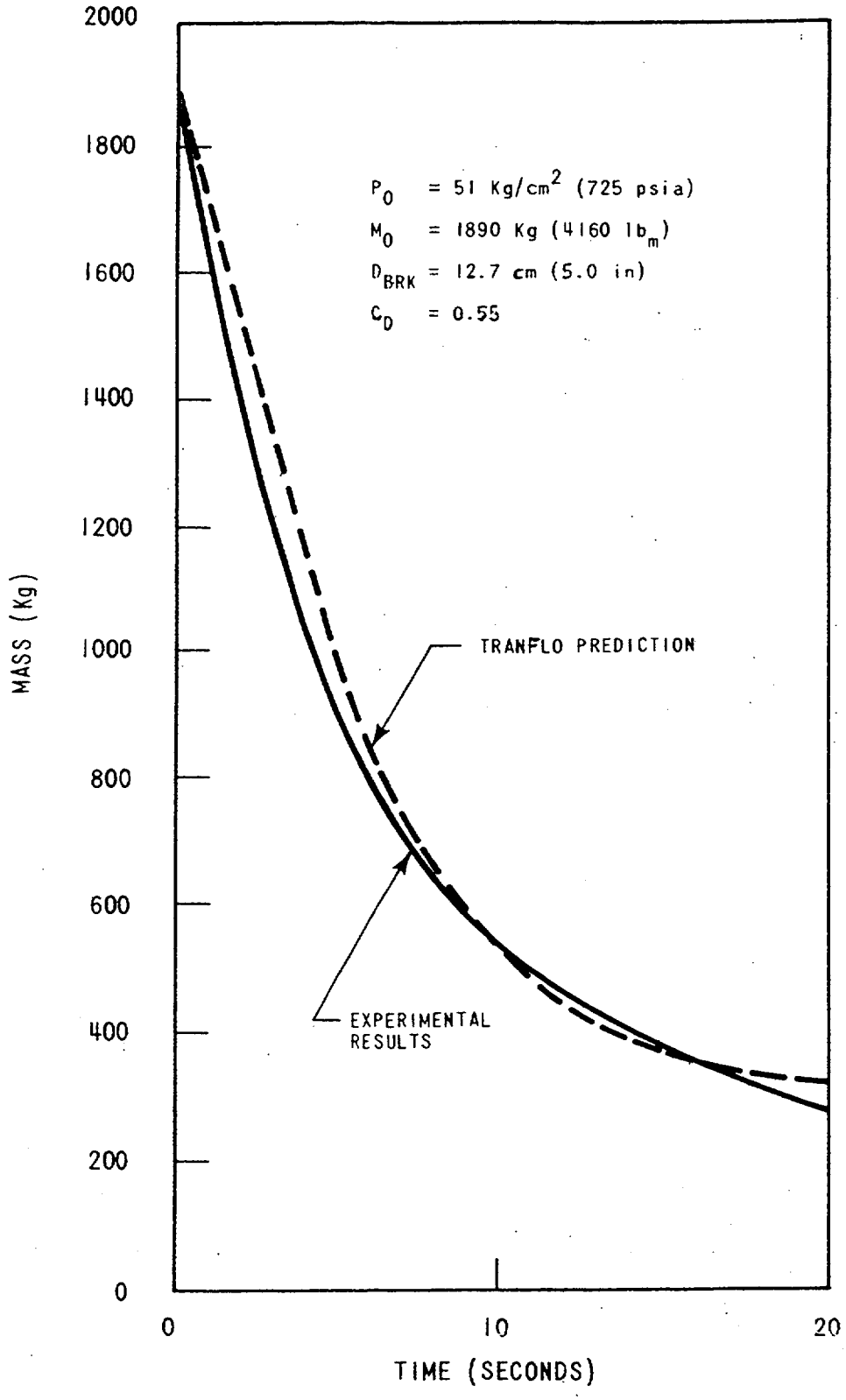

Figure 5.1.5.1-1 CISE Blowdown Test 1 - Mass Vs. Time

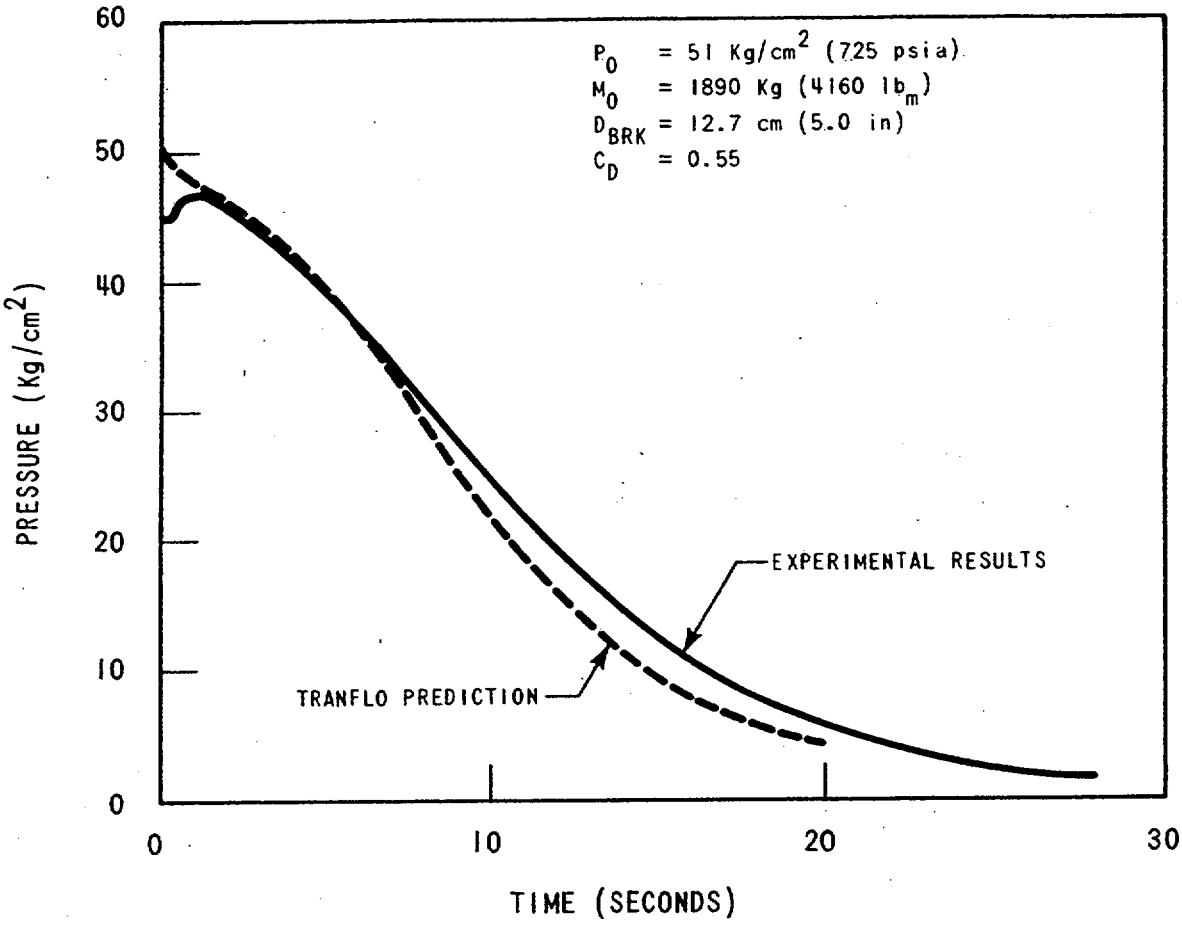

Figure 5.1.5.1-2 CISE Blowdown Test 1 - Pressure Vs. Time

5.1.5.2 CISE Test 2

Test case 2 models a blowdown from the lower nozzle shown in Figure 5.1.5-1 through an orifice 4 inches in diameter. The initial pressure is 51 kg/cm^2 (725 psia) and the water level is approximately 118 cm (3.87 ft) above the nozzle. A C_D of 1.00 was selected due to the long entrance length to the discharge point and the low quality of the flow. Results are shown in Figures 5.1.5.2-1 and 5.1.5.2-2.

As indicated by Figure 5.1.5.2-1, accurate prediction of the vessel mass with time is achieved; to predict the pressure transient TRANFLØ was modified to approximate the counter-current steam and water flow expected to occur in the region above the blowdown nozzle. Changes made to the flow models to approximate this steam/water separation were (1) flows from the upper region of the vessel towards the nozzle were modeled to be essentially all liquid, and (2) the blowdown flowrate was forced to be saturated water. The results of this pressure transient are shown on Figure 5.1.5.2-2.

As the transient shows, the mass remaining is closely predicted with these modifications, and the pressure trend is consistent with the test results.

5.1.5.3 CISE Test 3

A third test was modeled simulating a blowdown from the intermediate level nozzle shown in Figure 5.1.5-1. The initial pressure is 51 kg/cm^2 (725 psia) and the water level is at the lower edge of the nozzle. The diameter of the blowdown orifice is 2 inches. Results using a C_D of 0.85 are shown in Figures 5.1.5.3-1 and 5.1.5.3-2. Again good agreement of the mass and pressure transients were obtained.

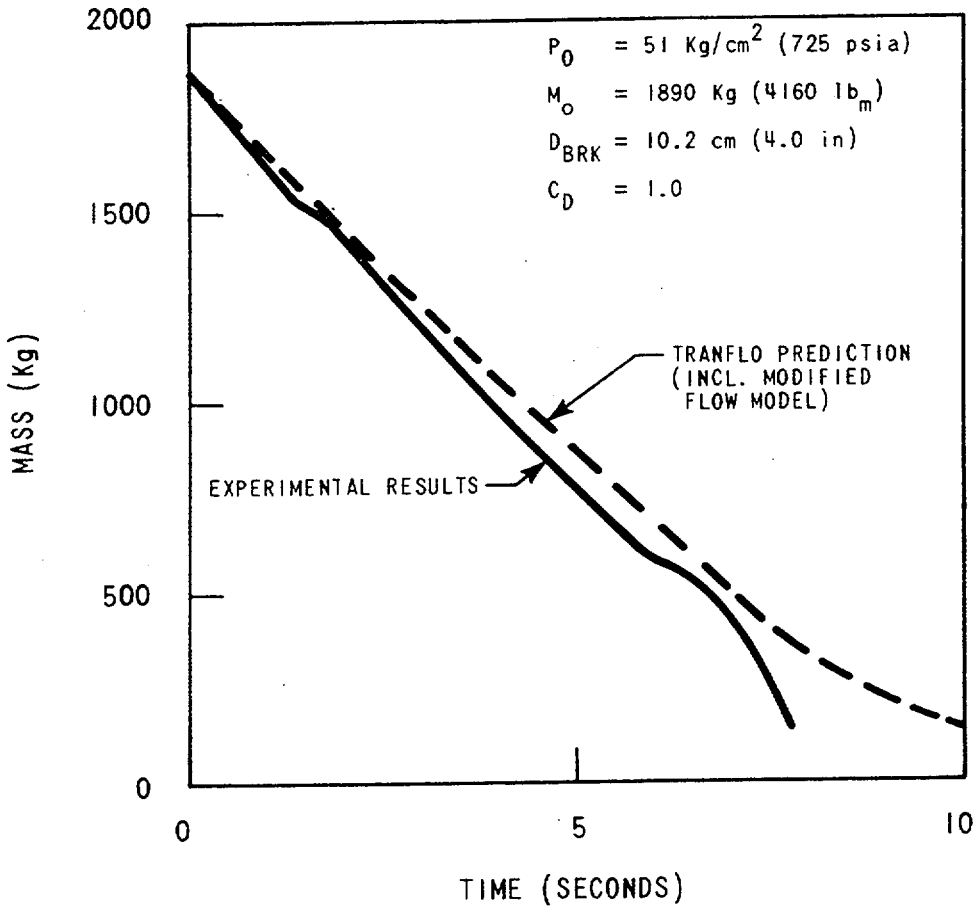

Figure 5.1.5.2-1 CISE Blowdown Test 2 - Mass Vs. Time

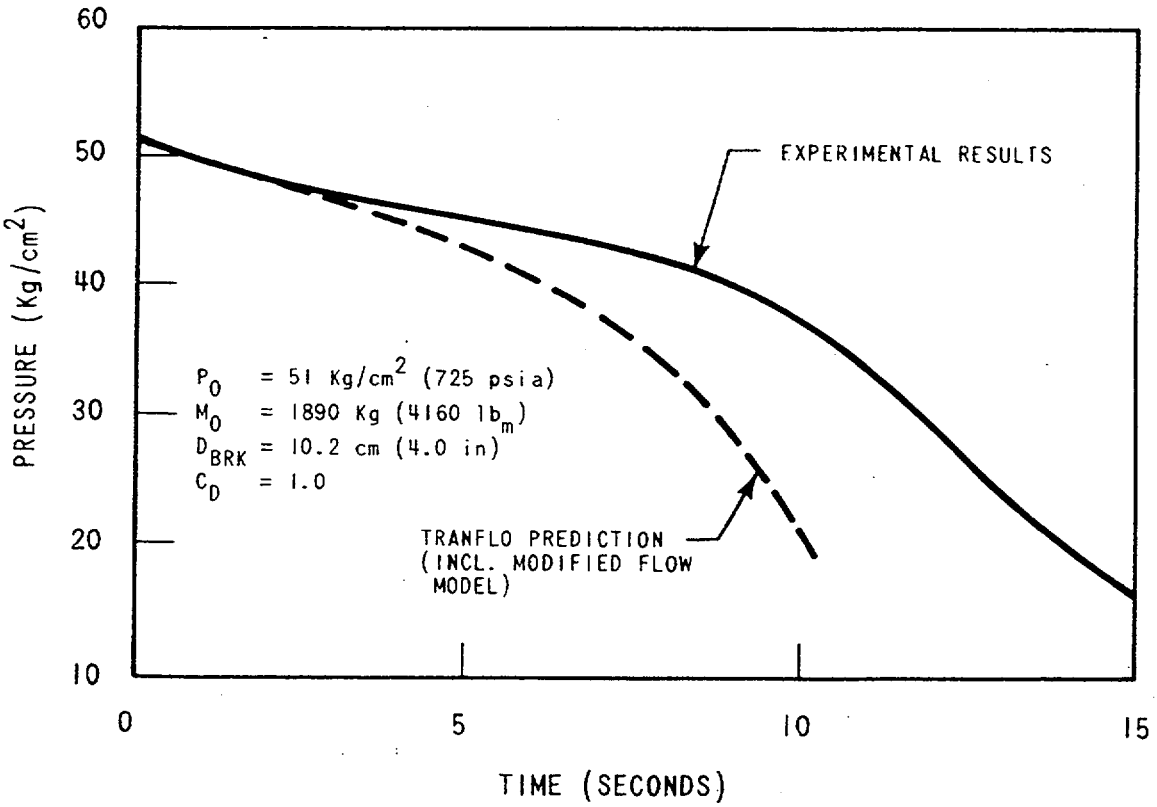

Figure 5.1.5.2-2 CISE Blowdown Test 2 - Pressure Vs. Time

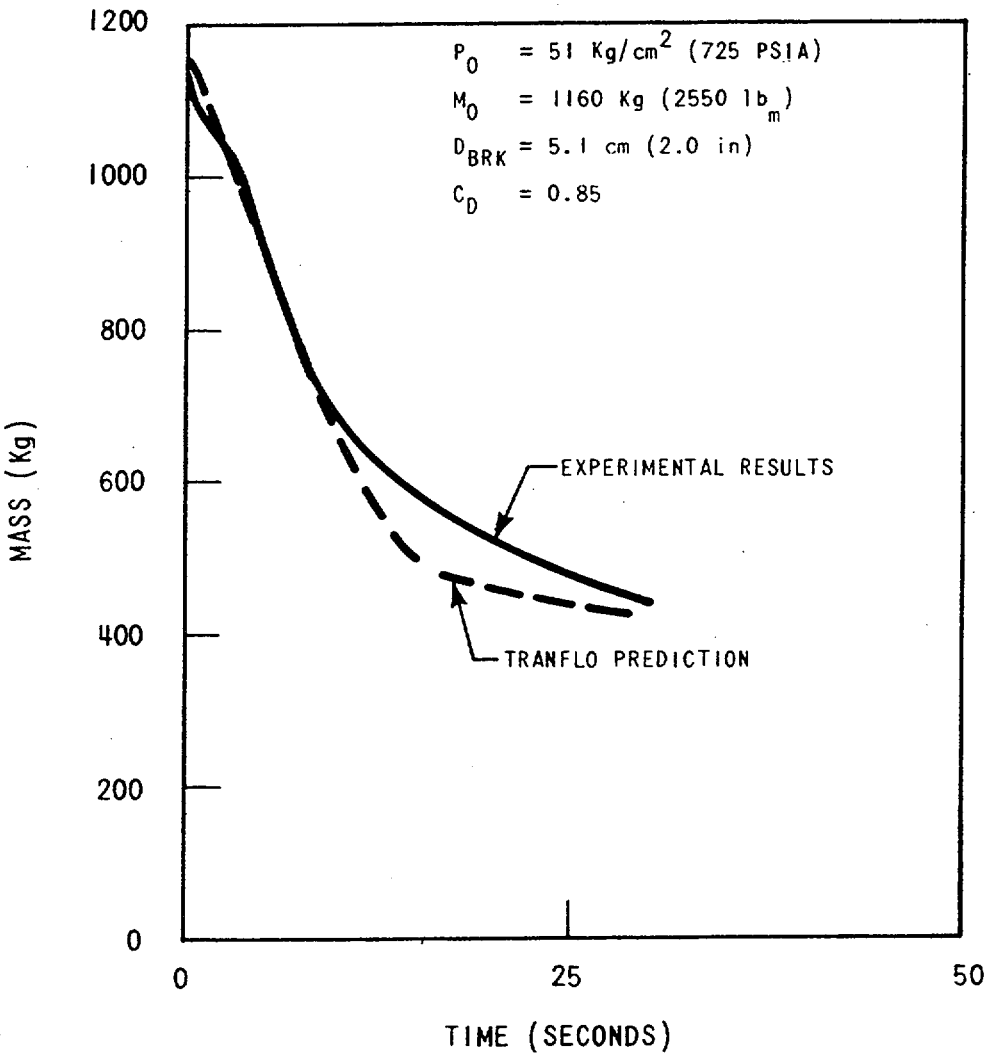

Figure 5.1.5.3-1 CISE Blowdown Test 3 - Mass Vs. Time

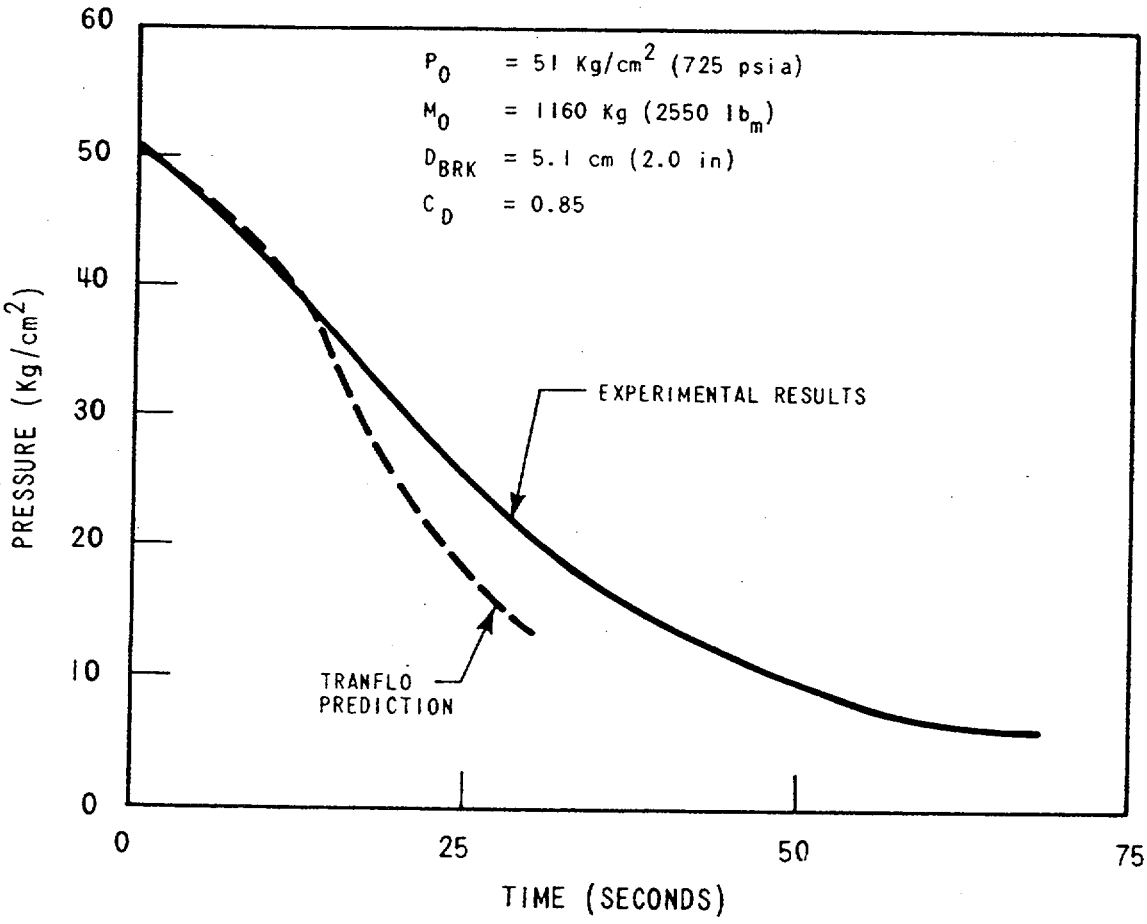

Figure 5.1.5.3-2 CISE Blowdown Test 3 - Pressure Vs. Time

5.2 COMPARISONS WITH SATAN CODE

The SATAN VI computer code is a well documented and accepted code for calculating high pressure steam/water blowdowns. A computer model (Figure 5.2-1) which duplicated the TRANFLØ steam generator model described in Section 4 was developed for use in SATAN to provide additional qualification of TRANFLØ blowdown calculations. Included in the SATAN model is the ability to simulate feedwater flows into the steam generator and to simulate heat flux between the primary and secondary systems.

Using both the SATAN and TRANFLØ codes, similar steam line break transients were modeled and the code results compared. The events modeled were a 4.6 ft^2, 1.4 ft^2, and 0.5 ft^2 rupture assumed to occur at initial steam generator power levels of hot standby, 102%, and 30%* of full power respectively. Results are compared in Figures 5.2-2 through 5.2-4.

In each comparison the time trends of the effluent quality variations are very similar. However, in each example the TRANFLØ prediction shows a delay before the start of entrainment. This is due to the modeling of the chevron separators. The time delay represents the time required to completely fill the drains and the banks of hooked vanes in the secondary separators with water (see Section 4.3.2). Until these are filled TRANFLØ calculates 100% quality steam in the upper head of the steam generator. If the SATAN results are shifted back in time by an amount equal to the time delay calculated by TRANFLØ, the results compare very well over the initial 4-6 seconds.

*Full power operation = 856 Mwt.

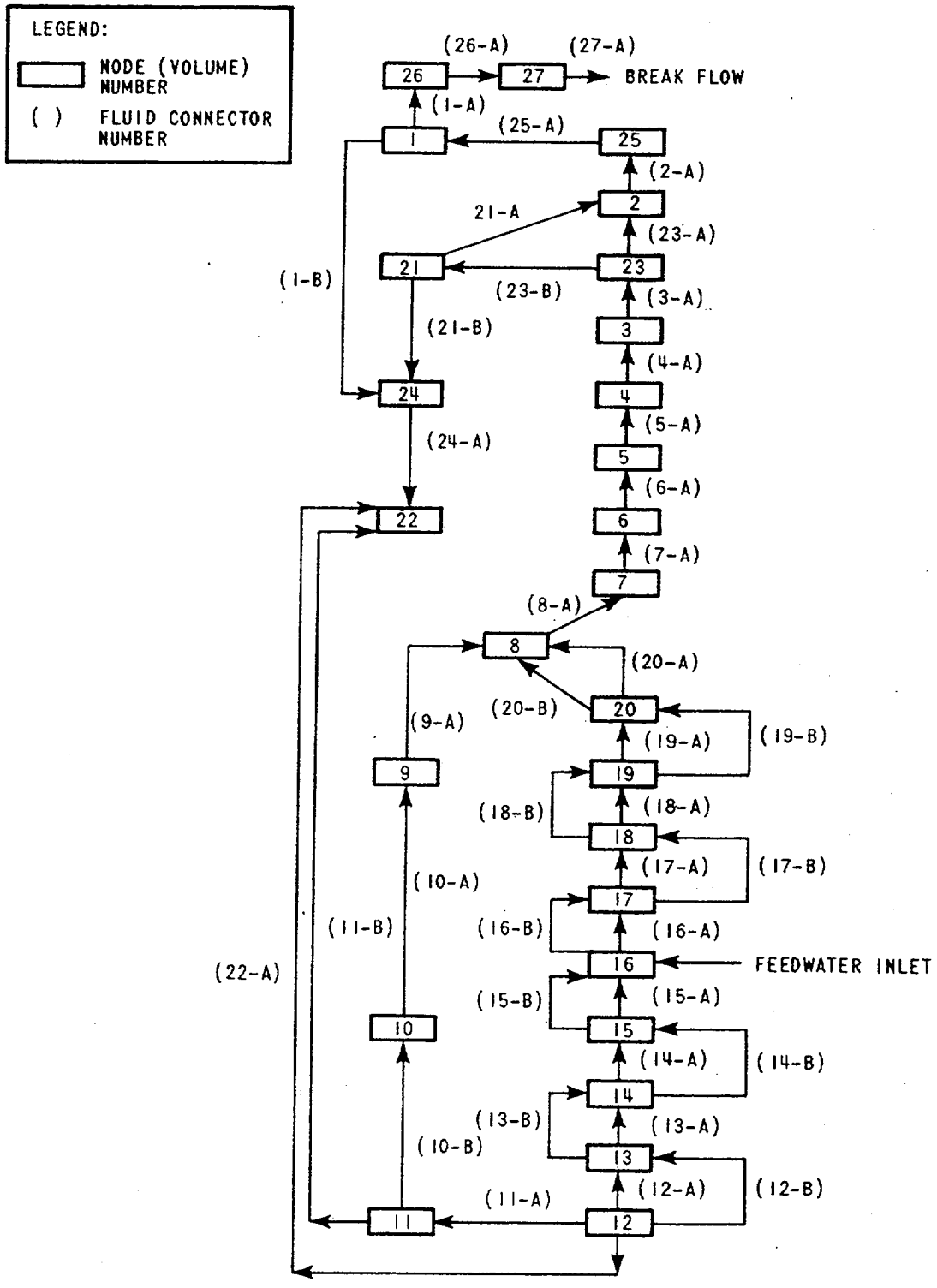

Figure 5.2-1 SATAN Steam Generator Computer Model

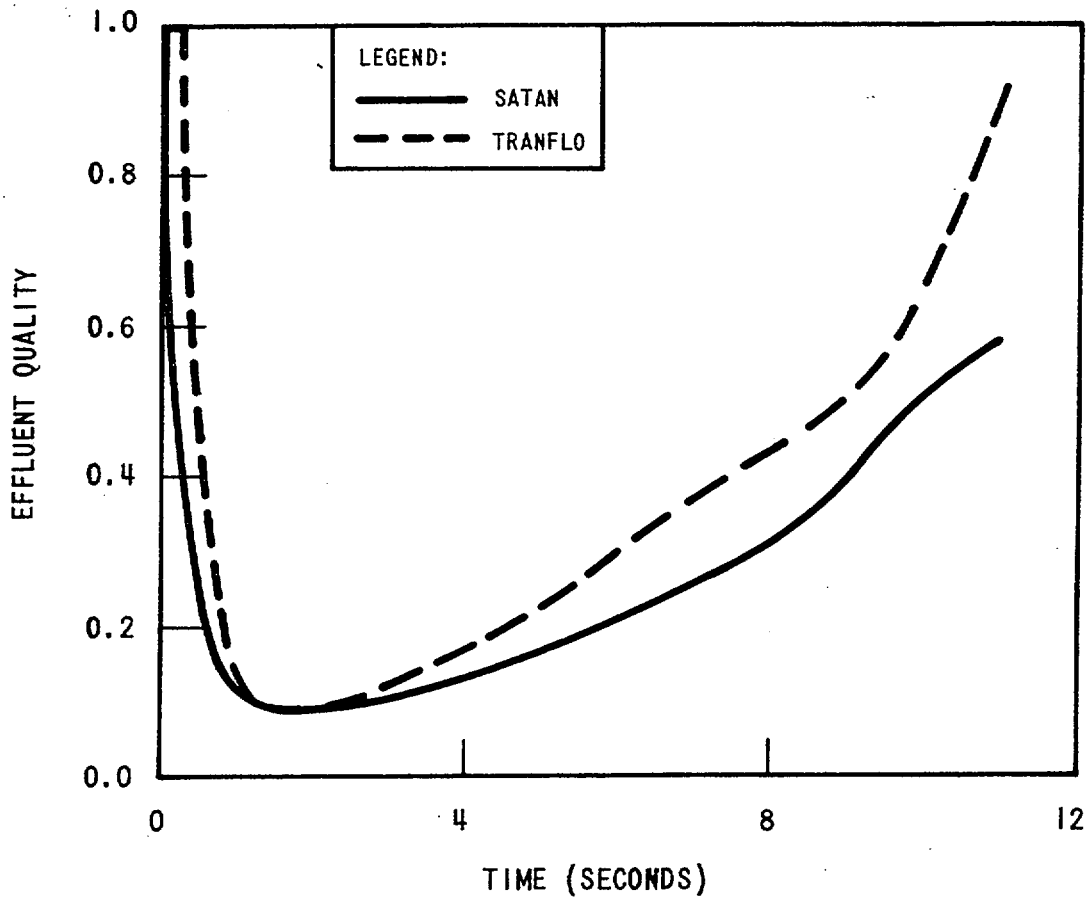

Figure 5.2-2 SATAN/TRANFLO Comparison
4.6 Ft^2 DER @ Hot Standby

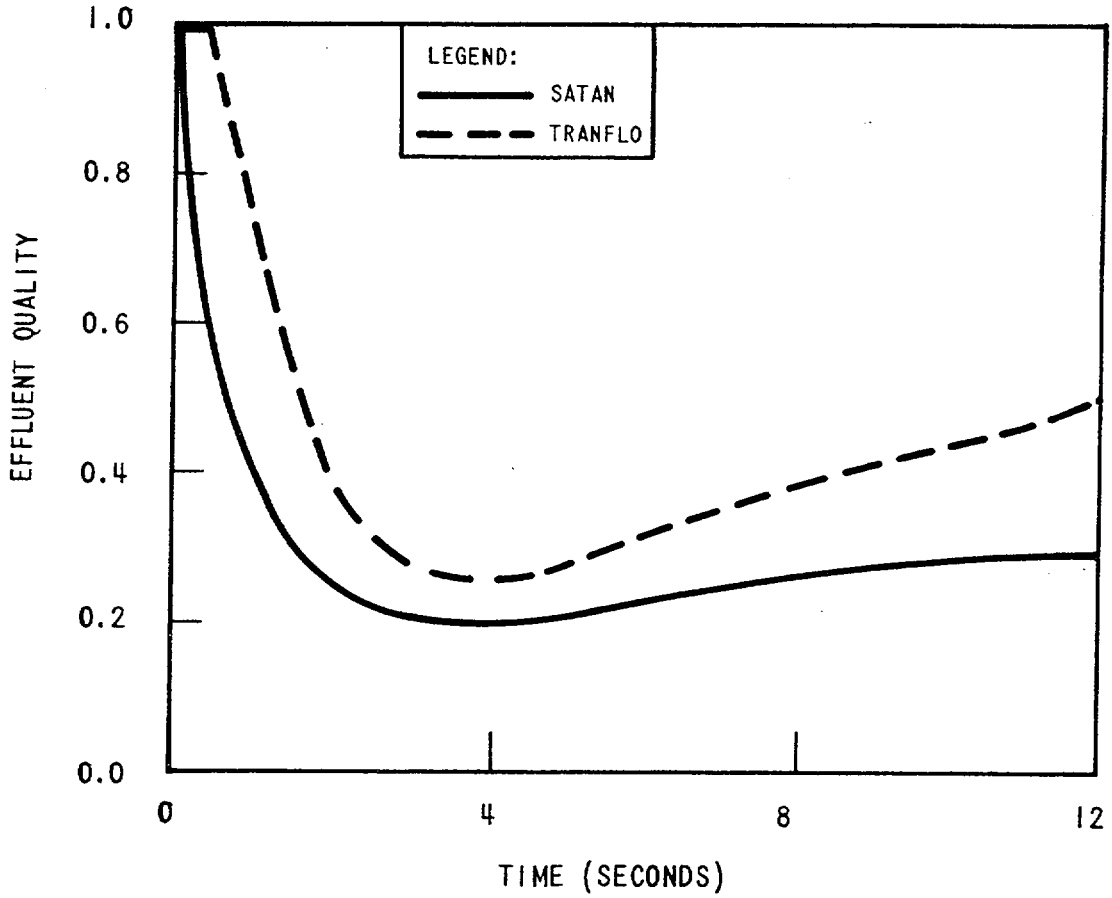

Figure 5.2-3 SATAN/TRANFLO Comparison
1.4 Ft^2 DER @ 102% Power

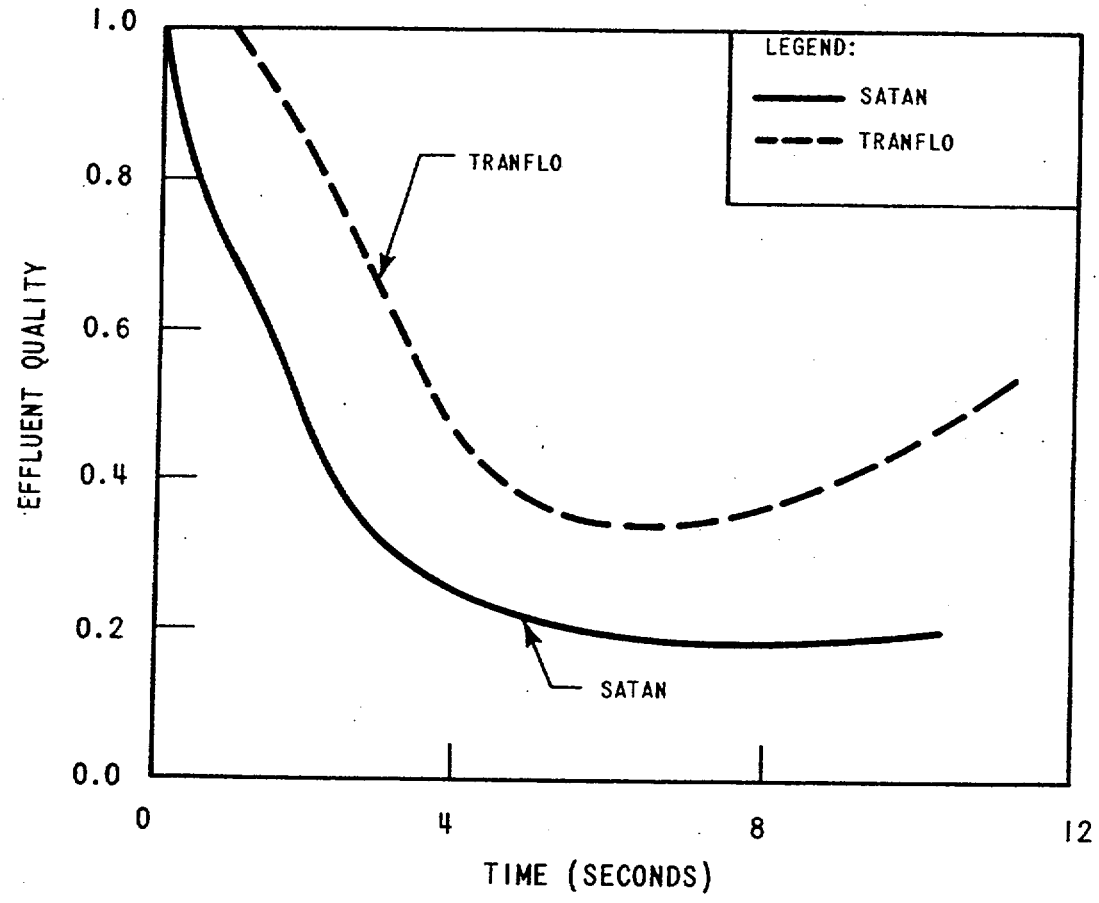

Figure 5.2-4 SATAN/TRANFLO Comparison
0.5 Ft^2 DER @ 30% Power

The close agreement of the two codes is a result of the steam separation equipment in the steam generator being ineffective during large portions of the transients depicted in Figures 5.2-2 through 5.2-4. The flow through the swirl vane drains is reversed during the entirety of all the transients shown making totally ineffective the separative work of the swirl vanes. The flow is also reversed in the chevron drains during the initial part of each transient. For the 4.6 ft^2 break there is back flow through the chevron drains until 7.2 seconds have elapsed. The chevron drain flows are reversed in the 1.4 ft^2 and 0.5 ft^2 breaks until 3.8 seconds and 1.4 seconds respectively. During these time intervals the secondary separators also lose all their effectiveness. Deviations between the results prior to these times indicate differences between the SATAN and TRANFLØ slip models and calculational methods (if the delay time displayed in the TRANFLØ results is removed). Subsequent to these times the deviations are a result of both the code differences and the effects of the separators on quality.

5.3 MODEL SENSITIVITY STUDIES

Several parametric studies were conducted with the TRANFLØ code and the steam generator models described in Section 4 to evaluate the impacts of modeling changes on predicted blowdown results. A discussion of these studies follows.

5.3.1 GEOMETRICAL MODELING

The loss coefficients used to describe the momentum pressure losses in each flow path in the steam generator models (see Appendix A) were determined using the geometrical characteristics of the generator internals and commonly accepted modeling practices as described in references

6, 14, and 15. In some instances the modeling criteria of the references could not be matched completely for some flow paths. For this reason several blowdown transients were run in which the values of the loss coefficients of all flow paths were arbitrarily changed by ±10% from the calculated values to evaluate the sensitivity of the blowdown results to the modeling. Results of the transients are shown in Figure 5.3.1-1 and indicate only a slight sensitivity to the changes made. For example a 10% change in the loss coefficients for all flow paths results in a maximum of only a 1% - 2% change in results. Thus it can be concluded that the sensitivity to the loss coefficients for any single flow path is negligibly small and that extreme accuracy in defining these coefficients is not required.

5.3.2 STEAM SEPARATOR EQUIPMENT MODELING AND EFFECTIVENESS DURING BLOWDOWN

One item having obvious potential for affecting the moisture entrainment calculated during a steam generator blowdown is the modeling of the steam separator equipment. Modeling of these devices has been described in Sections 4.3.1 and 4.3.2. Since experimental data on the performance of these devices is limited, studies were conducted to assure the modeling used is conservative for defining moisture entrainment in blowdowns. A description of these investigations and the results follow.

One parameter in the swirl vane modeling that affects fluid quality is the η_{sv} used in the equation described in Section 4.3.1. The separation model, which modifies the void fraction of the flow passing through the swirl vanes, was selected based on the fact that the separators are designed such that only a portion of the liquid phase is removed from the flow and that the amount of liquid removed is related to the area swept out by the scrubber (see Figure 4.3.1-2). Thus the swirl vane modeling should adjust void fraction rather than quality.

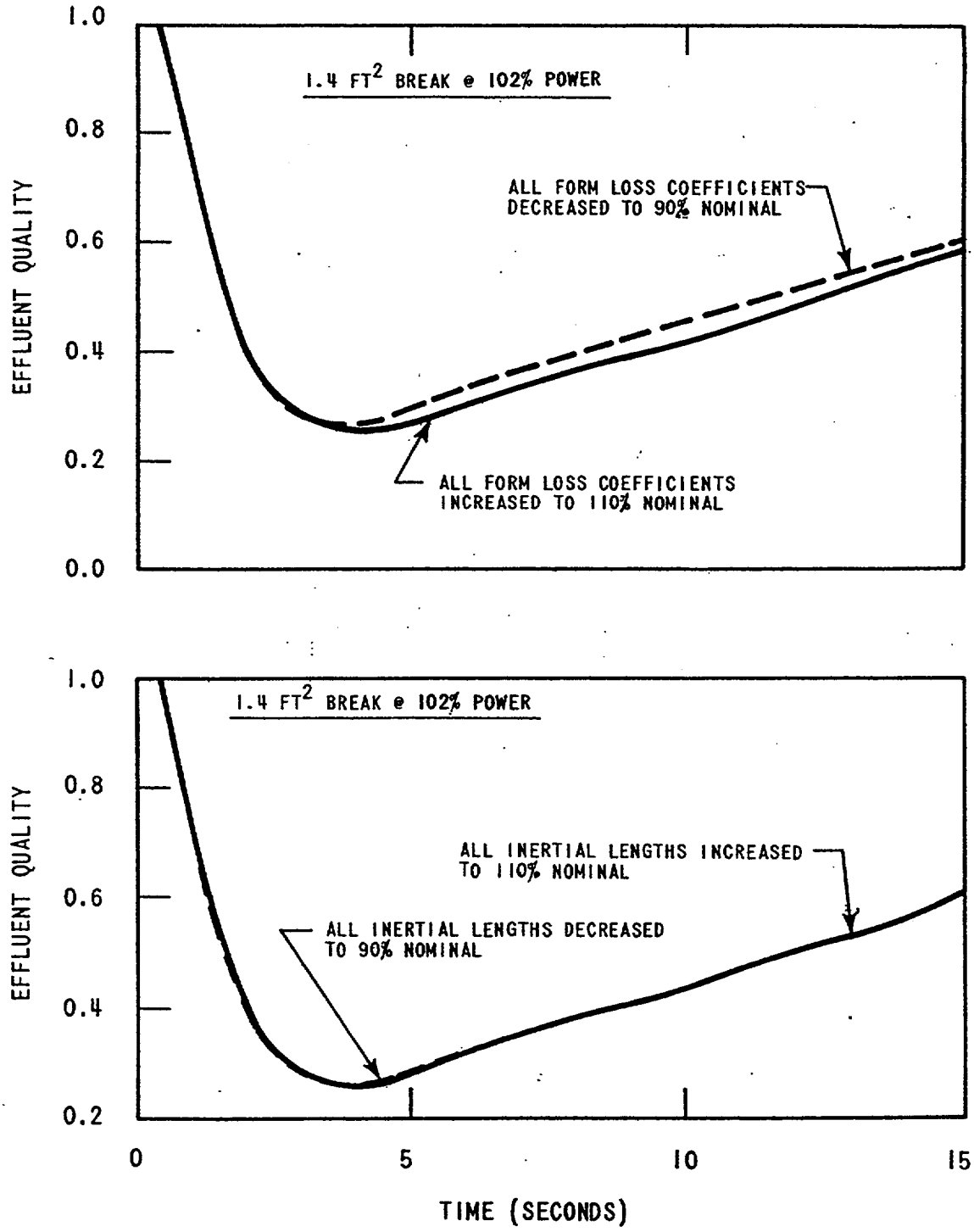

Figure 5.3.1-1 Sensitivity to Geometrical Modeling

Studies were conducted to evaluate the sensitivity of the entrainment results to the value chosen for η_{sv}. This was done by computing several identical blowdown transients using different values of η_{sv}. Results are shown in Figure 5.3.2-1. The principle effect of varying η_{sv} is to change the average quality of the small break blowdowns slightly. For the example in Figure 5.3.2-1, there is no change in entrainment in the full double-ended rupture transient due to changes in η_{sv}. The smaller 0.7 ft^2 rupture, however, shows a change in average quality between 0 and 19 seconds of -1.5% for a change of η_{sv} between 0.8 and 0.6. A similar analysis of a 0.5 ft^2 rupture at 30% power shows a change in average quality over the first 16 seconds of blowdown of approximately 4.8% for the same variation of η_{sv}.

The lack of sensitivity of blowdown entrainment to the separator equipment model is primarily a result of flow reversal through the separator drains during the blowdown. The rapid depressurization occurring in the upper head causes a large pressure drop between the upper downcomer region of the steam generator and the separator exits. The pressure drop is in a direction to force a flow reversal through both the swirl vane annular drains and the drain pipes out of the secondary chevron separators (see Figures 4.1-1 and 4.2-1). Once flow reverses in these drains the separator effectiveness is completely lost. Table 5.3.2-1 lists for the blowdowns shown in Figure 5.3.2-1 the times during which flow through the separator drains is reversed. In every case a significant portion of the period during which entrainment occurs includes the time in which the swirl vanes cannot function due to the reverse flow in the drains. This fact minimizes the effects of the swirl vane model on blowdown results.

The swirl vane model, using a value of $\eta_{sv} = 0.7$, was also compared to steady state test data taken from operating steam generators and found in general, to overpredict the separation performance as shown in Figure

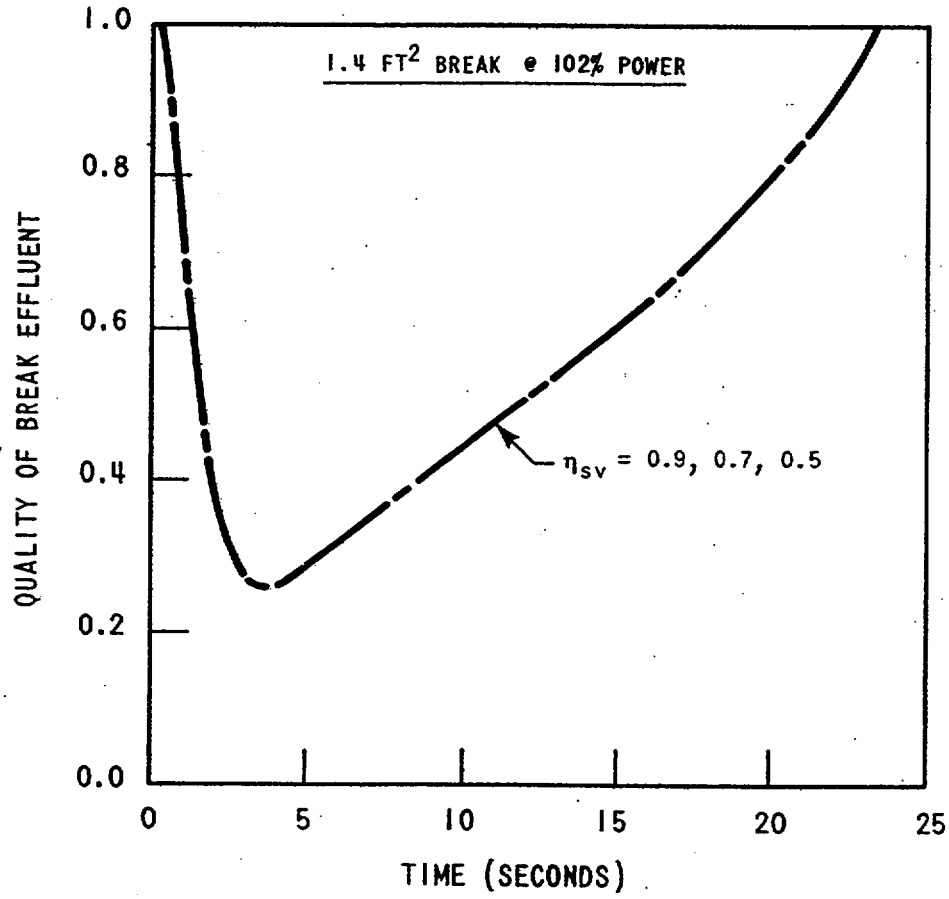

Figure 5.3.2-1a Entrainment Sensitivity to η_{sv}

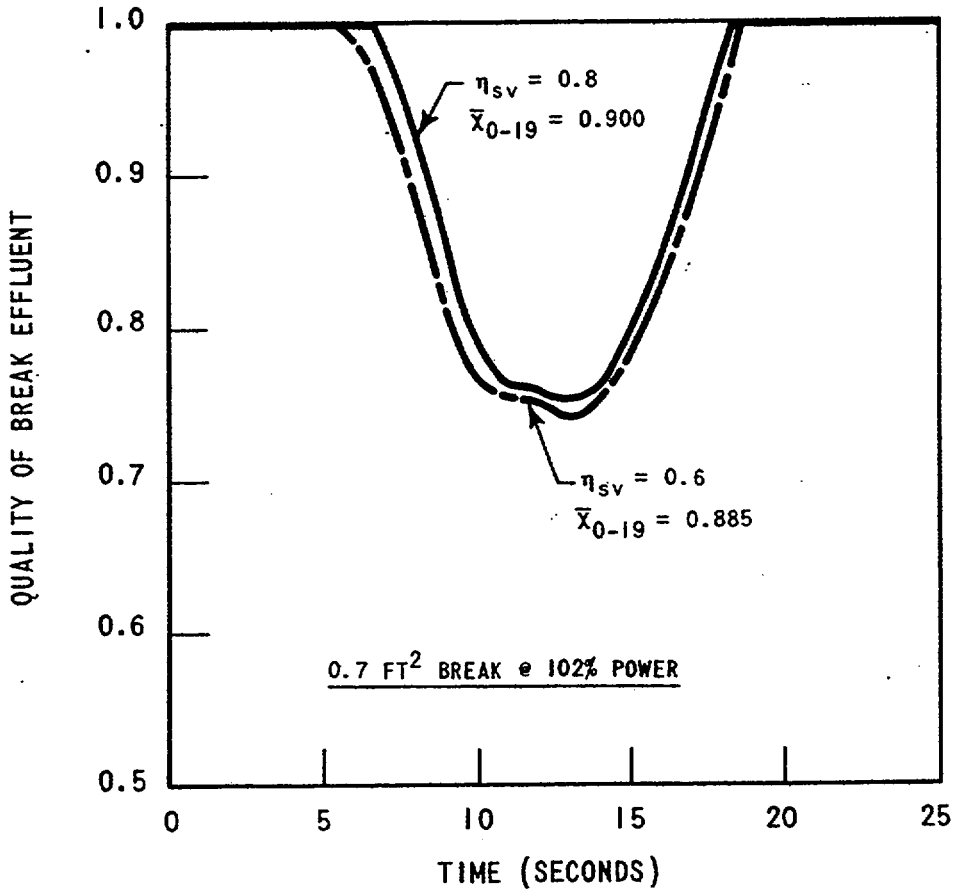

Figure 5.3.2-1b Entrainment Sensitivity to η_{sv}

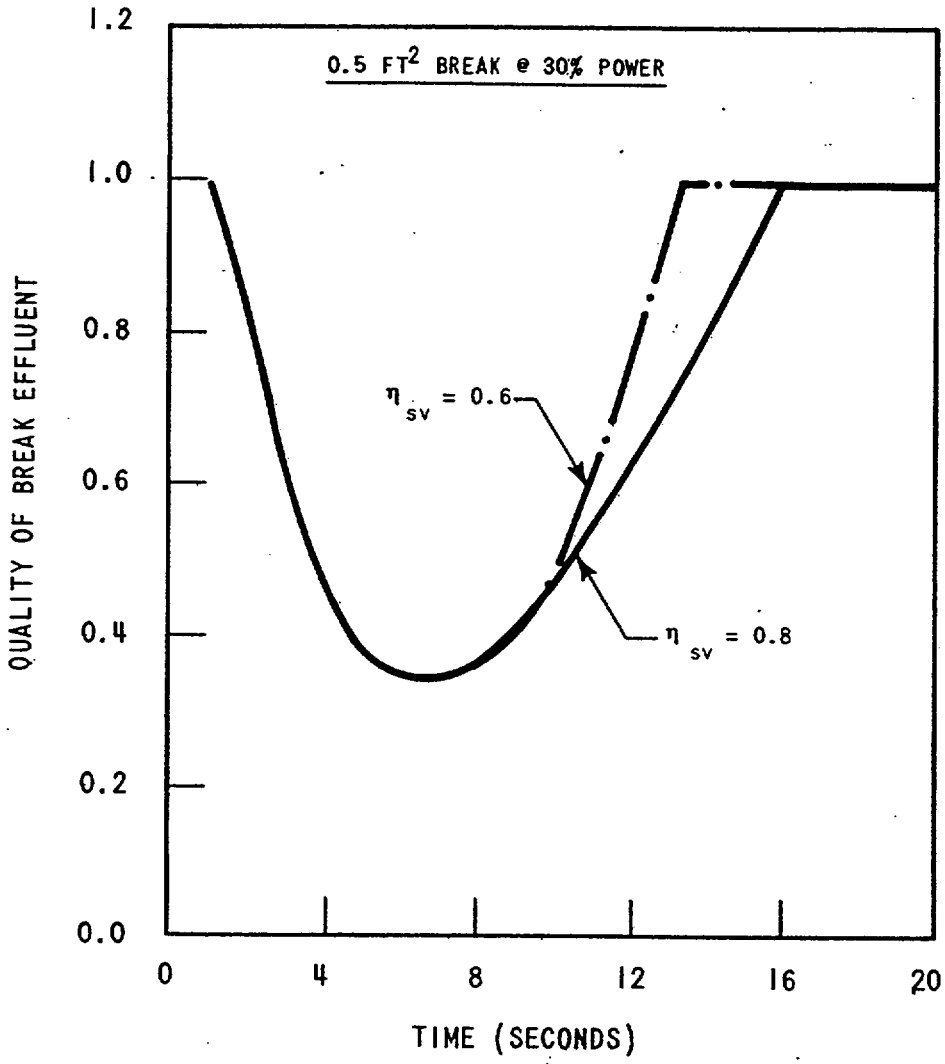

Figure 5.3.2-1c Entrainment Sensitivity to η_{sv}

TABLE 5.3.2-1

TABLE OF FLOW REVERSALS IN SEPARATOR DRAINS DURING BLOWDOWNS

Break Description	Time of Flow Reversal (sec)	
	Swirl Vanes	Secondary Separators
I. 1.4 Ft^2 Break at 102% Power		
$\eta_{sv} = 0.9$	0.1 - >30.0	0.1 - 3.7
$\eta_{sv} = 0.7$	0.1 - >30.0	0.1 - 3.7
$\eta_{sv} = 0.5$	0.1 - >30.0	0.1 - 3.7
II. 0.7 Ft^2 Break at 102% Power		
$\eta_{sv} = 0.8$	6.5 - 13.5*	-
$\eta_{sv} = 0.6$	6.3 - 13.7*	-
III. 0.5 Ft^2 Break at 30% Power		
$\eta_{sv} = 0.8$	0.08 - 4.7	0.02 - 1.4
$\eta_{sv} = 0.6$	0.08 - 4.6	0.01 - 1.4

*Flow oscillates between forward and reverse direction during this time. Flow magnitude is small.

5.3.2-2. A more informative comparison of the test data with the computer model was obtained by calculating a value of η_{sv} for each test data point. This was done using the correlation techniques developed during the test program which uses the energy difference between the liquid and gas phases to predict moisture separation. The comparison is shown in Figure 5.3.2-3 along with a least squares curve fit to the data points shown. From this figure it is obvious that a value of $\eta_{sv} = 0.7$ should result in over predicting the swirl vane performance.

Both Figures 5.3.2-2 and 5.3.2-3 indicate the TRANFLØ swirl vane model is conservative for steady state operation. Since the performance would not improve under blowdown conditions, the model should be conservative for prediction of moisture entrainment during steam line break transients.

Additional field test data was available for model 51 steam generators currently in operation. Empirical correlations used to quantify the test data predict separator performance as shown in Figures 5.3.2-4 and 5.3.2-5. These empirical relationships were programmed into the TRANFLØ code and several blowdown transients were computed. Comparisons of those results with results of the same transient computed using the standard computer model show that entrainment to be significantly increased (see Figures 5.3.2-6 through 5.3.2-8). Again the conclusion is that the computer model provides conservative entrainment results.

Several important points should be made about the conservatisms of the empirical correlations shown in Figures 5.3.2-4 and 5.3.2-5. First, the test data used to develop the correlations covered only those ranges of pressure, flow, and quality shown on the figures. Extrapolations beyond those limits must be made carefully. For example, the extrapolation of the secondary separator performance curves, though they show reasonable trends, should be considered to have wide variation in the region of low inlet qualities. Secondly, the extrapolation of the

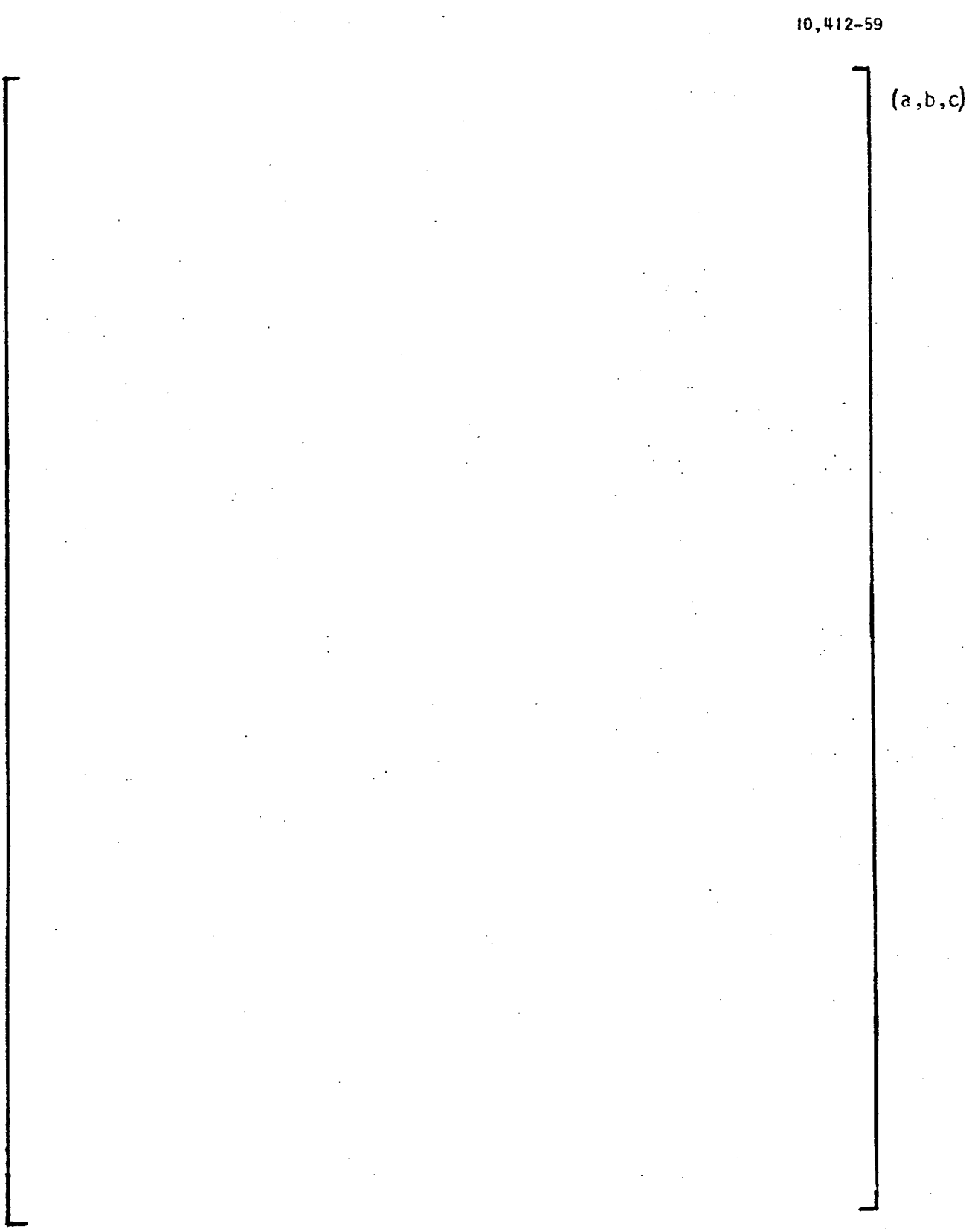

(a,b,c)

Figure 5.3.2-2 Comparison of TRANFLO Swirl Vane Model with Steady-State Test Data

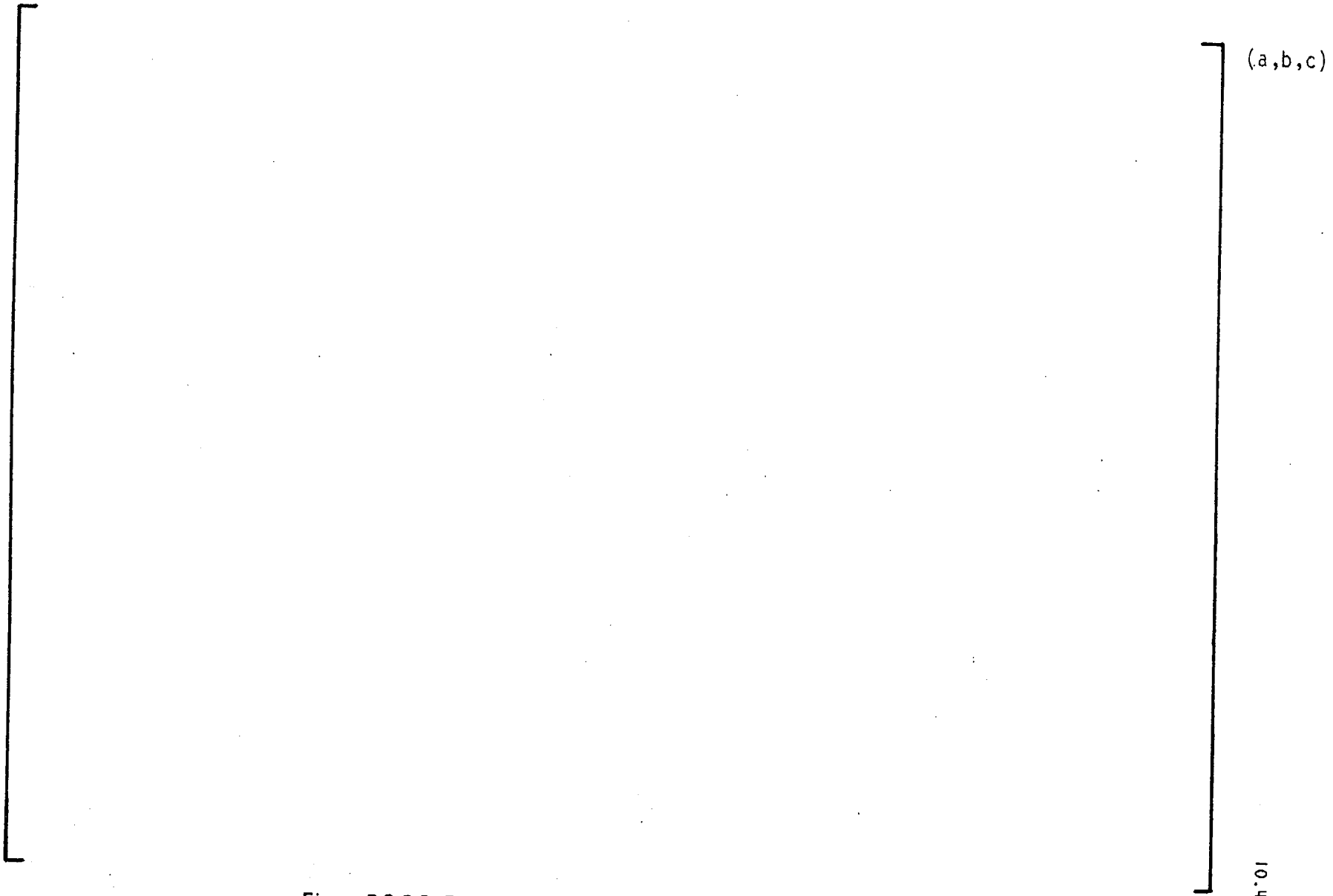

(a,b,c)

Figure 5.3.2-3 Empirical Values of η_{sv} (S.S. Test Data)

(a,b,c)

Figure 5.3.2-4 Swirl Vane Performance (Based on Steady-State Test Data)

10.412-54

Figure 5.3.2-5 Secondary Separator Performance (Based on Steady-State Test Data)

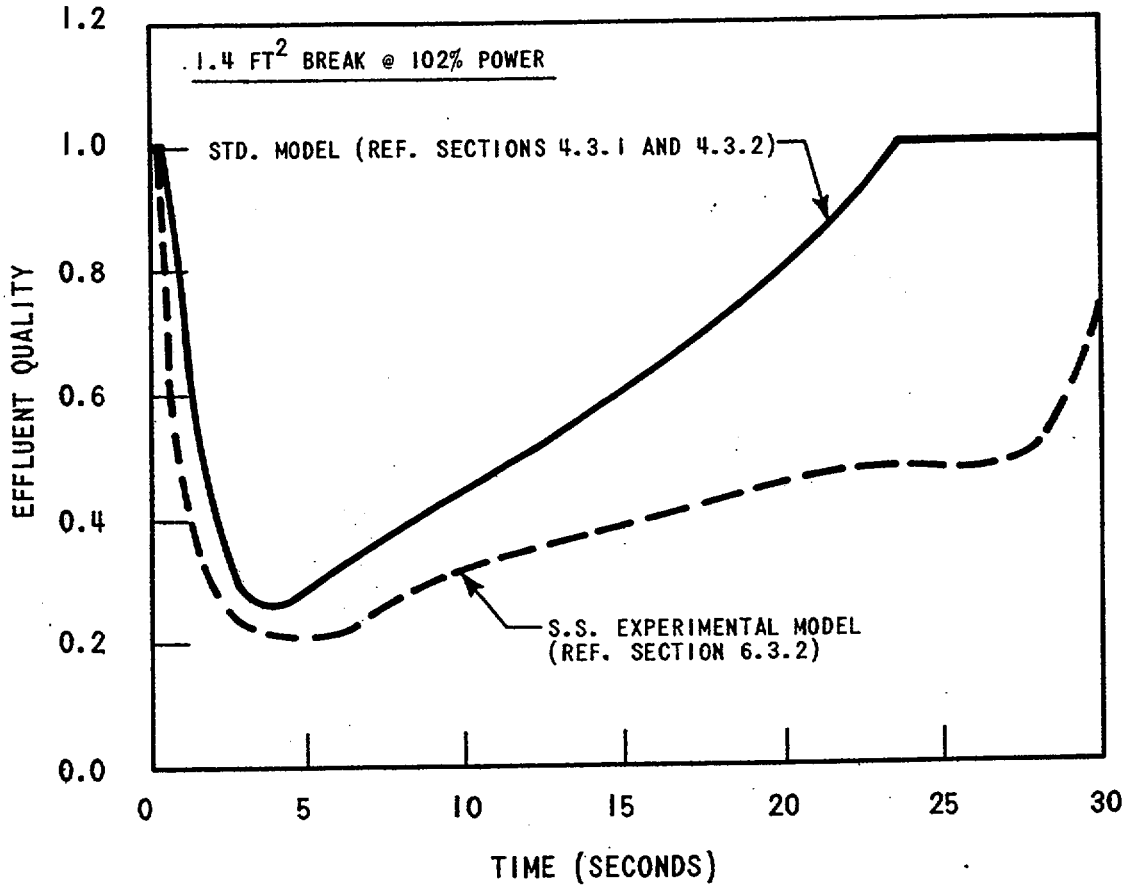

Figure 5.3.2-6 Effects of Separator Equipment Modeling on Blowdown Results

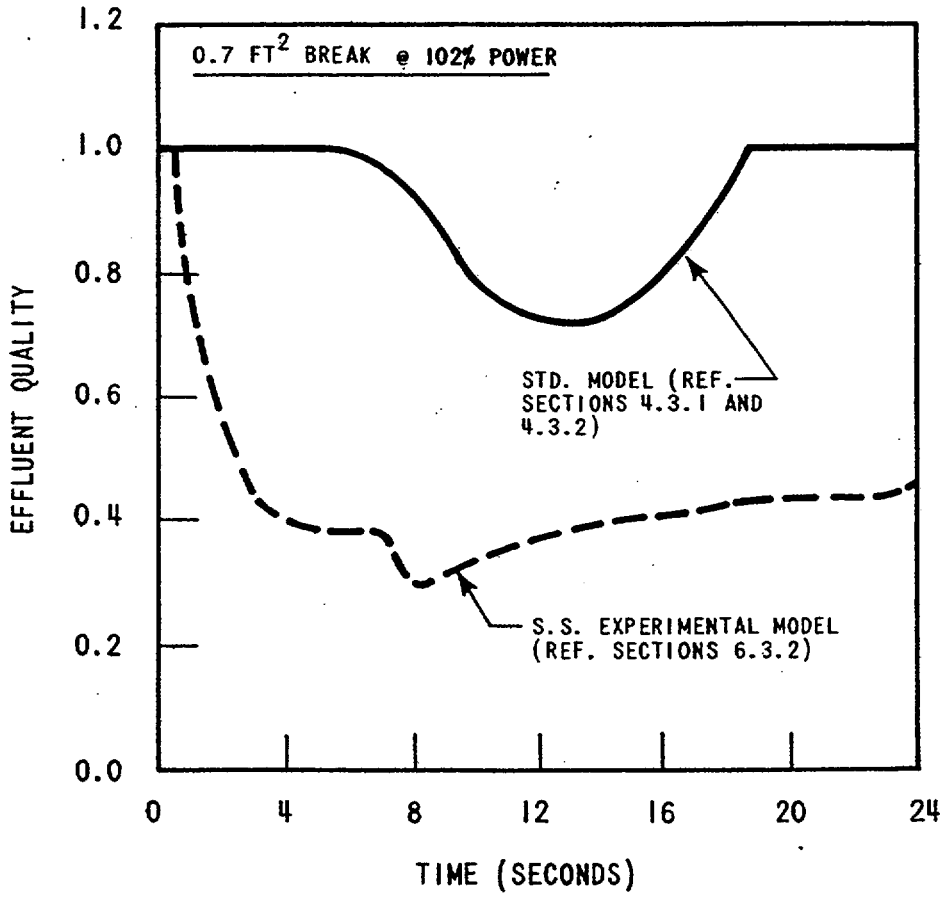

Figure 5.3.2-7 Effects of Separator Equipment Modeling on Blowdown Results

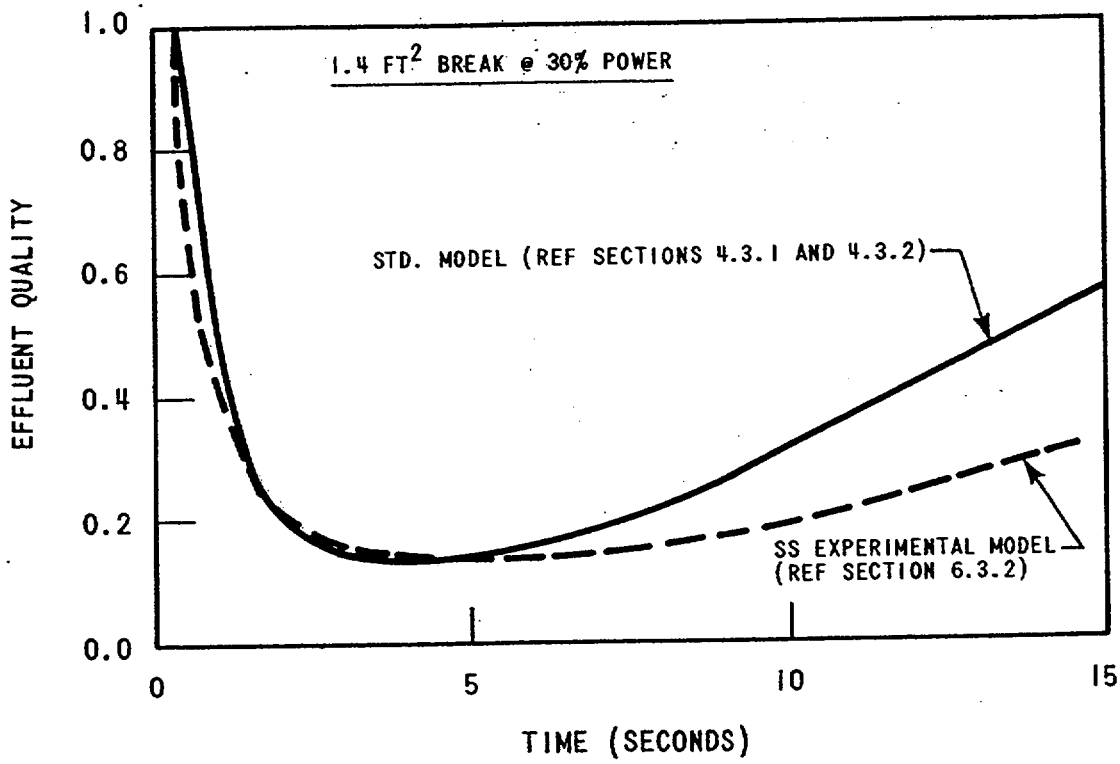

Figure 5.3.2-8 Effects of Separator Equipment Modeling on Blowdown Results

primary separator performance curves to the higher flowrates are overly conservative. Outlet quality of the swirl vanes at high flowrates will not approach 100% when inlet quality does not approach 100%. In fact, the 1000 lbm/sec-700 psia curve shown on Figure 5.3.2-4 is near the expected upper limit of the performance capability of the swirl vanes. However, the curves, as shown, result in more separation than would be expected and were used without limitations for the analyses described above.

6.0 CONCLUSIONS

The computer code described here can be used as a comprehensive thermal-hydraulic model of a U-tube steam generator or many other steam/water systems. It is capable of modeling all phases of steam line break blowdowns and can also be applied to many other transients involving steam generators. Fluid conditions within the system may be subcooled, saturated, or superheated in any or all parts of the model. Appropriate mass and energy transfers within the system are determined at all times.

The calculations allow inclusion of the effects of phase velocity differences, water separation due to gravity, heat transfer into the system from external sources, special phase separation equipment, and critical leaks in the system from either subcooled, saturated, or superheated regions. Checks for critical heat flux conditions during heat transfer are also made.

Specific models which can be used for simulating particular Westinghouse steam generators are also presented. Modeling of special phase separation equipment in these steam generators is discussed and shown to be adequate for prediction of steam line blowdowns.

Finally, verification of the code capability is presented by means of numerous predictions of experimental blowdown data. In most comparisons the results are extremely favorable. In those comparisons where analytical and empirical results differ, reasons for the discrepancies are readily identified and accountable.

The particular purpose for which the TRANFLØ code was developed was the conservative prediction of the characteristics of steam generator blowdowns following a steam line rupture. The results of these predictions are intended for use in reactor containment building and equipment integrity analyses to assure the safe operation of nuclear power

plants. For this purpose it is conservative to maximize the energy releases with time, and this has been an objective consistently pursued in the code development. Modeling is unilaterally designed to underpredict the amount of low energy liquid which would be carried out with the blowdown effluent and thereby maximize the energy release. Verification of this goal has been achieved by performing sensitivity studies for key parameters and comparisons with experimental data. The result is a conservative analysis tool totally capable of performing blowdown calculations.

Thus the objectives set forth in the introduction have been achieved; i.e., the development of a means to conservatively examine secondary system high energy line breaks which includes all important factors which effect the results.

7.0 REFERENCES

1. F. M. Bordelon, et. al, "SATAN VI Program: Comprehensive Space-Time Dependent Analysis of Loss-of-Coolant", WCAP-8302 (June 1974).

2. V. J. Esposito, K. Kesavan, B. Maul, "WFLASH-A Fortran IV Computer Program for Simulation of Transients in a Multi-Loop PWR", WCAP-8200, Revision 2 (June 1974).

3. T. A. Porsching, et. al, "FLASH 4: A Fully Implicit Fortran IV Program for the Digital Simulation of Transients in a Reactor Plant", WAPD-TM-840 (March 1969).

4. "Proprietary Redirect/Rebuttal Testimony of Westinghouse Electric Corporation", USAEC Docket RM-50-1, Page 25-1, October 26, 1972.

5. A. A. Armand, "The Resistance During the Movement of a Two-phase System in Horizontal Pipes", AERE-Trans-828 (1959).

6. J. W. Murdock, "Two-phase Flow Measurements with Orifices", Journal of Basic Engineering, Transactions of ASME, p. 419 (December 1962).

7. R. F. Davis, "The Physical Aspects of Steam Generation at High Pressure and the Problem of Steam Containment", I. Mech. Engr. (1940).

8. F. J. Moody, "Maximum Flow Rate of a Single Component, Two-phase Mixture", Journal of Heat Transfer, Transactions of the ASME, pp 134-142 (February 1965).

9. F. R. Zaloudek, "Steam-Water Cricital Flow from High Pressure Systems-Interim Report", HW-80535, UC-38, TID-4500, 29th Ed. (January 1964).

10. Battelle Northwest Laboratories, "Coolant Blowdown Studies of a Reactor Simulator Vessel Containing a Perforated Sieve Plate Separator", BNWL-1463 (February 1971).

11. ORNL-tr-2587 and ORNL-tr-2588, "Study of Processes During Blowdown of Water-cooled Reactors. Tests with the Large 11.2 m Vessel Without Inside Equipment", Battelle Institute e.v., Frankfurt am Main, West Germany (July 1971).

12. R. Carzaniga, et. al, "An Investigation on the Blowdown of a Tank Filled with Saturated Steam-Water, Part 1: Experiments", CISE-R-303 (December 1970).

13. A. Premoli and C. Sandri, "An Investigation on the Blowdown of a Tank Filled with Saturated Steam-Water, Part 2: Theoretical Analysis", CISE-R-304 (June 1971).

14. Crane Company, "Flow of Fluids Through Valves, Fittings and Pipe", Technical Paper No. 410 (1969).

15. Fluid Meters, Their Theory and Application, Report of ASME Research Committee on Fluid Meters, Fifth Edition (1959).

16. J. G. Collier, Convective Boiling and Condensation, pp. 141, 1972, McGraw-Hill.

17. J. R. S. Thom, W. M. Walker, T. A. Fallon, and G. F. S. Reising, Boiling in Subcooled Water During Flow Up Heated Tubes or Annuli, Proceedings of the Institute of Mechanical Engineers, 1965-66, Vol. 180, Pt 3C, pp 226-246. (Paper 6)

18. R. O. Sandberg, A. A. Bishop, and L. S. Tong, "Forced Convection Heat Transfer at High Pressure After the Critical Heat Flux", ASME Paper 65-HT-31, 1965.

19. L. S. Tong, Boiling Heat Transfer and Two-Phase Flow, pp 162-166, 1965, Wiley.

20. R. S. Dougall, and W. M. Rohsenow, "Film Boiling on the Inside of Vertical Tubes with Upward Flow of the Fluid at Low Qualities", MIT Report No. 9079, September 1963.

21. V. E. Schrock and L. M. Grossman, "Forced Convection Boiling Studies Forced Convection Vaporization Project", USAEC Report TID-14632 (1959).

22. J. F. Heineman, An Experimental Investigation of Heat Transfer to Superheated Steam in Round and Rectangular Channels, pp 32-35, September 1960, ANL-6213, Argonne National Laboratory.

8.0 APPENDIX A - CODE INPUT

The following input data is required to run the TRANFLØ code.

8.1 CONTROL CARD (FORMAT 9I5)

Variable Name		Description
NBGIN	-	If 0, data is read from cards; if 1, data is read from a restart tape
NEND	-	IF 0, no restart tape is written; if 1, restart tape is written
NPRINT	-	Maximum number of cycles between printout
NOSLIP	-	If 1, slip flow will not be included in calculations
NOSEP	-	If 1, natural separation will not be included in calculations
ISS	-	If 1, a steady state initial condition will be calculated (available only for Model 51 steam generators)
MØNIT	-	Number of variables to be monitored for summary output

8.2 TITLE CARD (FORMAT 8A10)

Eighty character title

8.3 MODEL DESCRIPTION CARD (FORMAT 9I5)

Variable Name		Description
NUMNP	-	Number of elemental control volumes

NUMFC - Number of flow paths

NUMFL - Number of flow leaks

NUMPC - Number of segments in the tube bundle heat source

8.4 CONTROL VOLUME DESCRIPTIONS (One card per control volume; FORMAT 8F10.2)

Variable Name		Description
VOL	-	Nodal volume (ft^3)
Z	-	Nodal elevation (ft)
P	-	Nodal pressure (psia)
T	-	Nodal temperature (°F)
VØID	-	Nodal void fraction
AN	-	Nodal area to be used in momentum flux pressure loss equation (ft^2)

8.5 FLOW CONNECTOR DESCRIPTIONS (One card per flow path; FORMAT 2I5, 6F10.2, 2I5)

Variable Name		Description
IU	-	Upstream node

ID - Downstream node

DE - Hydraulic diameter for use in skin friction pressure drop equation (ft)

AF - Cross-sectional flow area to be used with skin friction and form loss pressure drop equations (ft^2)

X - Length (ft)

EL - Inertial length (ft^{-1}), where $EL = \int \frac{dL}{Area}$ along the length of the flow connector.

FD - Form loss pressure drop coefficient defined by

$$\Delta P = \frac{FD \times W^2 \times \nu}{2g_c \times 144 \times AF^2} = \frac{FD \rho V^2}{2g_c \times 144}$$

(See list of nomenclature for definition of terms)

W - Initial flow rate (lbm/sec)

KFT - Flow connector type:

Enter 0 for regular connector
Enter +1 for saturated steam flow only
Enter +2 for saturated liquid flow only
Enter +3 for steam flow in positive direction and water flow in negative direction
Enter -1 for steam flow in positive direction and regular flow in negative direction

Enter -2 for water flow in positive direction and regular flow in negative direction
Enter +5 for cross flow through a tube bundle
Enter ±4 for call of the subroutine SCØNN for special connector models.

IFF - Enter 1 if no gravity separation is to be calculated for this connector

8.6 LEAK DESCRIPTION (One card per flow leak; FORMAT 2I5, 6F10.2, I5)

Variable Name		Description
IL	-	Node of leak
ILT	-	Leak type: Enter 1 if leak is constant Enter 2 if leak is a critical flow leak out Enter 3 if leak is constant with steam out only Enter 4 if leak is critical flow with steam out only Enter 5 if leak is input as a table (Note: If ILT = 3,4 and node is not two-phase, the leak reverts to type 1 or 2 respectively)
PL	-	External pressure (psia)
DL	-	Leak diameter (in)
HLX	-	External enthalpy (Btu/lbm)
ORCØF	-	Orifice coefficient

WL - Initial leak flow (lbm/sec)

ZL - Leak elevation (ft)

LTFIVE - Number used to identify type 5 leaks in output

8.7 SPECIAL LEAK DATA (Needed only for leaks of type 5, three data cards for each type 5 leak immediately following the leak description card; FORMAT 10F8.2)

Variable Name		Description
Card 1, Flow Data:		
FLIN	-	Nominal leak flow (lbm/sec)
FLT (1-9)	-	Table of 9 values of leak flow normalized to FLIN and corresponding to time TFL
Card 2, Enthalpy Data:		
ENTH	-	Nominal leak enthalpy (Btu/lbm) (If negative, enthalpy is internally calculated for leak flows out of the node)
ENTT (1-9)	-	Table of 9 values of leak enthalpy normalized to ENTH and corresponding to time TFL
Card 3, Time Data:		
TFL (1-9)	-	Time points for tables FLT and ENTT (sec)

8.8 HEAT SOURCE DATA (One card for each segment of the heat source; FORMAT I5, 2F10.2)

Variable Name		Description
IH	-	Secondary node receiving heat from the heat source segment
TPC	-	Initial temperature of the primary fluid in the heat source segment (°F)
HTL	-	Length of tubes in the segment (ft)

8.9 HEAT SOURCE DESCRIPTION (one card; FORMAT 7F10.2, 2I5)

Variable Name		Description
PCFLØ	-	Primary fluid flow rate (lbm/sec)
PC	-	Primary pressure (psia)
TH	-	Primary inlet temperature (°F)
RF	-	Tube bundle fouling factor
RI	-	Tube inside radius (ft)
RØ	-	Tube outside radius (ft)
NT	-	Total number of tubes
ITYPC	-	Enter 0 for constant primary coolant flow, Enter 1 to input primary coolant flow rate, temperature and pressure as functions of time

8.10 SPECIAL HEAT SOURCE DATA (Needed only if ITYPC=1; 8 cards; FORMAT 8F10.2)

Variable Name	Description
Cards 1-2, Temperature Data:	
TTH(1-10)	Primary fluid inlet temperature normalized to TH and corresponding to time THT (10 values)
Cards, 3-4, Flow Data:	
SFLØW(1-10)	Primary fluid flow rate normalized to PCFLØ and corresponding to time THT (10 values)
Cards 5-6, Pressure Data:	
TPCP(1-10)	Primary fluid pressure normalized to PC and corresponding to time THT (10 values)
Cards 7-8, Time Data:	
THT(1-10)	Time points for tables TTH, SFLØW, and TPCP (sec)

8.11 TUBE PITCH (One card; FORMAT F10.2)

Variable Name	Description
TP	Tube pitch (ft)

8.12 MONITOR DATA (One card per monitor variable; FORMAT 2I5, A10)

Variable Name	Description
IB	Number of common block containing monitor variable (beginning with common block NODE) (If negative, monitor variable is calculated in subroutine YEXMØN)*

*YEXMØN is a subroutine written by the user to calculate and store as monitor variables any information not available in the program's common block statements.

IM - Number of monitor variable in common block

VNAME - Monitor variable name

8.13 TIME DATA (One card; FORMAT 7F10.2)

Variable Name		Description
TINIT	-	Initial problem time (used only when NBGIN = 0) (sec)
TSTØP	-	Problem stop time (sec)
TPRINT	-	Time interval for data printout (sec)
TDELT	-	Maximum allowable time step (sec)
TMØN	-	Minimum time interval for monitor data printout (sec)
CØNV	-	Convergence criteria; maximum fractional change of mass or energy in any node during one time step
TLIM	-	Central processor time limit (sec).

9.0 APPENDIX B

MATHEMATICAL SOLUTION
OF SYSTEM DIFFERENTIAL EQUATIONS

The differential equations defined in Section 3.1 are solved using a fully implicit backward differencing technique[3]. Using this technique, values of W_k, WL_ℓ, U_i, M_i, $\frac{\partial P_i}{\partial U_i}$, $\frac{\partial P_i}{\partial M_i}$, and $\frac{\partial WL_\ell}{\partial P_i}$ at time "t" determine the values of M_i, U_i and W_k at time "$t + \Delta t$". As described in Reference 3, equation (1) - (3), (9), and (10) from Section 3.1 may be linearized to the form

$$[I - \Delta t\ J^n]\ (y^{n+1} - y^n) = \Delta t\ \dot{y}^n \qquad (11)$$

where "n" refers to the n^{th} time step, "J" is the Jacobian matrix of the transformation $\dot{y} = f(y)$, and

$$y = \begin{bmatrix} W_1 \\ \vdots \\ W_m \\ U_1 \\ \vdots \\ U_n \\ M_1 \\ \vdots \\ M_n \end{bmatrix}$$

The solution is then given by

$$\Delta y = y^{n+1} - y^n = A^{-1}\ (\Delta t\ \dot{y}^n) \qquad (12)$$

where $A = [I - \Delta t\ J^n]$

The above steps are accomplished by first defining the system flows and leaks as follows. Flow in flow path m connecting node i to node j is defined to be positive when the direction is from i to j. Leak flow ℓ associated with node i is defined to be positive when the direction is out of the node. The flow directions can then be accounted for mathematically by letting

$$\alpha = |W_m| \,/\, W_m \tag{13}$$

$$\beta = |WL_\ell| \,/\, WL_\ell \tag{14}$$

Equations (1) through (3) may then be written as

$$\dot{M}_n = \sum_{m=1}^{M} [\delta_{j(m),n} - \delta_{i(m),n}] W_m - \sum_{\ell=1}^{L} \beta_\ell \delta_{i(\ell),n} WL_\ell \tag{15}$$

$$\dot{U}_n = \sum_{m=1}^{M} \left[\left(\frac{1+\alpha_m}{2}\right) H_{i(m)} + \left(\frac{1-\alpha_m}{2}\right) H_{j(m)}\right] (\delta_{j(m),n} - \delta_{i(m),n}) W_m$$
$$- \sum_{\ell=1}^{L} \left[\left(\frac{1+\beta_\ell}{2}\right) H_{i(\ell)} + \left(\frac{1-\beta_\ell}{2}\right) H_\ell\right] \beta_\ell \delta_{i(\ell),n} WL_\ell + Q_n \tag{16}$$

$$\dot{W}_k = \frac{1}{L_k} (P_{i(k)} - P_{j(k)}) + F_k^* \alpha_k W_k^2 + E_k \tag{17}$$

Equations (9) and (10) become

$$P_n = P_n (U_n, M_n) \tag{18}$$

$$\text{and } WL_\ell = WL_\ell (U_{i(\ell)}, M_{i(\ell)}) \tag{19}$$

---

* F_K is a generalized pressure loss coefficient

Defining $$\Delta_m = \left[\left(\frac{1+\alpha_m}{2}\right) H_{i(m)} + \left(\frac{1-\alpha_m}{2}\right) H_{j(m)}\right] \quad (20)$$

and $$\Delta_\ell = \left[\left(\frac{1+\beta_\ell}{2}\right) H_{i(\ell)} + \left(\frac{1-\beta_\ell}{2}\right) H_\ell\right] \quad (21)$$

equation (16) becomes

$$\dot{U}_n = \sum_{m=1}^{M} \Delta_m \left(\delta_{j(m),n} - \delta_{i(m),n}\right) W_m - \sum_{\ell=1}^{L} \Delta_\ell \beta_\ell \delta_{i(\ell),n} WL_\ell + Q_n \quad (22)$$

Using equations (15), (17) and (22) and recalling that the independent variables are W_m, P_n, and U_n the following relationships are derived:

$$\frac{\partial \dot{W}_k}{\partial W_m} = 2F_k \alpha_k W_k \delta_{k,m} / L_k \quad (23)$$

$$\frac{\partial \dot{W}_k}{\partial U_n} = \frac{1}{L_k}\left[\frac{\partial P_{i(k)}}{\partial U_{i(k)}} \delta_{i(k),n} - \frac{\partial P_{j(k)}}{\partial U_{j(k)}} \delta_{j(k),n}\right] \quad (24)$$

$$\frac{\partial \dot{W}_k}{\partial M_n} = \frac{1}{L_k}\left[\frac{\partial P_{i(k)}}{\partial M_{i(k)}} \delta_{i(k),n} - \frac{\partial P_{j(k)}}{\partial U_{j(k)}} \delta_{j(k),n}\right] \quad (25)$$

$$\frac{\partial \dot{U}_n}{\partial W_k} = \sum_{m=1}^{M} \Delta_m \left(\delta_{j(m),n} - \delta_{i(m),n}\right) \delta_{m,k} \quad (26)$$

$$\frac{\partial \dot{U}_n}{\partial U_m} = - \sum_{\ell=1}^{L} \Delta_\ell \beta_\ell \delta_{i(\ell),n} \frac{\partial WL_\ell}{\partial U_m} \delta_{i(\ell),m} \quad (27)$$

$$\frac{\partial \dot{U}_n}{\partial M_m} = - \sum_{\ell=1}^{L} \Delta_\ell \beta_\ell \delta_{i(\ell),n} \frac{\partial WL_\ell}{\partial M_m} \delta_{i(\ell),m} \quad (28)$$

$$\frac{\partial \dot{M}_n}{\partial W_k} = \sum_{m=1}^{M} \left(\delta_{j(m),n} - \delta_{i(m),n}\right) \delta_{m,k} \quad (29)$$

$$\frac{\partial \dot{M}_n}{\partial U_m} = - \sum_{\ell=1}^{L} \beta_\ell \delta_{i(\ell),n} \frac{\partial WL_\ell}{\partial U_m} \delta_{i(\ell),m} \quad (30)$$

$$\frac{\partial \dot{M}_n}{\partial M_m} = - \sum_{\ell=1}^{L} \beta_\ell \, \delta_{i(\ell),n} \, \frac{\partial WL_\ell}{\partial M_m} \, \delta_{i(\ell),m} \tag{31}$$

Now define

$$y \equiv \begin{bmatrix} y_1 \\ \vdots \\ y_M \\ y_{M+1} \\ \vdots \\ y_{M+N} \\ y_{M+N+1} \\ \vdots \\ y_{M+2N} \end{bmatrix} \equiv \begin{bmatrix} W_1 \\ \vdots \\ W_M \\ U_1 \\ \vdots \\ U_N \\ M_1 \\ \vdots \\ M_N \end{bmatrix}$$

The Jacobian of $\dot{y} = f(y)$ is then (for p from 1 to N and q from 1 to M)

$$J_{k,p} = \frac{\partial \dot{W}_k}{\partial W_p} \tag{32}$$

$$J_{k,M+q} = \frac{\partial \dot{W}_k}{\partial U_q} \tag{33}$$

$$J_{k,M+N+q} = \frac{\partial \dot{W}_k}{\partial M_q} \tag{34}$$

$$J_{M+n,p} = \frac{\partial \dot{U}_n}{\partial W_p} \tag{35}$$

$$J_{M+n,M+q} = \frac{\partial \dot{U}_n}{\partial U_q} \tag{36}$$

$$J_{M+n,M+N+q} = \frac{\partial \dot{U}_n}{\partial M_q} \tag{37}$$

$$J_{M+N+n,p} = \frac{\partial \dot{M}_n}{\partial W_p} \tag{38}$$

$$J_{M+N+n,M+q} = \frac{\partial \dot{M}_n}{\partial U_q} \tag{39}$$

$$J_{M+N+n,M+N+q} = \frac{\partial \dot{M}_n}{\partial M_q} \tag{40}$$

Now all the terms of equations (11) and (12) are defined, i.e.

$$(\delta_{i,j} - \Delta t\, J_{i,j})\, \Delta y_j = \Delta t\, \dot{y}_i \tag{41}$$

where A from equation (12) is defined as

$$A \equiv (\delta_{i,j} - \Delta t\, J_{i,j}) \text{ and}$$

$$B \equiv \Delta t\, \dot{y}_i$$

Thus $$[A]\, \Delta y = [B] \tag{42}$$

The solution of the system equations is further simplified by eliminating the mass and energy components from the above sets of equations. Examination of equations (27), (28), (30) and (31) shows that only $J_{M+n,N+n}$, $J_{M+n,M+N+n}$, $J_{M+N+n,M+n}$, and $J_{M+N+n,M+N+n}$ are non-zero. Using this fact and separating (42) into its constituent flow, energy, and mass components

Flowrates Energy Mass

$$\sum_{p=1}^{M} A_{k,p}\,\Delta y_p + \sum_{q=1}^{N} A_{k,M+q}\,\Delta y_{M+q} + \sum_{q=1}^{N} A_{k,M+N+q}\,\Delta y_{M+N+q} = B_k \quad (43)$$

$$\sum_{p=1}^{M} A_{M+n,p}\,\Delta y_p + A_{M+n,M+n}\,\Delta y_{M+n} + A_{M+n,M+N+n}\,\Delta y_{M+N+n} = B_{M+n} \quad (44)$$

$$\sum_{p=1}^{M} A_{M+N+n,p}\,\Delta y_p + A_{M+N+n,M+n}\,\Delta y_{M+n} + A_{M+N+n,M+N+n}\,\Delta y_{M+N+n} = B_{M+n} \quad (45)$$

equations (44) and (45) can be used to eliminate Δy_{M+n} and Δy_{M+N+n}. This gives

$$\Delta y_{M+n} = (A_{22}B_1 - A_{12}B_2) - (A_{22}S_1 - A_{12}S_2)/D \quad (46)$$

$$\Delta y_{M+N+n} = (A_{11}B_2 - A_{21}B_1) - (A_{11}S_2 - A_{21}S_1)/D \quad (47)$$

where $1 \equiv M+n$

$2 \equiv M+N+n$

$$S_1 \equiv \sum_{p=1}^{M} A_{M+n,p}\,\Delta y_p$$

$$S_2 = \sum_{p=1}^{M} A_{M+N+p}\,\Delta y_p$$

$$D_1 = A_{11}A_{22} - A_{12}A_{21}.$$

Substituting (46) and (47) back into (44) and (45) gives Δy_{M+n} and Δy_{M+N+n} in the form

$$\Delta y_{\ell} = \sum_{p=1}^{M} C_{\ell p} \Delta y_p + H_{\ell} \quad \text{where } \ell = [M+1, M+2N]$$

such that

$$\Delta y_{M+n} = \sum_{p=1}^{M} \frac{(A_{12}A_{2p} - A_{22}A_{1p})}{D} \Delta y_p + \frac{(A_{22}B_1 - A_{12}B_2)}{D} \tag{48}$$

$$\Delta y_{M+N+n} = \sum_{p=1}^{M} \frac{(A_{21}A_{1p} - A_{11}A_{2p})}{D} \Delta y_p + \frac{(A_{11}B_2 - A_{21}B_1)}{D} \tag{49}$$

The mass and energy components of (43) are eliminated by using equations (48) and (49).

$$\sum_{p=1}^{M} A'_{kp} \Delta y_p = B'_k \tag{50}$$

where

$$A'_{kp} = A_{kp} + \sum_{q=1}^{2N} A_{k,M+q} C_{M+q,p}$$

and

$$B'_k = B_k - \sum_{q=1}^{2N} A_{k,M+q} H_{M+q}$$

Thus the 2N+M equations are reduced to M equations solving only for the flow rates, all other parameters being determined from them.

From equations (23) through (31) it is apparent that values for U_n, M_n, W_k, WL_n, $\partial P_n/\partial M_n$, $\partial P_n/\partial U_n$, and $\partial WL_n/\partial P_n$ are required initially to set up the Jacobian and the B vector. Also values for L_k, F_k, W_k and E_k for each connector are needed.

The solution described by equation (50) is a non-linear equation of the form

$$\dot{y}_i = f_i\ (y_j)$$

However, for small time steps, this may be linearized such that

$$\frac{d\dot{y}_i}{dt} = \frac{\partial y_i}{\partial y_j}\ \ \frac{dy_j}{dt} \cong J_{ij}\ \dot{y}_j$$

Interpolating linearly in a negative time direction

$$\dot{y}_i\ (t_o - \Delta t) = \dot{y}_i(t_o) - \Delta t\ J_{ij}\ \Big|_{t_o}\ \dot{y}_j(t_o)$$

or $$\dot{y}_i\ (t_o - \Delta t) = (\delta_{ij} - \Delta t\ J_{ij}\ \Big|_{t_o}\ )\ \dot{y}_j\ (t_o).$$

Inverting

$$\dot{y}_j\ (t_o) = [\delta_{ij} - \Delta t\ J_{ij}\ \Big|_{t_o}\ ]^{-1}\ \dot{y}_i\ (t_o - \Delta t)$$

and using $$\dot{y}_j\ (t_o) \equiv \lim_{\Delta t \to o}\ [y_j\ (t_o) - y_j\ (t_o - \Delta t)]/\Delta t$$

gives

$$y_j\ (t_o) = y_j\ (t_o - \Delta t) + \Delta t\ [\delta_{ij} - \Delta t\ J_{ij}\ \Big|_{t_o}\ ]^{-1}\ \dot{y}_i\ (t_o - \Delta t)$$

or $$\Delta y_j = \Delta t\ [\delta_{ij} - \Delta t\ J_{ij}]^{-1}\ \dot{y}_i\ .$$

This is the same form as equation (11) and is the linearized form of the system equations solved by TRANFLØ.

10.0 APPENDIX C - NOMENCLATURE

A	- Area (ft^2)
AF	- Connector Flow Area (ft^2)
AN	- Node Cross-sectional Area (ft^2)
C	- Flow coefficient (ft^{-1})
D	- Diameter (ft)
DE	- Hydraulic diameter (ft)
DP	- Therodynamic pressure drop (psi)
DPE	- Expansion loss pressure drop (psi)
DPF	- Form loss pressure drop (psi)
DPX	- Skin Friction pressure drop (psi)
E	- Elevation head (psi)
FD	- Form loss coefficient
G	- Mass flux (lbm/ft^2-sec)
H	- Heat transfer coefficient (Btu/sec-°F)
I	- Identity matrix
J	- Jacobian matrix
L	- Inertial Length (ft^{-1})
M	- Mass (lbm)
P	- Pressure (psia)
Pr	- Prandtl number
Q	- Total heat flux (Btu/sec)
Rc	- Reynolds number
T	- Temperature (°F)
U	- Internal energy (Btu)
V	- Specific volume (ft^3/lbm)
VIS	- Fluid viscosity (lbm/ft-sec)
VM	- Momentum averaged specific volume [11] (ft^3/lbm)
W	- Mass flow rate (lbm/sec)
WL	- Leak mass flow rate (lbm/sec)
X	- Length of a connector (ft)

Z	- Node elevation (ft)
F	- Darcy friction factor
g_c	- Gravitational constant
h	- Specific enthalpy (Btu/lbm)
k	- Thermal conductivity (Btu/ft-sec-°F)
t	- Time (sec)
q	- Heat flux (Btu/sec-ft^2)
ν	- Specific volume (ft^3/lbm)
x	- Quality
x_a	- Void fraction
x_f	- Flowing quality
δ	- Kronecker delta
Δ	- Difference
μ	- Viscosity (lbm/ft-sec)

Subscripts

l	- Refers to leak flows
k	- Refers to connectors
i,j	- Refer to nodes
w	- Refers to water
s	- Refers to steam
o	- Refers to initial value
H	- Refers to hydraulic value
in	- Refers to flow into a node
fb	- Refers to film boiling condition
fc	- Refers to forced convection condition
fg	- Refers to phase change between steam and water
fv	- Refers to forced convection vaporization condition
lb	- Refers to local boiling condition
sc	- Refers to subcooled condition
sv	- Refers to swirl vanes

eff - Refers to effective value of specific volume [11]

min - Refers to minimum value

out - Refers to flow out of a node

sat - Refers to saturation condition

crit - Refers to critical value

wall - Refers to value at tube wall

primary - Refers to primary heat source

Superscripts

s - Refers to steam

w - Refers to water